CAPITAL UNIVERSITY OF SCIENCE AND TECHNOLOGY, ISLAMABAD

Neuropharmacological Investigation of Chlorogenic Acid in Ketamine-Induced Mice Models of Schizophrenia

by

Anis Murtaza

A thesis submitted in partial fulfillment for the degree of Master of Philosophy

in the

Faculty of Pharmacy
Department of Pharmacology

2026

CERTIFICATE OF APPROVAL

Neuropharmacological Investigation of Chlorogenic Acid in Ketamine-Induced Mice Models of Schizophrenia

by

Anis Murtaza

(MPH243002)

THESIS EXAMINING COMMITTEE

S. No.	Examiner	Name	Organization
(a)	External Examiner	Dr. Muhammad Faheem	RIU, Islamabad
(b)	Internal Examiner	Dr. Fazlullah Khan	CUST, Islamabad

Dr. Muzaffar Abbas
Thesis Supervisor
September, 2026

Dr. Fazlullah khan
Head
Dept. of Pharmacology
September, 2026

Dr. Muzaffar Abbas
Dean
Faculty of Pharmacy
September, 2026

Author's Declaration

I, **Anis Murtaza** hereby state that my MPhil thesis titled "**Neuropharmacological Investigation of Chlorogenic Acid in Ketamine-Induced Mice Models of Schizophrenia**" is my own work and has not been submitted previously by me for taking any degree from Capital University of Science and Technology, Islamabad or anywhere else in the country/abroad.

At any time if my statement is found to be incorrect even after my graduation, the University has the right to withdraw my MPhil Degree.

(Anis Murtaza)

Registration No: MPH243002

Plagiarism Undertaking

I solemnly declare that research work presented in this thesis titled "**Neuropharmacological Investigation of Chlorogenic Acid in Ketamine-Induced Mice Models of Schizophrenia**" is solely my research work with no significant contribution from any other person. Small contribution/help wherever taken has been duly acknowledged and that complete thesis has been written by me.

I understand the zero tolerance policy of the HEC and Capital University of Science and Technology towards plagiarism. Therefore, I as an author of the above titled thesis declare that no portion of my thesis has been plagiarized and any material used as reference is properly referred/cited.

I undertake that if I am found guilty of any formal plagiarism in the above titled thesis even after award of MPhil Degree, the University reserves the right to withdraw/revoke my MPhil degree and that HEC and the University have the right to publish my name on the HEC/University website on which names of students are placed who submitted plagiarized work.

(Anis Murtaza)
Registration No: MPH243002

Acknowledgement

To start with, I would like to thank **Almighty Allah (SWT)**, the supreme provider of all power and wisdom, whose boundless mercy and blessings helped me to survive all the hardships of my M.Phil journey. Only through His grace did I manage to gain the strength and courage to pass all the challenges. Peace and blessings upon **Prophet Muhammad (PBUH)** whose teachings of compassion, integrity and search of knowledge have always been a source of inspiration and guidance to me since my early years. I am grateful to a great extent to **Capital University of Science and Technology (CUST), Islamabad**, which offered me the great opportunity to get my M.Phil in Pharmacy and to help me in my studies.

I owe a special debt to my great supervisor, **Dr. Muzaffar Abbas (Dean, Faculty of Pharmacy, Capital University of Science and Technology, Islamabad)**. The variety of his intellectual rigour, visionary direction, uncompromising support and endless enthusiasm of his research has made my academic experience to become a most enriching and fulfilling experience. I am still extremely grateful to him because he has opened new knowledge horizons, ensured necessary resources, and accompanied me on my way in all its challenges. His extraordinary talent of developing the exciting scientific stories out of the complicated material has not only refined my vision of research but also given me a desire to discover something new all my life. He has significantly influenced my life in very positive aspect. I owe a lot of gratitude also to **Dr. Reem Altaf** who gave me invaluable tips, encouragement, and support. She has been one of the greatest inspirational guides in my academic career.

I want to use this chance to express my gratitude to my esteemed instructors and seniors: **Dr. Sohail Riaz, Ms. Ibtesam Zakir, Mr. Ibrar Khan, Mr. Shamas Gulfam** and **Mr. Farhan Ali Khan**. You have been invaluably helpful to me, with your technical help, and your precious collaboration, your moral support.

(Anis Murtaza)

Abstract

Schizophrenia is a complex neuropsychiatric disorder that is characterized by positive, negative and cognitive symptoms, and chronic neuroinflammation. The current study evaluated neuropharmacological potential of chlorogenic Acid (CGA) in a ketamine-induced mouse model of schizophrenia at three different doses of CGA (10, 50, or 100 mg/kg) using haloperidol (1mg/kg) as a positive control drug. A multidisciplinary method was used which involved a combination of *in vivo* behavioral evaluation, biochemical and histopathological evaluation and detailed *in silico* studies. Behavioral testing showed that CGA treatment reduced ketamine-induced hyperactivity, social interaction, spatial working memory, and depressive-like behavior. The biochemical studies revealed that there was significant decrease in pro-inflammatory cytokines (TNF-α and IL-1β) expression in brain. At the behavioral and biochemical levels, the CGA at 10 mg/kg was determined to be the most effective. The histopathological analysis showed neuronal integrity in the hippocampus, prefrontal cortex, and striatum. The analysis of network pharmacology revealed that CGA and schizophrenia-associated genes had 196 overlapping targets, and the key hub proteins, such as IL6, TNF, IL1B, NFKB1, AKT1, and CASP3, enriched the TNF signaling pathway and IL-17 signaling pathway pathway. Molecular docking of Schrodinger Maestro 13.4 showed good interactions of CGA with these hub targets with the docking scores reaching up to -6.6 kcal/mol, mostly through hydrogen bonding with key amino acids. All these findings indicate that CGA has promising antipsychotic-like and neuroprotective potential due to its inhibitory effect on neuroinflammation and the regulation of major inflammatory and apoptotic processes. Therefore, CGA might be is a possible multi-target natural therapeutic candidate in the treatment of schizophrenia.

Contents

List of Figures

List of Tables

Abbreviations

AAALAC	Association for Assessment and Accreditation of Laboratory Animal Care International
AKT1	Protein Kinase B (AKT Serine/Threonine Kinase 1)
ANOVA	Analysis of Variance
BCA	Bicinchoninic Acid
CASP3	Caspase-3
CGA	Chlorogenic Acid
DMSO	Dimethyl Sulfoxide
ELISA	Enzyme-Linked Immunosorbent Assay
FST	Forced Swim Test
GO	Gene Ontology
H&E	Hematoxylin and Eosin
HRP	Horseradish Peroxidase
IAEC	Institutional Animal Ethics Committee
IL-1β	Interleukin-1 Beta
IL-6	Interleukin-6
i.p.	Intraperitoneal
KEGG	Kyoto Encyclopedia of Genes and Genomes
NF-κB	Nuclear Factor Kappa B
OFT	Open Field Test
OMIM	Online Mendelian Inheritance in Man
PDB	Protein Data Bank
PFC	Prefrontal Cortex
PPI	Protein-Protein Interaction

SD	Standard Deviation
SEM	Standard Error of the Mean
SIT	Social Interaction Test
ShinyGO	Shiny Gene Ontology
SP	Standard Precision (docking mode)
STITCH	Search Tool for Interactions of Chemicals
STRING	Search Tool for the Retrieval of Interacting Genes/Proteins
TMB	Tetramethylbenzidine
TNF-α	Tumor Necrosis Factor Alpha

Symbols

$*$	$P < 0.05$ (statistically significant)
$**$	$P < 0.01$ (highly significant)
$***$	$P < 0.001$ (very highly significant)
$\#$	$P < 0.05$ vs control group
$\#\#$	$P < 0.01$ vs control group
$\#\#\#$	$P < 0.001$ vs control group
$\pm$	Plus or minus (used with mean $\pm$ SD or mean $\pm$ SEM)
N	Number of animals per group
%	Percentage
μg	Microgram
ng	Nanogram
mg/kg	Milligram per kilogram
μL	Microliter
mL	Milliliter
cm	Centimeter
s	Second
°C	Degree Celsius
M	Molar (e.g., 2 M H_2SO_4)

Chapter 1

Introduction

1.1 Background of Schizophrenia

Severe disturbances in social relationships, emotional response and thought and perception are hallmarks of schizophrenia, a severe and chronic neuropsychiatric illness [1]. Emil Kraepelin first described dementia praecox in the late 19th century, emphasizing the disorder's early start and progressive cognitive loss. At first, the term was used in 1908 by Eugen Bleuler who was a Swiss psychiatrist to highlight the split or fragmentation of thinking, mood, volition and psychic processes rather than the dementia that was believed to be inevitable. Bleuler replaced the idea of a merely degenerative process with a more diverse diagnosis of fundamental disruptions in mental integration. Modern diagnostic systems have their roots in this redefinition [2].

Schizophrenia is considered by the World Health Organization to be a disorder that is characterized by abnormalities in perception, thinking, emotions and behavior that greatly affect functioning [3]. According to the most recent estimates, schizophrenia affects nearly 23.18 million people globally, or a prevalence of roughly 0.29 percent or 0.43 percent among adults. Due mostly to population expansion, absolute numbers have increased dramatically from 13.62 million cases

in 1990 to over 23 million in 2021. Age-standardized rate changes have resulted in minor prevalence and disability-adjusted life-year changes [4].

Schizophrenia etiology is multifactorial, due to intricate interactions involving genetic predisposition and environmental factors. Genome-wide association studies reveal a highly polygenic architecture with thousands of common variants with small individual effects and rare copy number variants, despite twin and adoption studies showing strong heritability, estimated at over 80% [5]. Prenatal infections, obstetric complications, urban upbringing, teenage cannabis use and long-term psychosocial stress are some of the determinants that interfere with genetic predisposition through epigenetic pathways to influence the development of disease, which usually occurs in late adolescence or early adulthood [6, 7].

Lifetime risk of schizophrenia is comparatively consistent across cultures (around 0.5 to 1 percent) but there exist significant regional differences in disease burden and access to care [8]. In South Asia, such as Pakistan, the number of cases is high because of the high population. In various provinces of Pakistan, regional estimates indicate a prevalence of between 1 and 2.5 percent although in most cases, it is higher in urban areas mostly due to stressors associated with rapid urbanization and scarcity of mental health resources. The burden is further worsened in the region by cultural stigma and treatment gaps of over 80 per cent in most of the low-resource settings [9, 10].

Preclinical animal studies are important in getting the insight of pathology of disease and the evaluation of interventions. Of these, the ketamine-induced model has been prominent since sub-chronic ketamine treatment of rodents leads to behavioral changes similar to positive symptoms (hyperlocomotion), negative symptoms (social withdrawal) and cognitive impairments and replicates neuroinflammatory and glutamatergic changes in human schizophrenia [9].

1.2 Significance of Schizophrenia Research

Schizophrenia has a significant socioeconomic impact globally due to direct medical expenses, lost productivity and carer stress [11]. Global Burden of Disease

studies indicate that the prevalence cases have increased in 2021 to 23.18 million, compared to 13.62 million in 1990 and the disability-adjusted life years have surged to 14.82 million in 2021 in comparison to 8.76 million in 1990. Even though the age-standardized incidence rates have demonstrated a slight decrease, it's contributions along with disability-adjusted life years rates have demonstrated small positive changes, demonstrating the chronic nature of the disorder and its effects throughout the lifespan [4].

In countries with low- and middle-income, such as in South Asia, the issue is exacerbated by a lack of mental health infrastructure and high treatment gaps as well as widespread stigma [9].

Pakistan has specific problems and it has been estimated that schizophrenia is a foremost factor contributing for mental health-related disability-adjusted life years in the area. Vulnerability is further exacerbated by urban stressors, consanguinity and socioeconomic factors and cultural beliefs tend to delay diagnosis and resort to non-specialist care [8, 10].

Because the number of absolute instances is increasing as a result of global population increase, the implications for public health are substantial. It has been projected that the prevalence and disability burden will continue to increase by 2030 [4]. The resistance to treatment occurs in approximately 30 per cent of patients and traditional treatment methods have not been associated with high levels of effectiveness in negative and cognitive symptoms which are significant factors in the long-term impairment and poor life quality. Such gaps indicate the necessity of developing new multi-target strategies that would deal with the underlying neuroinflammatory and synaptic processes [12].

The scientific importance of the research on schizophrenia is in the ability to identify new targets of treatment in the face of the ongoing difficulty with available interventions. As nearly a third of patients are now treatment-resistant and conventional antipsychotics often do not treat negative and cognitive domains, there is a rising interest in adjunctive agents with an anti-inflammatory and multi-target profile, including natural polyphenols [6, 7].

TABLE 1.1: Global versus regional burden of Schizophrenia (selected indicators from GBD 2021 data)

Region	**Prevalent cases (millions, 2021)**	**Age-standardized prevalence rate (per 100,000)**	**DALYs (millions, 2021)**	**Ref**
Global	23.18	277.71	14.82	[4]
South Asia	High absolute contribution (part of ∼14.96 million in Asia)	Elevated in several countries	Substantial regional share	[9, 10]
High-income countries	Lower absolute numbers	Comparable to global average	High per capita costs	[4, 10]

1.3 Symptoms of Schizophrenia

The three main symptom domains of schizophrenia are positive, negative and cognitive symptoms [13]. Positive symptoms, which indicate an excess or distortion of normal functioning, include hallucinations, delusions and disordered cognition or behavior. Due to the persecutory or grandiose aspects of the delusions, the most common auditory hallucinations are between 70 and 80 percent auditory. Frequent derailment or incoherence are examples of disordered speech and catatonic or extremely disorganized behavior can seriously impair day-to-day functioning [14].

Negative symptoms are associated with impaired or absent normal functioning and encompass impaired expression of emotions, avolition, anhedonia, asociality and alogia [15]. The symptoms occur in 50 to 95 percent of patients in the clinical setting and are highly linked with low functional outcomes and low quality of life. Negative symptoms tend to arise sooner and continue despite positive symptoms being treated and are quite significant in terms of long-term disability [15, 16].

Impairments in a number of areas, including working memory, executive function, processing speed and language learning, might emerge as cognitive symptoms [16].

These disabilities impact between 75 and 85 percent of the people with schizophrenia and is experienced in different levels since the prodromal stage. The cognitive deficits are regarded as fundamental characteristics of the disorder and are robust are consistent determinants of impaired daily functioning and they tend to be less responsive to the existing antipsychotics [17, 18].

The disease is usually progressive, starting with a prodromal phase that may span several years, with subtle negative and cognitive impairments and acute episodes with pronounced positive symptoms followed by a chronic phase where negative and cognitive impairments may be more prominent [14].

This course provides an insight into the heterogenic nature of schizophrenia and the necessity of early treatment to prevent long-term disability [13].

TABLE 1.2: Summary of symptom categories in Schizophrenia with clinical examples and Neurobiological correlates

Symptom Category	**Clinical Examples**	**Neurobiological Correlates**	**Ref**
Positive	Hallucinations (mainly auditory), delusions (persecutory or grandiose), disorganized speech or behavior	Mesolimbic dopamine hyperactivity	[14]
Negative	Avolition, anhedonia, social withdrawal, blunted affect, alogia	Prefrontal cortex dysfunction, reduced motivation circuits	[15, 16]
Cognitive	Deficiencies in executive control, attention and processing speed	Glutamate/ N-methyl-D-aspartate (NMDA) hypofunction, widespread cortical inefficiency	[16]

1.4 Diagnostic Criteria for Schizophrenia

The most important international classification systems for diagnosing schizophrenia are DSM-5 and ICD-11. Delusions, hallucinations, or disordered speech must

be one of the two or more distinctive symptoms that have been found for a considerable amount of duration within one month (reduced time if treatment is successful) in order for the DSM-5 to make the diagnosis [19].

Additional requirements include the absence of schizoaffective illness, mood disorders with psychotic aspects, pharmacological actions, or other medical causes, as well as persistent symptoms of disruption lasting at least six months and a substantial functional handicap. When a comorbid history of autism spectrum disorder or a communication disorder is present, the diagnosis additionally requires that prominent delusions or hallucinations persist for a minimum duration of one month [14].

ICD-11 follows a similar pattern by focusing on symptoms but with more emphasis on a dimensional approach and eliminating the first-rank symptoms that were so prevalent in ICD-10. These two systems emphasize functional impairment and duration, but provide scope to cultural differences in symptom manifestation [19]. Diagnostic issues in Pakistan (and other South Asian settings) are associated with cultural explanations of symptoms (religious/ spiritual explanations of hallucinations), language difficulties and insufficient access to structured clinical interviews, such as the SCID [20, 21]. Prompt diagnosis is vital as early intervention can result in better prognosis and less untreated psychosis, which is linked to a poor prognosis [14]. Nevertheless, lack of valid biomarkers and overlap with other psychotic disorders still present a major challenge in diagnostic issues especially within resource restricted environments [22].

1.5 Overview of Pathophysiological Mechanisms

1.5.1 Neurotransmitter Dysregulation

The dopamine hypothesis has long served as a central framework for understanding schizophrenia pathophysiology, proposing that negative and cognitive symptoms arise from reduced activity within the mesocortical pathway, whereas positive

symptoms such as hallucinations and delusions stem from excessive mesolimbic dopaminergic activity. More contemporary integrative models have expanded beyond this framework, emphasizing dysregulation across multiple neurotransmitter systems, particularly glutamatergic and GABAergic signaling [23]. NMDA receptors on GABAergic interneurons are believed to be hypofunctional, causing imbalance between excitatory and inhibitory processes and downstream abnormalities of dopaminergic neurons and cortical disinhibition [24].

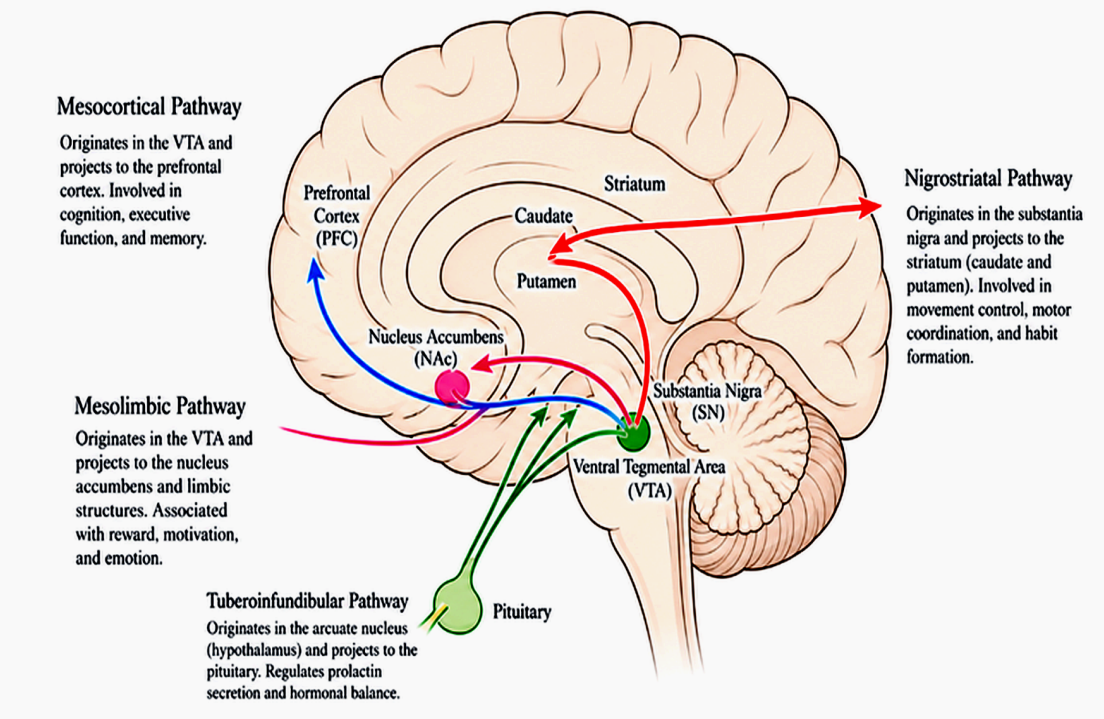

FIGURE 1.1: The interaction between anomalies in pathways in the etiology of schizophrenia:

Sagittal view of human brain illustrating the four major dopaminergic pathways implicated in schizophrenia pathophysiology. (A) Mesolimbic pathway (pink): VTA → nucleus accumbens, increased activity causes positive symptoms. (B) Mesocortical pathway (blue): VTA → prefrontal cortex, hypoactivity causes negative or cognitive symptoms. (C) Nigrostriatal pathway (yellow): substantia nigra → dorsal striatum, D2 blockade causes EPS. (D) Tuberoinfundibular pathway (green): hypothalamus → pituitary, D2 blockade causes hyperprolactinemia. Adapted from Howes & Shatalina (2022). (Image compiled by author and adapted from Howes, O.D. et al., 2022)

1.5.2 Neuroinflammation and Immune Dysregulation

Neuroinflammation has emerged as aa important mechanism in schizophrenia, with evidence of increased pro-inflammatory cytokines including IL-6, TNF-α and IL-1β in both peripheral blood and Central Nervous System (CNS) compartments [25]. Heightened microglial activation and compromised blood-brain barrier integrity further contribute to abnormal synaptic pruning and neuronal damage. These neurotransmitter systems interact with these inflammatory processes, which may worsen the glutamate hypofunction and dopaminergic imbalance and are linked with the persistence of negative and cognitive symptoms [24, 26].

1.5.3 Structural, Functional and Genetic Factors

The structural brain abnormalities that are regularly found in schizophrenia are decreased gray matter in the prefrontal cortex and hippocampus, expansion of the ventricles and impaired white matter connectivity [5]. These alterations are linked to polygenic risks scores comprising of thousands of shared variants and uncommon copy number variants. Disease vulnerability is additionally determined by gene-environment interaction, in which neuroimaging shows a change in functional connectivity, which is associated with symptom severity and cognitive impairment [6].

1.6 Overview of Preclinical Models in Schizophrenia Research

The utilization of animal studies in schizophrenia studies is necessary since it is possible to investigate the mechanisms of the disease and test possible therapeutic measures using animals that cannot be done in humans due to ethical and practical considerations [27]. These models attempt to model essential features of the disorder using face (similarity in symptoms), construct (similar underlying mechanisms) and predictive (response to known antipsychotics) validities. Although

none of the models is a complete representation of the complex human condition, they offer informative understanding of neurobiological pathways and enable the bridging of basic science to clinical translation [28].

The preclinical models of schizophrenia can be broadly divided into pharmacological, genetic, developmental and lesion based models. One of the most common types of pharmacological models is the type which involves the use of NMDA receptor antagonists because they are able to cause the development of schizophrenia-like behavior and neurochemical changes [29].

Genetic models aim to address individual risk genes discovered in genome-wide association studies, whereas developmental models include early-life exposures (e.g. maternal immune activation or prenatal stress) to recap neurodevelopmental etiologies of the disorder [30].

The model of ketamine induced has become one of the most popular pharmacological models [27]. Related to schizophrenia symptoms, sub-anesthetic doses of ketamine when administered repeatedly or sub-chronically cause a spectrum of behavioral changes in rodents that include hyperlocomotion (positive symptoms), social withdrawal (negative symptoms) and working memory and attention impairment (cognitive symptoms).

This model is especially applicable since it recreates the NMDA receptor hypofunction, which is among the major pathophysiological characteristics that are backed by human research and causes neuroinflammatory alterations [31, 32].

The ketamine model has great translational power to test new drugs, even natural agents that have anti-inflammatory effects [27]. Nevertheless, there are some limitations that have to be taken into account by researchers: strain-specific effects, dose-specific effects and that it mainly simulates an acute or sub-chronic glutamatergic impairment and not the entire chronic process of schizophrenia. When formulating such studies, ethical aspects in animal research, such as the 3Rs principle (Replacement, Reduction, Refinement) are the crucial steps to take [28].

1.7 Current Treatments and Their Limitations

1.7.1 Pharmacological Approaches

Antipsychotics remain the cornerstone of schizophrenia treatment, encompassing two main classes: first-generation agents (e.g., haloperidol, chlorpromazine) and second-generation agents (e.g., risperidone, olanzapine, clozapine). FGAs are useful in treating positive feelings since they primarily function as dopamine D2 receptor antagonists. SGAs are frequently used because of their comparatively lower risk of EPS and their wider receptor profiles, which include serotonin 5-HT2A antagonism [33, 34].

1.7.2 Non-Pharmacological and Combination Therapies

Approaches to non-pharmacological interventions, such as psychosocial approaches including cognitive behavioral therapy for psychosis (CBTp), family-based interventions, training in social skills and vocational intervention. These strategies, together with pharmacotherapy, enhance functional outcomes and decrease the relapse rates. Psychosocial support models of integrated care, which involve the use of medication, have demonstrated superior long-term outcomes compared to the use of medication alone, especially in negative symptoms and quality of life [35].

1.7.3 Limitations

Although the treatment has advanced, the modern treatments are still quite limited. FGAs have been associated to high incidence of extrapyramidal symptoms with many SGAs inducing significant weight increase, metabolic imbalances and sedation. The two classes demonstrate low efficacy rates against negative and cognitive symptoms, with about 30 percent of the patients being considered as treatment-resistant [33, 36].

The difficulty in compliance because of side effects and inadequate symptom control continues to be a significant issue. Such gaps underscore the necessity of adjunctive therapies with a focus on neuroinflammation and multi-pathway processes [34].

1.8 Introduction to Chlorogenic Acid

Chemically referred to as 5-O-caffeoylquinic acid (5-CQA) CGA is a primary dietary polyphenol of the hydroxycinnamic acid group. It's structure is an ester of caffeic and quinic acids [37]. CGA is very rich in different plant sources with green coffee beans being the richest source of diet with it having up to 54 percent of the extract in certain varieties. It is also present in fruits like apples or pears, berries, or vegetables like potatoes and artichokes and traditional medicinal plant like *honeysuckle* and *Eucommia ulmoides* [38].

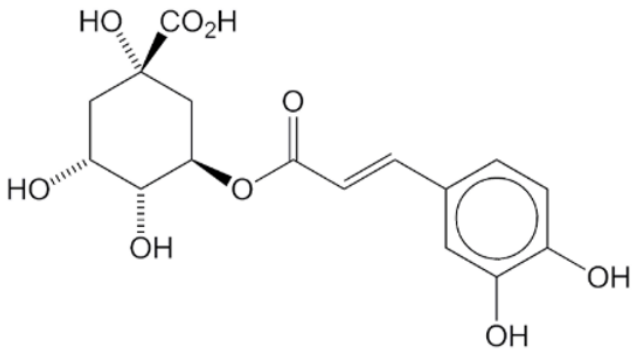

FIGURE 1.2: Chemical Structure of Chlorogenic Acid [39]

CGA has moderate bioavailability in terms of pharmacokinetics. Small amount of it is absorbed intact in small intestine after oral ingestion with a large percentage being hydrolyzed by gut microbiota in colon to produce metabolites like caffeic acid and ferulic acid. These metabolites with a few intact CGA are able to enter the brain and have pharmacological actions on the CNS. CGA has a half-life of relatively low value (1-2 hours) and exhibits dose-dependent plasma concentrations [38, 40].

The neuroprotective and anti-inflammatory potential of CGA is mediated, in part, through its inhibitory action on critical inflammatory pathways, particularly NF-κB signaling and the downstream production of cytokines including TNF-α, IL-6 and IL-1β. CGA has also been reported to modulate microglial activation states, favoring a transition from the pro-inflammatory M1 phenotype to the reparative, anti-inflammatory M2 phenotype.

These effects, along with its capacity to lower oxidative stress and maintain neuronal integrity, make CGA a viable option for neuroinflammatory illnesses like schizophrenia [41, 42].

Recent data on preclinical studies of CGA in models of neuroinflammation and cognitive dysfunction suggests its ability to enhance behavioral outcomes and prevent damage mediated by cytokines [42]. Its multi-target profile is in line with the complicated pathophysiology of schizophrenia, in which neuroinflammation is at the heart of the process [43].

1.9 Research Gap, Objectives, Hypothesis and Study Rationale

Regardless of the tremendous advances in the study of schizophrenia, there are still notable gaps in the creation of effective treatment options that can improve negative symptoms, cognitive impairments and neuroinflammatory basis [44]. The existing antipsychotics exhibit partial efficacy in these domains and treatment resistance occurs in about 30 percent of the patients. Although preclinical data indicate that natural polyphenols such as CGA have anti-inflammatory and neuroprotective properties in a variety of CNS models, there is limited literature regarding network pharmacology, molecular docking and extensive *in vivo* investigative research of ketamine-induced schizophrenia model. Moreover, the dose-response relationships of CGA in neuroinflammatory psychiatric models need to be clarified [14].

1.9.1 Objectives

i. To assess the dose-dependent effects of CGA (10, 50, or 100 mg/kg) on ketamine-induced schizophrenia-like behaviors in mice.

ii. To assess the effects of CGA on brain levels of TNF-α and IL-1β using ELISA.

iii. To examine the protective effects of CGA on histopathological changes in hippocampus, prefrontal cortex and striatum.

iv. To identify molecular targets and signaling pathways of CGA against schizophrenia using network pharmacology.

v. To validate the interaction of chlorogenic acid with key targets using molecular docking analysis.

1.9.2 Hypothesis

Chlorogenic acid attenuate ketamine-induced schizophrenia-like symptoms primarily through modulation of neuroinflammatory pathways.

1.9.3 Study Rationale and Scope

This preclinical research integrated behavioral, biochemical and histopathological evaluations with *in silico* to offer mechanistic understanding of the therapeutic potential of CGA. The study provides a translational basis of future research on CGA as an adjunctive natural agent by assessing three doses within the ketamine model, which is a dependable and reliable way to induce neuroinflammation and behavioral impairments similar to those of schizophrenia. It has been restricted to mice the results of which are supposed to help in the subsequent creation of multi-target treatments that will be applied to neuroinflammation in schizophrenia.

Chapter 2

Literature Review

2.1 Historical Evolution of Schizophrenia Understanding

There has been considerable change in the conceptual understanding of schizophrenia in the last century and a half. Dementia praecox is the term, coined by Emil Kraepelin in the late 19^{th} century, to describe a category of psychotic disorders that have onset at an early age and progressive worsening of cognitive functions. A major difference between manic-depressive illness and a primarily biological and degenerative course was highlighted by Kraepelin, which was clinical outcome and longitudinal observation. His classification established the basis of a disease-entity approach that was categorical and shaped the psychiatric nosology over several decades [1, 45].

The term schizophrenia (origins in Greek: schizophrenia) was coined in 1911 by the Swiss psychiatrist Eugen Bleuler, to characterize the disintegration of psychic functions, such as the defect of association, affect, autism and ambivalence (the four As). In contrast to Kraepelin who concentrated on the invariable degradation, Bleuler considered schizophrenia as a heterogeneous entity comprising of organic and psychological components. He emphasized the division of mental activities

over early dementia, creating a gap to psychological interpretations without abandoning a biological basis. This change carried the discipline beyond a strictly degenerative paradigm to a more complex and dynamic interpretation [1, 46].

The further evolution was observed in the mid-20th century due to the impact of psychoanalytic views and the introduction of operational diagnostic criteria. The first-rank symptoms described by Kurt Schneider focused on diagnostic anchors that were particular psychotic phenomena (thought insertion and auditory hallucinations) [47]. But the hegemony of the biological paradigm was challenged as social psychiatry and anti-psychiatry movements emerged and challenged the medical model, emphasizing environmental and social factors [48].

The modern knowledge is a significant paradigm change to neurodevelopmental and integrative models. Schizophrenia is now considered as a disease with powerful genetic backgrounds that interacts with environmental injuries at critical developmental intervals instead of an entirely degenerative disease [7]. Neuroimaging, genetics, immunology have advanced the understanding to include neuroinflammation, glutamate dysregulation and synaptic pruning abnormalities in their framework. Latest views suggest that the rigid categorical diagnosis should be replaced with dimensional and transdiagnostic models, as the manifestations of the clinical phenomena are heterogeneous and clinical manifestations are overlapping with those of other psychiatric disorders [13, 49].

2.2 Epidemiology and Risk Factors

2.2.1 Global and Regional Prevalence

Epidemiology trends on schizophrenia across the globe show an increasing absolute burden against a relatively stable age-standardized rates. According to the Global Burden of Disease (GBD) 2021 study, schizophrenia affected an estimated 23.18 million individuals worldwide in 2021, with approximately 1.22 million new cases reported during that year. Lifestyle diseases and chronic illnesses have risen

up to 23.18 million prevalence cases in 2021 compared to 13.62 million prevalence cases in 1990 that was mainly influenced by an increase in population. The age-standardized prevalence rate increased only slightly (261.98 to 277.71 per 100,000 individuals) with an age-standardized DALY rate that increased slightly (177.75 per 100,000). It is projected that both absolute prevalence and DALYs will keep increasing until 2036, although incidence age-standardised will experience a marginal decrease [4, 50].

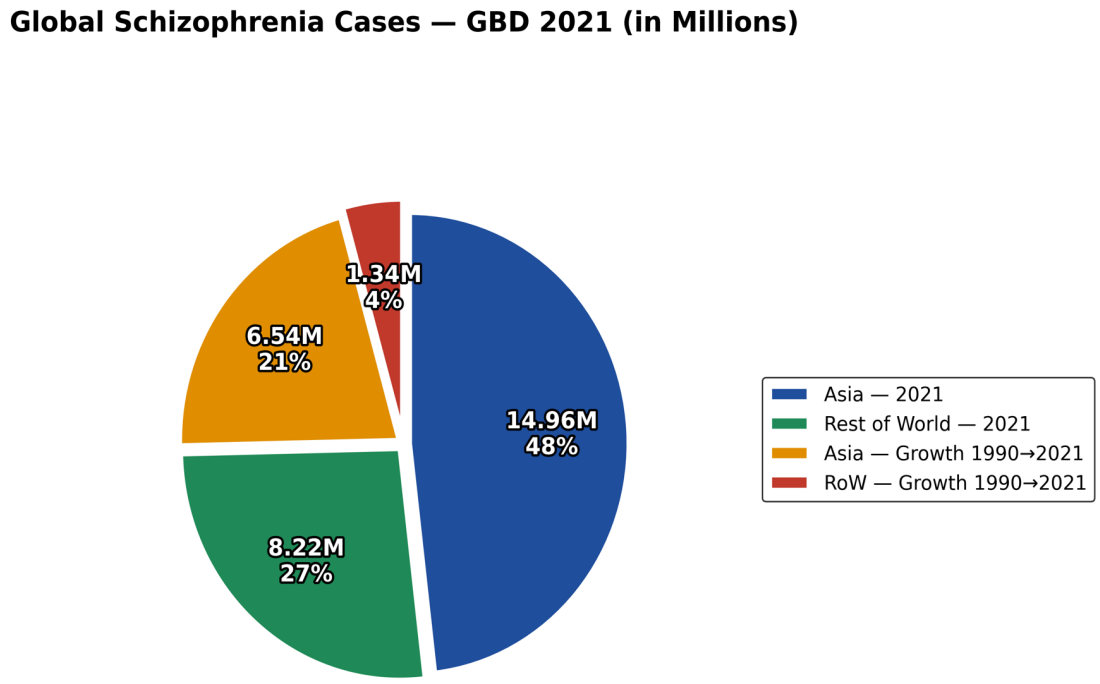

FIGURE 2.1: Global schizophrenia burden, 2021 (GBD Study). Asia bears 64% of cases amid population-driven growth

The given 3D globe infographic represents the trends of global schizophrenia epidemiology based on the GBD 2021 study. Asia leads on deep red shading, having 14.96 million prevalent cases in 2021 (an increase of 78% since 8.42 million prevalent cases in 1990), 64% of the global prevalent cases of 23.18 million cases. The orange color on South Asia (including Pakistan) indicates high absolute burdens (0.5-1% lifetime prevalence) and urban peaks associated with psychosocial stressors, whereas lighter red colors represent other areas. The upward arrows indicate

the estimated absolute variations in prevalence and DALYs up to 2036 even with the stable age-standardized rates (277.71 per 0.1 million). Incidence (20-24 years) and prevalence/DALYs (30-34, males higher) peak age figures, against blue oceans in a clean medical style. (Image compiled by author and adapted from GBD 2021 Schizophrenia Collaborators 2025 and Peng and Hu 2025).

The pressure is especially high in Asia because of high population levels. Asia also reported prevalent cases rising to 14.96 million in 2021 and a significant proportion of the global cases in 1990 of 8.42 million. The onset of the peaks is at the age group of 20-24, the prevalence and DALYs are highest at the ages of 30-34 and the burden tends to be higher among the males. In South Asia, such as in Pakistan, absolute numbers are high, but there is limited national prevalence data because of underreporting and difficulties in diagnosis. It is found that in the region the lifetime prevalence can be 0.5-1% and in urban areas there are higher rates which have been associated with psychosocial stress factors [4, 51].

2.2.2 Risk Factors

Schizophrenia is a result of intricate interactions between genetics and the environmental factors. Genetics show a significant impact with estimates of heritability being approximately 80%. Genome-wide association studies discover thousands of small effect genetic risk arising from both prevalent common variants and less frequent copy number variations. The family history is still one of the most powerful predictors and the first-degree relatives present significantly high risk (odds ratio of about 7-11 over the general population) [5, 6, 52].

The critical modulating role goes to environmental risk factors. Increased risk is always linked to prenatal infections, obstetric problems, upbringing in the city, use of cannabis in adolescence and chronic psychosocial stress. Other factors like consanguinity, high rates of urbanization, socioeconomic disadvantage as well as inaccessibility to perinatal care in South Asia contribute to vulnerability. Meta-analyses show that exposure to cannabis during adolescence presents odds ratio of about 2-4, whereas urbanicity and migration have odds ratio of about 1.5-2 [9, 10].

TABLE 2.1: Major risk factors for schizophrenia with approximate odds ratios from meta-analyses (2019–2026)

Risk Factor	**Approximate Odds Ratio (95% CI)**	**Ref**
Family history (first-degree relative)	7.0–11.0	[6, 52]
Cannabis use in adolescence	2.0–4.0	[14]
Urban upbringing / migration	1.5–2.5	[10]
Prenatal infection / obstetric complications	1.5–3.0	[5]
Consanguinity (South Asia-specific)	Elevated (variable)	[9]

These risk factors are dynamically interacting, with genetic liability enhancing environmental impacts via epigenetics. Cultural stigma, treatment gaps greater than 80 percent and other socioeconomic stressors also add to the burden in Pakistan and South Asia more broadly, underscoring the necessity of context-specific prevention approaches [9].

2.3 Pathophysiology of Schizophrenia: In-Depth Critical Analysis

2.3.1 Neurotransmitter Systems

Recent PET imaging research has reinforced the dopamine hypothesis by showing enhanced presynaptic dopamine synthesis and capability of releasing specifically in the area of striatum, which is highly correlated positive symptoms and antipsychotic response. Nevertheless, negative and cognitive impairments are more reliably associated with prefrontal hypo-dopaminergia, which implies a regionally decoupled, but not general, dopaminergic impairment. Critical reviews observe that although striat hyperdopaminergia is also one of the most replicated observations, most of the patients do not have this abnormality, indicating pathophysiological heterogeneity [13, 23].

Strong evidence that NMDA receptor hypofunction, especially on parvalbumin-containing GABA interneurons, causes the disinhibition of pyramidal neurons and the cortical excitatory-inhibitory imbalance has led to the dominance of the glutamate theory. It is this mechanism which is thought to be upstream of the dopaminergic dysregulation in most models [53]. Recent meta-analyses and pharmacological challenge studies confirm that glutamate abnormalities can be antecedents of dopaminergic alterations but the timing relationship and direction of causation is controversial. The situation is further complicated by serotonergic and GABAergic input, where 5-HT2A receptor modulation had a role in the domains of symptoms and therapeutic response. In general, neurotransmitter theories have been replaced by integrated network dysfunction rather than isolated transmitter excess/deficit, but there are major gaps in terms of individual variability and stage of illness specific alterations [24].

2.3.2 Neuroinflammation and Immune Dysregulation

Modern literature is trending in placing neuroinflammation as a primary cause and no longer as a secondary effect of schizophrenia [44]. Multiple lines of evidence including PET imaging of microglial activation, elevated peripheral and CSF cytokines (particularly IL-6, TNF-α and IL-1β) and post-mortem findings support sustained low-grade inflammation. Over-activation of microglia is believed to lead to surge in synaptic pruning in adolescence and continued loss of neurons, which leads to further gray matter loss [26].

The neurotransmitter systems are also under the control of inflammation: pro-inflammatory cytokines enhance the release of glutamate and reduce the functioning of NMDA receptors through the metabolites of the kynurenine pathway. The present evidence on maternal immune activation supports a multiple-hit hypothesis in which initial inflammation predisposes the brain against subsequent environmental stressors [24]. The critical analysis, however, shows that there is significant heterogeneity. Patients do not all exhibit a pro-inflammatory pattern

and in some studies, anti-inflammatory responses are inconsistent or even compensatory. Much of this variability is probably due to medication status, duration of illness and methodological variations (peripheral vs. central measures). Nevertheless, the inflammation is becoming considered as an encouraging transdiagnostic object particularly in negative and cognitive symptoms which cannot be easily measured with dopamine blocking agents [54].

2.3.3 Structural, Functional and Genetic Abnormalities

Extensive neuroimaging meta-analyses also verify extensive and usually progressive gray matter losses, predominantly in the prefrontal cortex, hippocampus and temporal gyrus, along with enlargement of ventricular and impaired white matter connectivity. Such structural changes are already evident during the prodromal and high-risk stages but they are more likely to be more prominent with increased duration of illness and the occurrence of repeated psychotic episodes. Functional MRI investigations also indicate dysconnectivity patterns, especially in fronto-striatal and default mode networks, both of which have a strong correlation with cognitive deficits and poor functional outcomes. The reduction of white matter integrity, specifically in the fronto-temporal and fronto-striatal tracts, deteriorates with time of the disease [13, 55].

The neuroimaging results in different stages of illness reveal a tendency of progressive changes in the brain. The loss of gray matter in frontal and temporal areas, ventricular enlargement and white matter disconnectivity are more pronounced in the first-episode period compared to the chronic period and are linked to the degree of symptom severity and functional impairment of many patients. The findings of these studies reinforce the neuroprogression notion in a subgroup of schizophrenics [56].

Schizophrenia is a highly polygenic disorder that genetically gathers around synaptic, neurodevelopmental and immunological pathways [5]. Uncommon copy number variants have bigger impacts. The interaction of genes and the environment which are mediated by epigenetics has become the focus of the disease expression.

Nonetheless, genetic risk translation to definite brain phenotypes is not complete and polygenic risk scores only account for a relatively small percent of variance [6].

Overall, existing evidence can be in favor of a multifactorial, interactive theory according to which neuroinflammation is one of the intermediates between genetic susceptibility, neurotransmitter disgrouping and structural/functional alterations of the brain.

The high degree of heterogeneity in patients indicates that there are biological subtypes and patients might need individualized treatment [5, 13, 24].

2.4 Animal Models in Schizophrenia Research

2.4.1 Validity and Types of Models

Utilizing animal-based experimental models is still essential in schizophrenia studies because of its ability to allow mechanistic studies and preclinical trials of new interventions to be done in controlled settings [27].

Three conventional metrics are used to evaluate these models: construct validity (common underlying biological mechanisms), face validity (similarity to human symptoms) and predictive validity (accurate prediction of the action of clinical medications).

The convergence of pharmacological, genetic, developmental and lesion-based models has greatly advanced our understanding of human schizophrenia, despite the fact that no single model can fully account for its complexity and variety [28].

The most widely used ones are pharmacological models, especially using NMDA receptor antagonists, which have high construct validity. Genetic models focus on particular risk genes found by genome-wide association research, whereas developmental models use early-life environmental exposures, including maternal immune

activation or prenatal stress, to recapitulate neurodevelopmental etiology. Lesion-based models, also not so popular today, were used in the past to learn about certain circuits in the brain [29, 30].

2.4.2 Ketamine-Induced Model: Mechanisms and Applications

One of the most widely used pharmacological models in the present research on schizophrenia is the ketamine-induced model. In mice, repeated or subchronic administration to sub-anesthetic doses of ketamine is a reliable way to produce behavioral phenotypes resembling key symptoms of schizophrenia [27]. These include impairments in working memory, spatial learning and attention (cognitive symptoms) as assessed by tests such as the Open Field Test (OFT), Social Interaction Test (SIT), Y-maze and novel object recognition; hyperlocomotion (modeling positive symptoms); and social disengagement and decreased interaction time (negative symptoms) [31, 32].

Ketamine mechanistically causes NMDA receptor hypofunction on GABAergic interneurons, which causes excessive glutamate release, disinhibition of glutamatergic pyramidal neurons and downstream imbalance of dopaminergic neurons [27]. This paradigm is particularly useful for evaluating substances that affect neuroinflammation, like CGA, because it also induces neuroinflammatory changes like elevated pro-inflammatory cytokines and microglial activation [30].

2.4.3 Strengths, Limitations and Translational Relevance

The ketamine model has a number of strengths such as it has high reproducibility, high face and construct validity of glutamatergic dysfunction and good predictive validity of antipsychotics. It can be especially useful to study neuroinflammation and to test multi-target natural compounds [27]. Nevertheless, there are notable limitations. The model mainly measures the acute or sub-chronic glutamatergic underfunction and not the complete chronic progression of schizophrenia. The

effects of behavior may be strain-dependent and certain symptoms (particularly negative and cognitive) can be inconsistent across studies. Also, the direct psychotomimetic actions of ketamine can complicate the interpretation of changes in the long term. These limitations notwithstanding, the ketamine model is highly translational, particularly in conjunction with molecular and *In silico* methods. It offers a viable platform in testing new adjunctive therapy to neuroinflammation and pathophysiology of the synapses before proceeding to clinical trials [28].

TABLE 2.2: Comparison of major animal models of schizophrenia

Type	**Face Validity**	**Construct Validity**	**Predictive Validity**	**Strengths**	**Limitations**
Ketamine (Pharmacological)	High	High	Good	Reproducible, neuro- inflammation	Acute effects, strain variability [27, 28]
Genetic (e.g., DISC1)	Moderate	High	Moderate	Targeted gene effects	Limited behavioral phenotype [28]
Maternal Immune Activation	High	High	Moderate	Neuro- developmental relevance	Variable outcomes [27]

2.5 Pharmacological Treatments: Evolution and Evidence

2.5.1 First- and Second-Generation Antipsychotics

The pharmacological therapy of Schizophrenia commenced with the introduction of first-generation antipsychotics (FGAs) in the 1950s. Chlorpromazine and haloperidol became the primary treatment because they have strong blockade of dopamine D2 receptors which were very effective in decreasing positive symptoms like hallucinations. These agents had a tremendous effect of decreasing long-term hospitalization. But their efficacy in D2 blockade of the nigrostriatal pathway was

often accompanied by EPS including acute dystonia, tardive dyskinesia, parkinsonism and akathisia [33, 34]. Dyskinesia, parkinsonism and akathisia [33, 34].

One high-potency typical (first-generation) antipsychotic that is still used as the gold standard reference medication in preclinical schizophrenia research is haloperidol. Positive effects like hallucinations, delusions and psychomotor agitation are successfully reduced by its strong antagonistic effect on dopamine D2 receptors. Haloperidol is frequently given at a dose of 1 mg/kg (i.p.) as the positive control in ketamine-induced mouse models of schizophrenia because this dose consistently reverses ketamine-induced hyperlocomotion and other positive symptom-like behaviors while offering a reliable benchmark for assessing new therapeutic agents. It is quite efficient against positive symptoms because of its potent D2 receptor antagonist; however, the EPS of common antipsychotics, such as acute dystonia, tardive dyskinesia, parkinsonism and akathisia are also caused by this same mechanism [57].

Atypical antipsychotics, also referred to as second generation antipsychotics (SGAs), were designed to work on tolerability and to enhance the range of symptoms covered [33]. The prototype SGA, clozapine, was reintroduced in the late 1980s and continues to be the most effective in treating schizophrenia that is treatment resistant. Other popular SGAs are risperidone, olanzapine, quetiapine, aripiprazole and ziprasidone. These medications have D2 antagonism in combination with serotonin 5-HT2A receptor blockade, which lead to a reduced risk of EPS and smaller negative symptom improvements relative to FGAs. Severe network meta-analyses affirm that clozapine, olanzapine and risperidone tend to exhibit more favorable total efficacy, whereas aripiprazole has a superior metabolism. In spite of these achievements, there are significant shortcomings of both generations. FGAs have a large burden of EPS and most SGAs are linked to severe metabolic imbalances, including weight gain, dyslipidemia and diabetes risk, especially olanzapine and clozapine [34, 58].

Haloperidol especially is a high-potency typical (first-generation) antipsychotic, still used as a gold-standard reference drug in preclinical studies of schizophrenia. It has its main therapeutic action as strong antidopamine D2 receptors,

effectively alleviating positive symptoms like hallucinations, delusions and psychomotor agitation. Haloperidol (1 mg/kg i.p.) is commonly used as the positive control in ketamine-induced mouse models of schizophrenia since this dose consistently revert ketamine-induced hyperlocomotion and other positive symptom-like behaviours and provides a stable reference point when it comes to testing new therapeutic agents. Strong D2 receptor blockage makes it particularly efficient on positive symptoms, but it also has the same side effects as normal antipsychotics, such as acute dystonia, tardive dyskinesia parkinsonism and akathisia [59, 60].

2.5.2 Emerging and Adjunctive Therapies

With the limitations of monotherapy with traditional antipsychotics, interest has steadily increased regarding adjunctive and mechanism-based approaches to treatment. Glutamatergic agonists (bitopertin) and antagonists (pomaglumetad) have been studied to treat NMDA receptor hypofunction [41]. Promising anti-inflammatory drugs such celecoxib, minocycline and low-dose aspirin have shown some promise in reducing cytokine levels and adverse symptoms, especially in individuals with elevated baseline cytokine levels. Additionally, adjuncts including neuroprotective drugs and antioxidant chemicals are being studied [35]. Despite reports of some small improvements in adjunctive trials, findings are inconsistent, with many trials reporting small effect sizes or lack of replication. This heterogeneity raises the importance of patient stratification based on biomarkers in future studies [34].

2.5.3 Clinical Trial Evidence and Real-World Studies

Network meta-analyses are randomized controlled trials that involve hundreds of studies, which give the best evidence of antipsychotic effectiveness. Clozapine has always been the most successful treatment-resistant medication causing in a massive decline in the number of hospitalizations and deaths. Olanzapine and risperidone are also highly effective in positive symptoms and aripiprazole has

a good tolerance between efficacy and metabolic side effects [33]. Observational studies and registry data, however, have demonstrated high discontinuation rates (usually 60 to 70% during the first year) which are mostly caused by side effects and lack of total control of symptoms, particularly in negative and cognitive domains [34]. Pharmacogenomic testing of CYP enzymes and HLA variants are slowly being included to minimize adverse reactions although not commonly used in clinical practice. The treatment of most patients continues to be based on trial-and-error [33].

TABLE 2.3: Comparison of FGAs and SGAs.

Antipsychotic Class	**Examples**	**Efficacy on Positive Symptoms**	**Efficacy on Negative Symptoms**	**Major Side Effects**	**Ref**
First-generation	Haloperidol, Chlorpromazine	High	Low	EPS, tardive dyskinesia	[34]
Second-generation	Clozapine, Olanzapine, Risperidone, Aripiprazole	High	Moderate	Metabolic (weight gain, diabetes), sedation	[33, 58]

Despite the fact that, antipsychotics are the main pillar of the neuroinflammation treatment, their inability to tackle negative and cognitive symptoms, in addition to severe side-effect side-effects, highlight why, new multi-target adjunctive methods should be developed. Anti-inflammatory and neuroprotective compounds like chlorogenic acid are natural products that provide a potential source of future research [41].

FDA approved D2 antagonist versus new muscarinic/TAAR1 therapy: This infographic classifies contemporary pharmacological therapies of schizophrenia in six major mechanistic groups. Risperidone and Olanzapine are D2 antagonist types of dopamine blockade, whereas KarXT/Cobenfy, is an innovative muscarinic agonist that completely bypasses the D2 line. TAAR1 agonists (Ulotaront, Phase 3) and M4 modulators (NMRA-266) are broadly symptom targeting novel receptors. Weekly implants (Lyndra Risperidone) overcome adherence barriers and serotonin

modulators (Xanomeline-Trospium) are a combination. (The figure designed and compiled by author and adapted from Correll, C.U. et al., 2026).

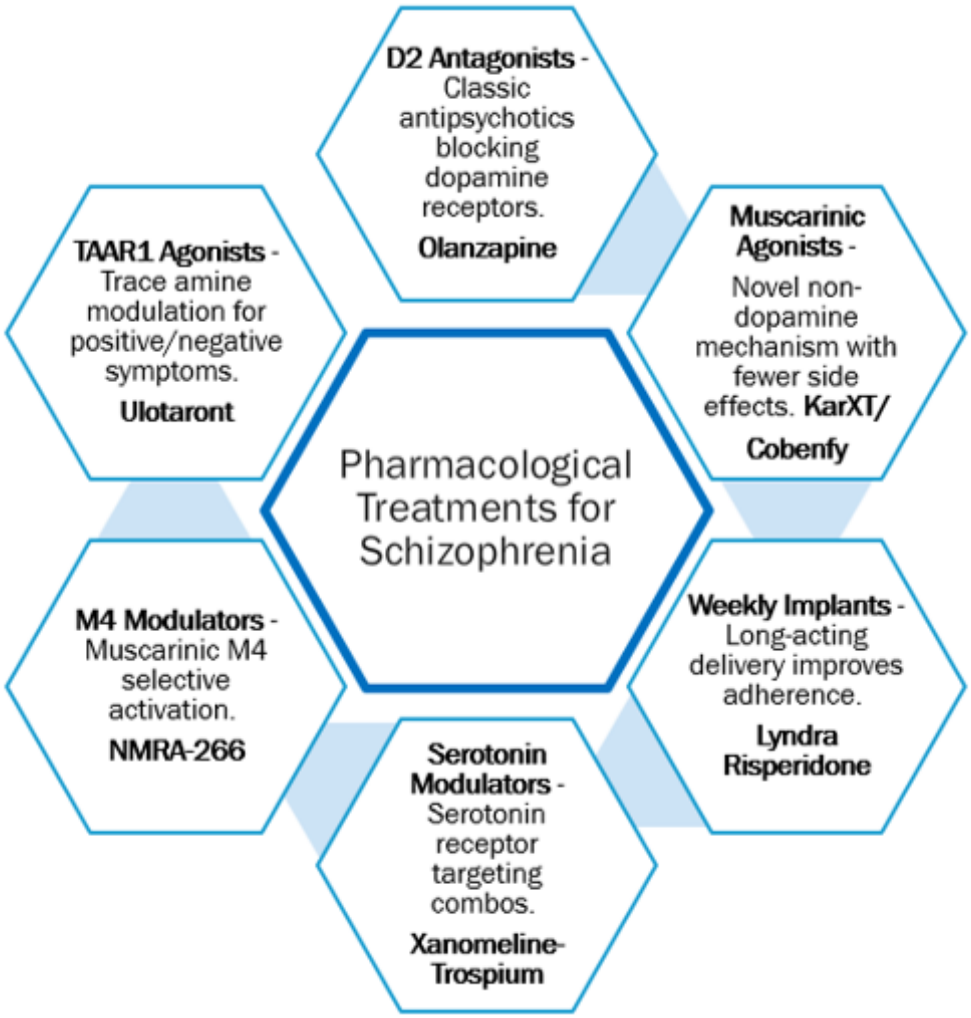

FIGURE 2.2: Classification of pharmacological schizophrenia treatments by mechanism (2026)

2.6 Non-Pharmacological Interventions and Integrated Care

Non-pharmacological treatment has come to be critical elements of holistic management of schizophrenia. One of the approaches that have been under the most extensive investigation is the Cognitive Behavioral Therapy of Psychosis (CBTp).

It aims at lessening distress related to persistent positive symptoms, difficult delusional beliefs and enhancing coping methods [61].

Pooled evidence from meta-analyses demonstrates that CBTp produces moderate-sized effects in reducing positive symptoms and overall functioning and that the effects are maintained when used concomitant with antipsychotic medication [35].

The goals of family interventions and structured psychoeducation programs are to lower high expressed emotion in families, enhance caregiver education and boost adherence to treatment. These strategies have proved to have substantial relapse and rehospitalization reduction. Social skills training and vocational rehabilitation also deal with social withdrawal and unemployment, which are two significant causes of long-term disability in schizophrenia [35].

Care models that involve the use of pharmacotherapy and psychosocial interventions always show better results compared to medication. Big data randomized trials and systematic reviews have shown better outcomes in negative symptoms, cognition and overall life quality. The strongest benefits have long-term outcomes in multimodal approaches incorporating CBTp, family therapy and vocational support [33, 61].

Although there is solid evidence on their effectiveness, there exist strong barriers to implementation, particularly in low- and middle-income countries. In Pakistan and South Asia, some of the complications are critical scarcity of qualified mental health practitioners, inaccessible CBTp programs, cultural stigma of psychological therapies and inadequate integration of psychosocial services into the existing healthcare systems. Therefore, pharmacological treatment remains almost the sole option of many patients because of the lack of accessibility and affordability [9, 10].

Culturally adapted, scalable and task-shifted interventions are urgently needed, as highlighted in the recent literature. Digital or group-based models and education of community health workers can be useful to close these gaps in resource-limited environments [33, 61].

2.7 Limitations of Current Treatments and Unmet Needs

Although the science of antipsychotic pharmacotherapy has developed over the decades, the existing schizophrenia treatment has significant limitations. The first- and second-generation antipsychotics have a strong effect on positive symptoms but moderate effect on negative symptoms and cognitive impairments, the major causes of long-term functional impairment and poor quality of life [34]. About 30% of patients can be categorized as being treatment-resistant with poor response despite an optimization regimen including clozapine. In practice, high discontinuation rates are always reported, usually more than 60 per cent. in the first year, mainly due to intolerable adverse effects and a failure to control symptoms completely [33, 58].

The majority of SGAs, such as olanzapine and clozapine, are linked with a high risk of metabolic complications, such as weight gain, dyslipidemia and newly developed diabetes, while FGAs, such as haloperidol and chlorpromazine, are linked with a high risk of EPS and tardive dyskinesia. Such negative outcomes do not only decrease adherence but also lead to higher cardiovascular morbidity and mortality in such population. Moreover, both classes show minimal effects on the neuroinflammatory and glutamatergic dysfunction underlying the disorder which is increasingly being considered central to the pathophysiology of the disorder [9, 35].

Non-pharmacological interventions are helpful where accessible, but lack accessibility, particularly in low-resource countries such as Pakistan. The lack of trained therapists, cultural stigma and insufficient incorporation into the regular care lead to the vast majority of patients receiving only partially pharmacological treatment with little psychosocial support. Such a disjointed approach does not focus on the entire range of symptoms and functional needs [9].

The greatest gaps in current therapeutic approaches to schizophrenia are interventions that are more effective in negative and cognitive symptoms, methods of overcoming treatment resistance and those that aim at neuroinflammation and

synaptic dysfunction, instead of only dopamine blockade. Existing interventions have minimal effect in stopping or reversing the gradual alterations in the brain of most patients.

Multi-target agents, which possess anti-inflammatory, neuroprotective and glutamatergic modulatory properties and can be used safely in adjunct to current antipsychotics are clearly needed [13, 44].

2.8 Pharmacology and Therapeutic Potential of CGA

2.8.1 Chemical Properties, Sources and Pharmacokinetics

CGA, a 5-O-caffeoylquinic acid, is one of the predominant dietary hydroxycinnamic acid esters of caffeic acid and quinic acid [43].

It is commonly found polyphenol in green coffee beans, which may contain 5-10 percent of the dry weight and is found in large amounts in apples, pears, berries, potatoes and other medicinal plants. Structurally, CGA has various hydroxyl groups which give it powerful antioxidant and metal-chelating effects [37, 38].

Pharmacokinetically, CGA shows moderate oral bioavailability [37]. Fractional absorption occurs to a small percentage in the small intestine, most of it is absorbed in the colon where gut microbiota break it down into caffeic acid and other metabolites.

These metabolites and certain intact CGA can pass by the blood-brain barrier and have CNS effects. The plasma half-life is not long (1-2 hours) and bioavailability depends on the dose and is affected by the individual gut microbiome composition [62].

2.9 Molecular Mechanisms

CGA exerts pronounced anti-inflammatory activity through inhibition of the NF-κB signaling cascade, thereby suppressing the production of pro-inflammatory cytokines including TNF-α, IL-6 and IL-1β [42]. Additionally, it controls the activation of microglia, polarizing them into the anti-inflammatory M2 type instead of the pro-inflammatory M1 type. Additionally, by directly scavenging free radicals and boosting endogenous antioxidant enzymes, CGA has antioxidant benefits. These systems work synergistically to lessen oxidative stress, neuroinflammation and neuronal death [63].

Recent research also indicates that CGA is able to regulate imbalance between glutamate-dopamine and safeguard synaptic integrity and therefore it is also mechanistically applicable to the pathophysiology of schizophrenia. Its multi-target profile is different to its traditional single-target antipsychotics [44].

2.9.1 Evidence in Neurological and Psychiatric Disorders

CGA has been shown to possess neuroprotective properties in multiple disorders of the CNS on preclinical grounds. It has been demonstrated that CGA cause decline in the cytokines levels, microglial activation and cognitive impairment in lipopolysaccharide-induced neuroinflammation models [37]. Sleep deprivation, chronic stress and ischemia model studies have reported improvements in memory, anxiety-like behaviour and depressive-like symptoms at doses between 5 and 100 mg/kg with some reporting a positive effect with lower-to-moderate doses [38, 43].

CGA supplementation (usually 300-500 mg/day) in human trials has been shown to have positive effects on cognitive functions like attention, psychomotor speed and executive functioning and on mental fatigue reduction. Nonetheless, there is a significant gap in research as there are no clinical trials specifically conducted in schizophrenia or psychotic disorders devoted to it [37, 38].

2.9.2 I*n Silico* and Preclinical Insights

Network pharmacology and molecular docking have been becoming a more commonly used tool to explain the multi-target effects of CGA in neuroinflammatory disease processes that are relevant to schizophrenia.

Network pharmacology analyses have shown that there is a significant overlap between the predicted targets of CGA and genes that are linked with neuroinflammation.

A single study determined robust targets including AKT1, TNF, MAPK1, MAPK-14, MMP9, PTGS2 and RELA and the TNF signalling pathway was highly enriched. Such results indicate that CGA might have its action by regulating major inflammatory centers that produce cytokines and activate microglia [42].

Molecular docking studies have provided further validation. CGA exhibits favourable binding affinities to several critical inflammatory proteins, including TNF, IL1β, AKT1 and NFκB1, primarily through hydrogen bonding and hydrophobic interactions at active sites. These computational results support CGA's potential to directly interfere with pro-inflammatory signalling cascades such as TNF/NF-κB and IL-17 pathways [42, 64].

These *In silico* predictions have been validated by preclinical research. CGA administration (doses range from 10–100 mg/kg) in lipopolysaccharide (LPS)-induced neuroinflammation models in mice and BV2 microglial cells TNF-α, IL-6 and IL-1β were among the pro-inflammatory cytokines whose expression and release were markedly decreased *In vivo* and at micromolar quantities in vitro.

Additionally, CGA reduced NF-κB activation, prevented microglial polarization toward the M1 phenotype and maintained synaptic integrity. Similar protective benefits have been seen in models of chronic stress and sleep deprivation, where CGA decreased neuroinflammatory markers and enhanced cognitive function [37, 42].

2.10 Synthesis of Literature, Research Gaps and Justification

The reviewed literature in this chapter demonstrates a steady shift in the interpretation of schizophrenia as a dopaminergic disorder to a multifactorial illness that entails dysregulation of glutamate, neuroinflammation, abnormalities of synaptic pruning and progressive structural brain alterations. Though first- and second-generation antipsychotics have continued to form the backbone of treatment, they have apparent deficiencies in the treatment of negative and cognitive symptoms, have serious side-effect profiles and result in treatment-resistance in about 30% of patients. Non-pharmacological and integrated care models have other advantages, but significant barriers to implementation exist, especially in low-resource environments [13, 34].

CGA has gained recognition as a promising natural polyphenol with potent anti-inflammatory, antioxidant and neuroprotective features [38]. *In silico* studies demonstrate that CGA interacts with multiple schizophrenia-relevant targets, particularly those involved in TNF, IL-17 and NF-κB signalling pathways. Preclinical evidence from LPS-induced neuroinflammation, chronic stress and cognitive deficit models supports CGA's ability to reduce pro-inflammatory cytokines, modulate microglial activation and improve behavioural outcomes. However, most existing research has focused on general neuroinflammation rather than schizophrenia-specific models and dedicated studies integrating network pharmacology with comprehensive *In vivo* evaluation in the ketamine-induced model are notably scarce [42].

Critical gaps in the literature are the small number of studies done on CGA in validated schizophrenia animal models, the lack of integration between computational target prediction and behavioural and biochemical outcomes and gaps in dose-response relationships in neuroinflammatory psychiatric models. In addition, studies exploring the effects of CGA on positive and negative symptom domains concomitantly in the ketamine model are scarce.

Chapter 3

Material and Methods

3.1 Animals

In this investigation, healthy male adult BALB/c mice weighing 25–30 g were employed. The animals were purchased from Capital University of Science and Technology's Animal House Facility in Islamabad. All of the mice were checked upon arrival for any indications of disease or trauma. The trial only involved animals in good health.

Capital University of Science and Technology, Islamabad's Institutional Animal Ethics Committee gave its approval to the study (Approval No. # REC /FOP /CUST /2025/01). The Association for Assessment and Accreditation of Laboratory Animal Care International's (AAALAC) recommendations and the Ethics Committee's criteria were strictly adhered to during all experimental procedures.

A computer-generated randomization schedule was used to allocate mice at random to six experimental groups (n = 6 each group). Ketamine-induced solely, ketamine plus CGA (10 mg/kg), ketamine + CGA (50 mg/kg), ketamine + CGA (100 mg/kg) and ketamine + haloperidol (1 mg/kg) served as the positive control group.

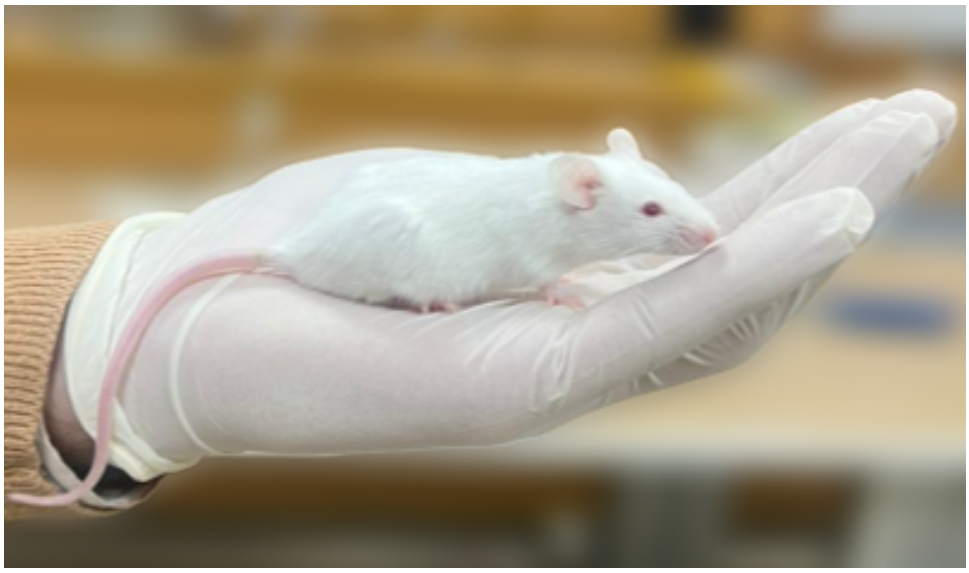

FIGURE 3.1: BALB/C mice utilized in study.

(Photography taken at Faculty of Pharmacy, Capital University of Science and Technology, Islamabad).

3.2 Housing Conditions

The mice were housed in groups and cages were placed on racks in a well-ventilated animal room. The room was maintained at a controlled temperature of 22 ± 2 °C, relative humidity of 50-60 % and a 12-hour light/dark cycle (lights on from 08:00 to 20:00 h) using an automatic timer system. Adequate ventilation was provided to ensure fresh air circulation and to maintain specific pathogen-free conditions.

The bedding material consisted of autoclaved wood shavings, which were changed every 48 hours or earlier if soiled to maintain hygiene and prevent ammonia accumulation. All cages were cleaned and disinfected regularly with 70 % ethanol. Special care was taken to avoid overcrowding and to provide sufficient space for normal locomotor activity.

3.3 Food Composition

Mice used in the study were fed a nutritionally balanced standard laboratory pellet diet formulated to meet their daily requirements. The diet consisted of locally

available ingredients that ensured consistent quality and reliable experimental outcomes.

TABLE 3.1: Composition of Animal's Food.

Food item	**Percentage (%)**	**5.0 Kg**
Wheat Flour	50	2.50 Kg
Chokar (Bran)	15	750 g
Fish Meal	15	750 g
Soybean Meal	10	500 g
Dry Skimmed Milk	5	250 g
Vitamins/Minerals Mix	5	250 g

3.4 Acclimatization

Before beginning any experimental procedures, all mice were given a fourteen-day acclimatization period upon arriving at the animal facility. The animals needed this time to adjust to the temperature, humidity, light-dark cycle and handling persons in their habitat. Mice were kept in groups of six in standard polycarbonate cages with corn cob bedding during this phase.

They were kept in controlled environments with a temperature of 24 ± 1°C, a relative humidity of 55-60% and a 12-hour light/dark cycle (lights on from 08:00 to 20:00). The normal pelleted meal and filtered water were available to the animals without restriction. Body weight, grooming, activity levels and any indications of illness or distress were all monitored through daily health checks.

Every day, each cage was gently handled for five to ten minutes in order to acclimate the animals to human contact. This made handling during subsequent drug administration and behavioral testing easier and decreased anxiety-related behaviors. To guarantee consistent distribution across treatment arms, mice were randomly assigned to experimental groups based on body weight at the conclusion of the acclimatization phase.

3.5 Mice Handling

All animal handling procedures were performed in compliance with institutional ethical Every animal handling method was carried out in accordance with institutional ethical standards that were authorized by the Capital University of Science and Technology (CUST), Islamabad, Ethics Committee. Before the tests started, animals were acclimated to the experimenter's gentle handling by being watched every day for any indications of disease, suffering, or unusual behavior.

Mice were gently restrained by holding the base of their tails and letting them clutch the wire cage lid in order to reduce stress during handling. Then, using the thumb and fingers to gently fix the loose skin over the scruff, the little finger was used to stabilize the tail. Without impairing ventilation or creating discomfort, this method offered sufficient constraint.

Throughout the experimental period, animals were monitored daily for body weight, food and water intake, grooming behavior and general activity. Any animal showing signs of severe distress or poor health was humanely euthanized via cervical dislocation following approved protocols.

3.6 Mice Bedding

Mice were housed in standard polycarbonate cages (dimensions $30 \times 20 \times 15$ cm) lined with corn cob bedding as the primary substrate. Corn cob bedding was selected due to its high absorbency, effective odor control, low dust content and non-toxic nature, making it suitable for maintaining animal health and experimental reliability. Bedding was provided at a depth of approximately 2-3 cm to allow natural burrowing and nesting behaviors.

Cages were thoroughly cleaned and bedding was replaced on each alternate day to maintain hygiene, prevent ammonia accumulation and minimize microbial contamination. During cage changes, mice were temporarily transferred to clean holding cages using gentle handling techniques to reduce stress.

The use of consistent bedding material across all experimental groups ensured uniform housing conditions, thereby reducing environmental variability that could affect behavioral and biochemical results.

3.7 Randomization

Before the trial began, animals were randomly randomized to treatment groups to guarantee impartial allocation and remove any possibility of bias in experimental results. A computer-generated random number sequence was used for randomization and body weight stratification was used to guarantee a consistent distribution among all groups.

For individual identification throughout the experimental period, mice were marked on the tail using non-toxic, permanent ink. The marking system employed circular bands of varying sizes and quantities to distinguish each animal within a cage. Animal #1 was identified by a single small circular band around the tail, while Animal #2 received two small circular bands with even spacing. Animal #3 was marked with three small circular bands and Animal #4 with four small circular bands. Animal #5 was distinguished by a single thick circular band and Animal #6 by one thick circular band followed by one small band, separated by a small gap.

This identification method allowed for accurate monitoring of individual animals throughout the experimental procedures, facilitating precise data collection and tracking of behavioral and biochemical outcomes for each subject.

3.8 Euthanizing Methods

At the conclusion of the study procedures, all animals were humanely euthanized to collect brain for biochemical and histopathological analyses. Euthanasia was performed under controlled conditions following institutional guidelines and ethical standards to minimize pain and distress.

3.8.1 Dislocation

Cervical dislocation was employed as the primary method of euthanasia. This technique was selected for its rapidity, reliability and compatibility with subsequent biochemical and histological analyses, as it avoids chemical interference from anesthetic agents. The procedure was performed by trained personnel only.

The mouse was first carefully restrained by holding onto the base of its tail in order to execute cervical dislocation. After that, the animal was put on a level platform and the base of its skull was firmly scraped with a wooden or stainless steel spatula. The cervical vertebrae were instantly separated from the skull by a quick, powerful tug on the tail. As a result, the brainstem-spinal cord link was instantly disrupted, causing fast unconsciousness in a matter of seconds. This was followed by respiratory arrest and cardiac collapse. The absence of a heartbeat and the stoppage of breathing were indicators of death.

3.8.2 Concussion

In cases where cervical dislocation was not feasible, concussion followed by cervical dislocation was employed as an alternative method. This two-step procedure ensured humane euthanasia while preserving tissue integrity for subsequent analyses.

The concussion method involved delivering a sharp, directed blow to the skull using a firm object, causing immediate brain trauma and loss of consciousness. This technique was performed by experienced personnel to ensure precise application. Following concussion, cervical dislocation was immediately performed to ensure irreversible cessation of vital functions, as concussion alone is considered a stunning technique rather than a complete euthanasia method by international standards.

Lack of breathing, heartbeat and corneal responses were indicators of death. Following euthanasia, brain tissues (prefrontal cortex, striatum and hippocampus) were immediately collected on ice for biochemical and histopathological analyses.

3.9 Chemicals and Drugs

All of the medications and chemicals employed in this investigation were purchased from commercial vendors and were of normal analytical grade. To guarantee stability and effectiveness, the test substance, CGA, ketamine and haloperidol were made fresh every day before being administered.

TABLE 3.2: List of chemicals and drugs used in the study along with their sources and suppliers.

Category	**Chemical/Substance**	**Source**
Test Compound	CGA	Sigma-Aldrich, USA
Drug	Ketamine	
	Haloperidol	
Solvent	Dimethyl Sulfoxide (DMSO)	
	Normal Saline (0.9% NaCl)	Amson Pharmaceuticals, Pakistan
Buffer	Phosphate Buffered Saline (PBS)	Sigma-Aldrich, USA
	RIPA Buffer	
ELISA Kit	Mouse IL-1β ELISA Kit	Biosharp, China
	Mouse TNF-α ELISA Kit	
Protein Assay Kit	BCA Protein Assay Kit	
Staining	Hematoxylin	Sigma-Aldrich, USA
	Eosin	
Solvent	Xylene	
	Ethanol	
Fixative	Formalin (10% neutral buffered)	

3.10 Ketamine-Induced Schizophrenia Model

A well-known ketamine paradigm that mimics important behavioral, neurochemical and neuroinflammatory aspects of the human condition was used to create a schizophrenia-like phenotype in mice. In rats, ketamine, a non-competitive NMDA receptor antagonist, causes a range of behavioral abnormalities that are similar to the positive, negative and cognitive symptoms of schizophrenia [65].

Ketamine was injected intraperitoneally (i.p.) at a dose of 30 mg/kg body weight after being dissolved in regular saline. For every animal, the injection volume was kept at 10 mL/kg. For 14 days in a row, ketamine was given once daily to create a chronic state similar to schizophrenia.

Throughout the course of the experiment, this repeated dose paradigm results in long-lasting changes in glutamatergic neurotransmission, neuroinflammation and behavioral impairments [65].

To confirm the development of schizophrenia-like phenotype, animals were monitored daily for behavioral changes following each ketamine administration. Parameters assessed included locomotor activity, rearing behavior, stereotypic movements and overall behavioral reactivity.

Observations were conducted for 60 minutes post-injection in a quiet, well-lit environment. Ketamine-treated mice typically exhibited hyperactivity, increased stereotypic behaviors and disrupted social interaction patterns characteristic of the model.

In the reversal treatment protocol, CGA (10, 50 and 100 mg/kg) or haloperidol (1 mg/kg) was administered 30 minutes after to ketamine injection from day 8 to day 14. This design allowed evaluation of therapeutic efficacy in reversing established schizophrenia-like symptoms. The control group received vehicle (2% DMSO in normal saline) following the same schedule. Behavioral assessments were conducted on day 14 (post-treatment) to evaluate therapeutic reversal.

3.11 Behavioral Assessments

Behavioral testing was conducted to evaluate schizophrenia-like symptoms across all experimental groups. Tests were performed in a quiet, lit room between 09:00 and 17:00 to minimize circadian variability. Animals were acclimatized to the testing room for 30 minutes before each test. Tests were ordered from least to most stressful to minimize carryover effects between assessments.

3.11.1 Open Field Test

Anxiety-like behavior and spontaneous locomotor activity were evaluated using the OFT. The device was a square arena made of opaque acrylic that was 40 cm in length, 40 cm in width and 35 cm in height. It was separated into peripheral zones and a central zone that measured 20 cm by 20 cm. After being positioned separately in the middle of the arena, each mouse was given five minutes to freely explore. A digital video camera installed above the arena was used to capture behavior. The overall distance traveled (in centimeters) in the chamber over a five-minute period was one of the parameters examined. In order to remove smell cues, the device was washed with 70% ethanol in between sessions.

FIGURE 3.2: OFT Chamber

(Photography taken at Faculty of Pharmacy, Capital University of Science and Technology, Islamabad).

3.11.2 Social Interaction Test

A three-chamber device called the SIT was used to assess social behavior, one of the main negative symptoms of schizophrenia. The device was made up of three connected rooms with detachable doors that measured 20 cm by 20 cm by 20 cm. The three stages of the test were social novelty, sociability and habituation. The test mouse was kept in the middle chamber with empty wire cups in both side chambers for five minutes during the habituation period. An unfamiliar mouse (stranger 1) was positioned beneath one wire cup for the sociability phase. For

five minutes, the amount of time spent interacting with each mouse was recorded. In order to eliminate smell cues, the device was cleaned in between sessions. The formula used was:

$$\% \text{ Social Preference} = \frac{\text{Time spent interacting with social partner}}{\text{Total exploration time}} \times 100 \quad (3.1)$$

FIGURE 3.3: SIT Chamber

(Photography taken at Faculty of Pharmacy, Capital University of Science and Technology, Islamabad).

3.11.3 Y-Maze Test

Spatial working memory was evaluated via spontaneous alternation behavior in the Y-Maze Test. Three arms measuring 35 cm in length, 6 cm in breadth and 15 cm in height were positioned at 120° angles to form the Y-maze contraption. After being positioned at the end of one arm, each mouse was given five minutes to freely explore. When all four paws entered an arm, it was considered an entrance. Consecutive inserts into all three arms without repetition, such as ABC, BCA and CAB sequences, were considered spontaneous alternation. Percentage spontaneous alternation was calculated as:

$$\% \text{ Correct Alterations} = \frac{\text{Number of alternations}}{\text{Total arm entries - 2}} \times 100 \quad (3.2)$$

FIGURE 3.4: SIT Chamber

(Photography taken at Faculty of Pharmacy, Capital University of Science and Technology, Islamabad).

3.11.4 Forced Swim Test

The purpose of the FST was to evaluate depressive-like behavior, which is indicative of negative symptoms in schizophrenia. Each mouse was put in a clear cylinder measuring 25 cm in height by 15 cm in diameter that was filled with water (23-25°C) to a depth of 15 cm, making sure the mice couldn't touch the bottom. The remaining five minutes of each six-minute session were used to record immobility time. Immobility was described as floating with the least amount of limb movement required to maintain head elevation. Following each experiment, the mice were taken out, towel-dried and put in a heated cage to recuperate before being put back in their original cage. In order to maintain hygienic conditions and temperature, water was replaced in between trials. The calculations were made using formula:

$$\% \text{ Immobility} = \frac{\text{Time spent immobile}}{\text{Total test duration}} \times 100 \tag{3.3}$$

FIGURE 3.5: FST Experiment

(Photography taken at Faculty of Pharmacy, Capital University of Science and Technology, Islamabad).

3.12 Study Design

This study combines *In Vivo* and *In Silico* approaches to evaluate the anti-schizophrenic effects of CGA in a ketamine-induced model. The *In Vivo* design includes KET induction, CGA treatment, behavioral assessments (OFT, SIT, Y-maze, FST), followed by biochemical (IL-1β, TNF-α ELISA, BCA) and histological (H&E) analyses in key brain regions (PFC, striatum, hippocampus).

The *In Silico* workflow identifies CGA targets, intersects them with Schizophrenia-related genes and validates key pathways and hub proteins through network analysis and molecular docking.

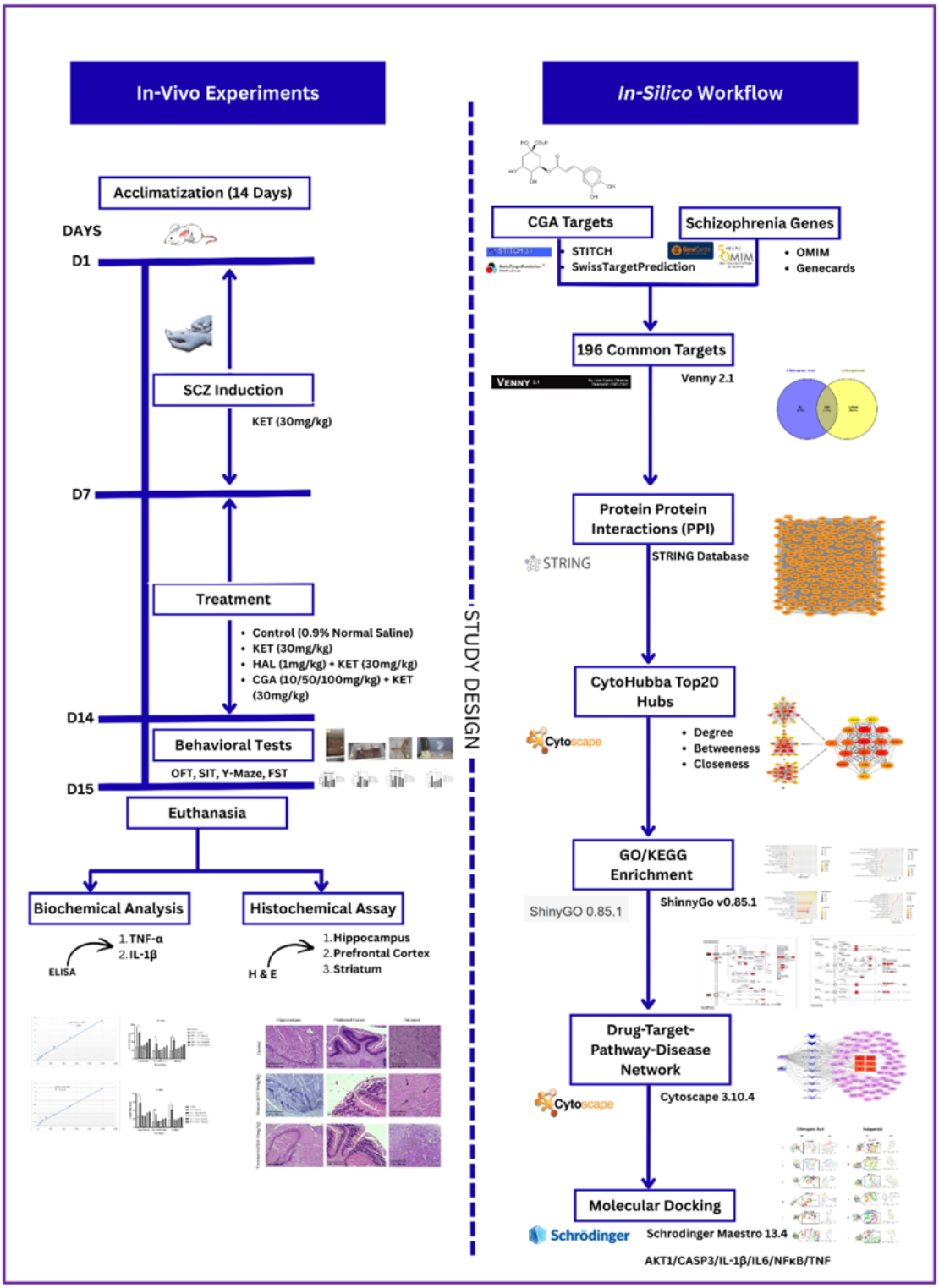

FIGURE 3.6: Study Design

The left side shows the *in vivo* timeline with steps from acclimatization to euthanasia, including treatment groups and behavioral tests, supported by minimal relevant icons (syringe, maze, brain, lab tools).

The right side presents the *in silico* workflow, moving from target prediction and gene databases to PPI analysis, hub gene identification, pathway enrichment and docking, using clean database and molecular icons.

3.13 Experimental Design and Grouping of Animals

Mice were divided into six experimental groups (n = 6 per group) at random based on body weight after the acclimation phase to guarantee even distribution. Haloperidol (1 mg/kg) was used as the positive control in this investigation to assess the neuroprotective effects of CGA at three different doses (10, 50 and 100 mg/kg) against ketamine-induced schizophrenia-like symptoms.

All treatments were administered via intraperitoneal (i.p.) injection. The study employed a reversal protocol wherein ketamine was administered daily for 14 consecutive days to induce Schizophrenia-like phenotype. Treatment with CGA or haloperidol was administered from day 8 to day 14, 30 minutes after the ketamine injection, allowing assessment of therapeutic reversal of established symptoms.

3.14 Drug Administration

Before drug administration, each mouse was individually weighed to ensure accurate dose calculations for ketamine, CGA and haloperidol. Fresh solutions of all drugs were prepared daily to maintain stability and efficacy.

All medications including CGA were injected intraperitoneally (*i.p.*) using a 26-gauge needle and a 1 mL sterile syringe. To maintain uniformity among groups, the injection volume was kept constant at 10 mL/kg body weight for every session. To reduce circadian variability, drug administrations were performed under sterile settings at the same time every day (16:00-17:00).

In order to produce a schizophrenia-like phenotype for the reversal protocol, ketamine (30 mg/kg, i.p.) was given once everyday for 14 days in a row. 30 minutes following the ketamine injection, CGA (10, 50, or 100 mg/kg, i.p.) or haloperidol (1 mg/kg, i.p.) were given between days 8 and 14. Using the same schedule, the control group was given an equivalent volume of vehicle (2% DMSO in regular saline).

3.15 Dose Preparation

All drug solutions were prepared fresh daily under sterile conditions to maintain stability and prevent degradation. Doses were calculated based on individual animal body weight (average 30 g), with the injection volume maintained at 10 mL/kg for consistent administration across all groups. Drug doses for individual mice were calculated according to the following formula:

$$\text{Dose of Mouse (mg)} = \text{Dose level} \left(\frac{\text{mg}}{\text{kg}}\right) \times \text{Body weight of mouse (kg)} \quad (3.4)$$

The body weight of each mouse was recorded prior to dosing and used individually in the calculation. The corresponding injection volume (in mL) was then determined as:

$$\text{Injection volume per mouse (mL)} = \text{Body weight (kg)} \times \frac{10 \text{ mL}}{\text{kg}} \quad (3.5)$$

Drug solutions were prepared at appropriate concentrations (mg/mL) such that:

$$\text{Concentration} \left(\frac{\text{mg}}{\text{mL}}\right) = \frac{\text{Dose per mouse (mg)}}{\text{Injection volume per mouse (mL)}} \quad (3.6)$$

For solutions requiring a vehicle (e.g., CGA in 2% DMSO in normal saline), the drug was first dissolved in the specified volume of DMSO and then diluted to the final volume with normal saline to achieve the calculated concentration. The vehicle control group received 10 mL/kg of the corresponding vehicle solution (2% DMSO in normal saline) without the active drug.

TABLE 3.3: Dose calculation for ketamine, CGA and Haloperidol during *in vivo* Studies

Group	**Compound**	**Dose (mg/kg)**	**Avg. Weight (kg)**	**Mouse Dose per Mouse (mg)**	**Total Mice**	**Total Dose for Group (mg)**
I	Saline	10 mL/kg	0.03	0.3 mL	6	25.2 mL
II	Ketamine	30 mg/kg	0.03	0.9	6	75.6
III	Haloperidol	1 mg/kg	0.03	0.03	6	1.26
	Ketamine	30 mg/kg	0.03	0.9	6	75.6
IV	CGA (Low)	10 mg/kg	0.03	0.3	6	12.6
	Ketamine	30 mg/kg	0.03	0.9	6	75.6
V	CGA (Medium)	50 mg/kg	0.03	1.5	6	63
	Ketamine	30 mg/kg	0.03	0.9	6	75.6
VI	CGA (High)	100 mg/kg	0.03	3	6	126
	Ketamine	30 mg/kg	0.03	0.9	6	75.6

All drug solutions were freshly made immediately before use of administration using 2% dimethyl sulfoxide (DMSO) in normal saline as the vehicle. The saline (vehicle) group received 10 mL/kg of a solution containing 40 μL DMSO and 960 μL normal saline. Ketamine solution (30 mg/kg) was prepared by dissolving 3 mg of ketamine in 1 mL of normal saline to obtain a concentration of 3 mg/mL. Haloperidol solution (1 mg/kg) was prepared by dissolving 0.1 mg of haloperidol in 1 mL of normal saline to obtain a concentration of 0.1 mg/mL. For CGA treatment groups, the required amount of CGA was first dissolved in 40 μL DMSO and then diluted with 960 μL normal saline to achieve final concentrations of 1 mg/mL (10 mg/kg), 5 mg/mL (50 mg/kg) and 10 mg/mL (100 mg/kg), respectively.

TABLE 3.4: Preparation of Solutions

Compound	**Dose**	**Concentration**	**Preparation**
Saline (Vehicle)	10 mL/kg	-	40 μL DMSO + 960 μL normal saline (2% DMSO)
Ketamine	30 mg/kg	3 mg/mL	3 mg ketamine dissolved in 1 mL normal saline

Table 3.4 continued from previous page

Compound	Dose	Concentration	Preparation
Haloperidol	1 mg/kg	0.1 mg/mL	0.1 mg haloperidol dissolved in 1 mL normal saline
CGA (Low)	10 mg/kg	1 mg/mL	1 mg CGA in 40 μL DMSO + 960 μL normal saline
CGA (Medium)	50 mg/kg	5 mg/mL	5 mg CGA in 40 μL DMSO + 960 μL normal saline
CGA (High)	100 mg/kg	10 mg/mL	10 mg CGA in 40 μL DMSO + 960 μL normal saline

All solutions were vortexed thoroughly to ensure complete dissolution before administration. Drug solutions were stored in sterile Eppendorf tubes at 4°C and used within 24 hours of preparation.

Intraperitoneal injections were performed using a 1 mL sterile syringe with a 26-gauge needle, with the injection volume adjusted to 10 mL/kg body weight for all treatments.

3.16 *In Silico* Studies

In *In Silico* Studies network pharmacology and molecular docking is performed. Network pharmacology methodology predicted CGA targets using STITCH and SwissTargetPrediction databases (confidence $\geq$0.7), intersecting with Schizophrenia genes from OMIM and GeneCards.

Common targets underwent STRING PPI network construction (medium confidence $\geq$0.4) and Cytoscape 3.10.4 analysis with CytoHubba for hub gene identification (Degree/Betweenness/Closeness centrality).

GO/KEGG enrichment utilized ShinyGO v0.85.1 (FDR<0.05), while molecular docking validation employed Schrodinger Maestro 13.4 (Glide SP mode) on hub protein structures from PDB (AKT1:3CQU, IL1B:9ILB, TNF:2AZ5 etc.) following protein/ligand preparation with OPLS4 force field.

3.16.1 Network Pharmacology

This network pharmacology investigation explored the potential therapeutic mechanisms of CGA against Schizophrenia. Potential targets of CGA were predicted using STITCH (http://stitch.embl.de) and Swiss Target Prediction (https://www.swisstargetprediction.ch) and Gene Cards (https://www.genecards.org) databases, applying a confidence threshold ≥0.7 in STITCH and default parameters in Swiss Target Prediction, which resulted in 277 unique targets after deduplication (combining predictions from both databases and removing overlaps/duplicates). Schizophrenia - associated genes were retrieved from OMIM (https://www.omim.org) and Gene Cards using the keyword "Schizophrenia," yielding 15,142 unique genes following removal of duplicates.

The overlap between the 277 CGA targets and 15,142 Schizophrenia genes was determined using Venny 2.1 (https://bioinfogp.cnb .csic.es/tools/venny) to generate a Venn diagram, identifying 196 common targets as candidate molecules mediating CGA's effects.

These 196 common targets were submitted to the STRING database (medium confidence ≥0.4, Homo sapiens) to construct a protein-protein interaction (PPI) network, with the interaction data exported as "string _interactions _short (2).tsv" and imported into Cytoscape version 3.10.4 for visualization and further analysis using a force-directed layout.

Hub genes were identified with the CytoHubba plugin in Cytoscape by applying three topological centrality measures: Degree centrality (DC, measuring local connectivity), Betweenness centrality (BC, assessing control over information flow) and Closeness centrality (CC, evaluating global reach).

The top 20 hubs were ranked independently for each metric. To identify robust core hubs, a Venn intersection analysis was performed on the three top-20 lists using Venny 2.1, yielding 17 common genes shared across all metrics.

3.16.1.1 Gene Ontology

Gene Ontology (GO) enrichment analysis was carried out on the common genes using ShinyGO v0.85.1 (https://bioinformatics.sdstate.edu/go/), an archived version based on Ensembl Release 104, to identify enriched categories in Biological Processes (BP), Molecular Functions (MF) and Cellular Components (CC). Analysis was conducted separately for BP, MF and CC with default parameters, including Homo sapiens as the species and a false discovery rate (FDR) threshold < 0.05 for significance. Enriched terms were ranked by P-value and visualizations were generated to highlight fold enrichment, gene count and -log10(FDR) for specific interpretation of significance levels.

3.16.1.2 Kyoto Encyclopedia of Genes and Genomes Pathway

Kyoto Encyclopedia of Genes and Genomes (KEGG) pathway enrichment analysis was similarly conducted on common genes using ShinyGO v0.85.1 to uncover multi-pathway mechanisms. The analysis focused on pathways with FDR ¡ 0.05, ranked by P-value and the top 15 pathways were selected for reporting. Visualizations, including bar charts and bubble plots, were created using ShinyGO to display enrichment metrics such as -log10(FDR) and fold enrichment. Specific pathways like TNF signaling and IL-17 signaling were visualized separately with red rectangles highlighting key hub genes to emphasize their central roles in inflammation.

3.16.1.3 Drug-Target-Pathway-Disease Network

To integrate findings into a holistic view, a drug-target-pathway-disease network was constructed using Cytoscape version 3.10.4. CGA was linked to the common genes based on predicted interactions from STITCH and SwissTargetPrediction. Common genes were connected to enriched KEGG pathways based on gene membership from ShinyGO and all pathways were associated with Schizophrenia.

3.16.2 Molecular Docking

To validate the predicted interactions between CGA and the core hub proteins identified from the protein-protein interaction (PPI) network, molecular docking studies were performed on the six most prominent hub targets: AKT1, CASP3, IL1β, IL6, NFKB1 and TNF. These proteins were selected on the basis of their high centrality scores across Degree, Betweenness and Closeness metrics, as well as their critical roles in inflammation, apoptosis and signaling pathways relevant to Schizophrenia.

3.16.2.1 Protein Preparation

The following accession IDs were used to get the target proteins' three-dimensional crystal structures from the Protein Data Bank (PDB): AKT1 (PDB ID: 3CQU), CASP3 (PDB ID: 1RE1), IL1β (PDB ID: 9ILB), IL6 (PDB ID: 1ALU), NFKB1 (PDB ID: 8TQD) and TNF (PDB ID: 2AZ5). The Protein Preparation Wizard in Schrodinger Maestro 13.4 was used to prepare protein structures. Assigning proper bond ordering, optimizing hydrogen bonding networks and inserting missing hydrogen atoms were all part of the preparation procedure. To reduce steric hindrance during docking, water molecules that were more than 5 Åaway from the ligand binding site were eliminated. The OPLS4 force field was then used to reduce the protein structures in order to obtain a stable, energetically favorable conformation.

3.16.3 Ligand Preparation

The PubChem database was used to obtain the three-dimensional structure of CGA (CID: 1794427). The LigPrep module in Schrödinger Maestro 13.4 was used to prepare ligands. The module produced tautomers, stereoisomers and potential ionization states at physiological pH (7.0 $\pm$ 0.5). To find the most stable ligand shape for docking studies, energy reduction was performed using the OPLS4 force field.

3.16.4 Receptor Grid Generation

For each target protein, receptor grids were generated around the predicted active sites or key residue clusters identified from literature and structural analysis using the Receptor Grid Generation module in Schrödinger Maestro. The grid boxes were centered on the coordinates of co-crystallized ligands where available, or on critical residues known to be involved in the protein's biological function. The active site residues and grid coordinates were identified using PrankWeb (Prankweb.cz), a web-based tool for predicting ligand binding sites. The grid framework was set to 20 Å× 20 Å× 20 Åto completely cover the binding pocket while maintaining computational efficiency.

Table 3.5: Grid center coordinates for Molecular Docking

Target Protein	**PDB ID**	**Grid Center Coordinates (X, Y, Z)**
AKT1	3CQU	23.45, 18.92, 31.67
CASP3	1RE1	12.78, -5.34, 45.21
IL1B	9ILB	-18.45, 24.63, 52.19
IL6	1ALU	35.82, -42.16, 28.94
NFKB1	8TQD	-27.54, 16.83, -33.47
TNF	2AZ5	-20.80, 70.95, 37.70

3.16.5 Molecular Docking

Molecular docking was executed using the Glide module in Schrödinger Maestro 13.4 with Standard Precision (SP) mode. This protocol allowed flexible ligand sampling while keeping the protein structure rigid.

The docking algorithm generated multiple poses for each protein-ligand complex, which were ranked based on their GlideScore (docking score expressed in kcal/mol). The top-ranked pose for each complex was selected for further analysis based on the most favorable binding energy and interaction profile.

3.16.6 Interaction Analysis

The best binding conformation for each protein-ligand complex was visualized and analyzed using the Maestro interface. Hydrogen bonds, hydrophobic interactions, π-π stacking, π-cation interactions and other non-covalent contacts were identified and measured. Hydrogen bond lengths were measured in Ångstroms (Å) for all interacting residues. Two-dimensional interaction diagrams were generated to have a comprehensive visualization of the binding mode and key residues involved in stabilizing the CGA-protein complexes.

This *in silico* docking approach provided direct evidence of the binding affinity and interaction modes of CGA with the selected hub targets, supporting the network pharmacology findings and offering mechanistic insights into the potential therapeutic effects of CGA in Schizophrenia.

3.17 Tissue Preparation

Following behavioral assessments on day 15, animals were euthanized on day 15 for collection of brain tissues. Euthanasia was performed via cervical dislocation under controlled conditions to minimize stress and maintain tissue integrity.

The entire brain was taken right away after the skull was properly dissected in order to obtain brain tissue. Under a stereomicroscope, brain areas such as the hippocampus, striatum and prefrontal cortex were dissected on an ice-cold glass plate. To get rid of blood and debris, ice-cold phosphate-buffered saline (PBS, pH 7.4) was used to wash the dissected tissues. Tissue samples intended for biochemical analysis were snap-frozen in liquid nitrogen right away and kept at -80°C until they were processed further. For 48 hours at room temperature, tissues intended for histological examination were preserved in 10% neutral buffered formalin.

Frozen brain tissue was homogenized in ice-cold RIPA buffer (50 mM Tris-HCl, pH 7.4, 150 mM NaCl, 1% NP-40, 0.5% sodium deoxycholate, 0.1% SDS) containing a protease inhibitor cocktail (1:100) for protein extraction. A mechanical

homogenizer operating at 4°C with three 10-second pulses was used for homogenization. After centrifuging the homogenates at 14,000 rpm for 30 minutes at 4°C, the soluble protein-containing supernatant was gathered and kept at -80°C.

3.18 Biochemical Assays

3.18.1 Protein Quantification Using Bicinchoninic Acid Assay

Total protein concentration in hippocampal tissue homogenates was determined using a bicinchoninic acid (BCA) protein assay kit (Beyotime, Cat. No. P0012S, China), following the manufacturer's protocol. This colorimetric method relies on the reduction of $Cu_2{}^+$ to Cu^+ by protein under alkaline conditions, with the resulting Cu^+ ions forming a purple-colored chelate complex with bicinchoninic acid that exhibits strong absorbance at 562 nm.

A standard curve was constructed using bovine serum albumin (BSA) at concentrations of 0, 25, 50, 100, 200, 400, 600, 800 and 1000 μg/mL. The working reagent was prepared by mixing Reagent A and Reagent B in a 50:1 ratio. For each well of a 96-well microplate, 25 μL of standard or sample (in duplicate) was combined with 200 μL of the BCA working reagent.

Plates were gently agitated to ensure thorough mixing, then incubated at 37°C for 30 minutes. After allowing the plates to cool to room temperature, absorbance was measured at 562 nm using a microplate reader (Thermo Fisher Scientific, USA). Protein concentrations (μg/mL) were derived by interpolating sample absorbance values against the standard curve via linear regression. To account for variation in total protein content across samples, cytokine concentrations obtained from ELISA were subsequently normalized using the formula:

$$\text{pg/mg protein} = \left[\frac{\text{Cytokine (pg/ml)}}{\text{Total protein}(\mu g/ml)}\right] \times 1000 \tag{3.7}$$

3.18.2 Enzyme-Linked Immunosorbent Assay for Cytokine Quantification

Commercial sandwich ELISA kits (Biosharp, China) were used to quantitatively analyze pro-inflammatory cytokines (TNF-α and IL-1β) in brain tissue homogenates. Using antibodies coupled to an enzyme, the enzyme-linked immunosorbent assay (ELISA) is a highly specific and sensitive immunological method for identifying and measuring target antigens in biological materials. The sandwich ELISA format uses immobilized capture antibodies on a solid phase (microplate wells) to bind the target antigen. A secondary antibody coupled to horseradish peroxidase (HRP) is then used for detection. A colorimetric signal proportionate to the target antigen's concentration is produced by the enzymatic reaction.

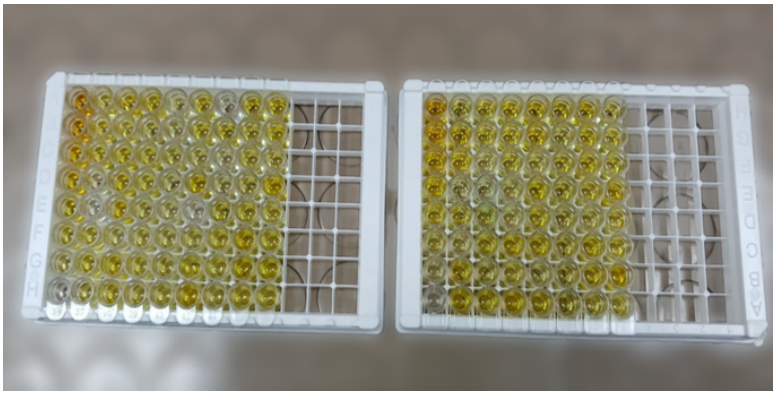

FIGURE 3.7: 96 well plates of ELISA.

(Photography taken at Faculty of Pharmacy, Capital University of Science and Technology, Islamabad).

3.18.2.1 Reagent Preparation

Before being used, all of the reagents were allowed to come to room temperature. To make 1× wash buffer, wash buffer (20× concentrate) was diluted with distilled water. The manufacturer's instructions were followed in the reconstitution of standards. To obtain the greatest standard concentration, lyophilized standards were reconstituted with standard diluent after being quickly centrifuged to collect contents from the bottom of the vial. A standard curve ranging from 0 to 1000 pg/mL for TNF-α and 0 to 500 pg/mL for IL-1β was obtained through serial

dilutions. To make sure quantities fell within the detectable range of the standard curve, tissue homogenate samples were diluted 1:2 with sample diluent, which was produced as specified.

3.18.2.2 Assay Procedure

The Biosharp Mouse TNF-α ELISA Kit (Cat. No. BSEM-004-96T) and Biosharp Mouse IL-1β ELISA Kit (Cat. No. BSEM-015-96T) were used in the ELISA method in accordance with the manufacturer's instructions. Monoclonal capture antibodies specific to mouse TNF-α or IL-1β were pre-coated in 96-well microplates for the experiment. To guarantee precision and repeatability, every sample and standard was run twice.

The selected wells were filled with 50 μL of each standard, sample, or control. The plate was incubated at 37 °C for 30 minutes to facilitate antigen-antibody binding after being gently tapped to ensure adequate mixing. Following incubation, an automated microplate washer was used to aspirate the plate and wash it five times with 300 μL of wash buffer in order to fully remove all unbound materials.

After adding 50 microliters of HRP-conjugated detection antibody to each well, the plate was incubated for 30 minutes at 37 °C. By binding to the trapped antigen, the detecting antibody was able to create a sandwich complex. After incubation, excess detection antibody was removed by aspirating the plate and washing it five times with 300 μL of wash buffer.

Each well received 50 μL of chromogen solution A (containing hydrogen peroxide) and 50 μL of chromogen solution B (containing tetramethylbenzidine, TMB) for color development. The HRP enzyme catalyzed the oxidation of TMB to create a blue-colored product after the plate was gently stirred and incubated for 15 minutes at 37 °C in the dark. The color changed from blue to yellow when 50 μL of stop solution (2 M H_2SO_4) was added to cease the enzymatic process. A Thermo Scientific Multiskan FC microplate reader was used to measure the optical density at 450 nm.

This procedure was strictly followed for both TNF-α and IL-1β assays to ensure consistent and reliable quantification of cytokine levels in hippocampal tissue.

3.18.2.3 Absorbance Measurement and Quantification

Absorbance readings were taken at 450 nm using a microplate reader, 15 minutes following the addition of the stop solution. A standard curve was generated by plotting the mean absorbance values of the standards against their respective known concentrations. The equation of the line and correlation coefficient (R2) were obtained using linear regression analysis. By interpolating absorbance values from the standard curve, sample concentrations were determined. The total protein content ascertained by the BCA assay was used to normalize the final cytokine values.

3.18.2.4 Quality Control

All assays were performed in duplicate and the coefficient of variation between replicates was maintained below 10%. Blank wells containing only sample diluent were included to get baseline results. Standard curves with R^2 values ≥ 0.99 were considered acceptable for quantification.

3.19 Histopathological Evaluation

Histopathological assessment was conducted on hippocampal tissue to evaluate alterations in neuronal architecture and morphology resulting from ketamine-induced schizophrenia-like pathology, as well as the impact of CGA treatment. Following collection, brain tissues were fixed for 48 hours in 10% neutral buffered formalin and subsequently subjected to paraffin processing. This involved dehydration through a graded ethanol series (70%, 80%, 95% and 100%), clearing in xylene and infiltration with molten paraffin prior to embedding into paraffin

blocks. Using a rotary microtome, coronal sections measuring 5 μm in thickness were obtained, transferred onto glass slides and allowed to dry overnight at 37°C.

For hematoxylin and eosin (H&E) staining, slides underwent deparaffinization in xylene followed by rehydration through a descending ethanol gradient and rinsing in distilled water. Nuclei were stained by immersion in Harris's hematoxylin for 5-7 minutes, after which slides were rinsed under running tap water.

A brief differentiation step was performed using 1% acid alcohol for 2-3 seconds and nuclear bluing was achieved with 0.2% ammonia water. Cytoplasmic counter-staining was subsequently carried out using 1% eosin Y for 30-60 seconds. Slides were then dehydrated through an ascending ethanol series, cleared in xylene and coverslipped using a permanent mounting medium.

Examination of stained sections was performed under light microscopy at 10× and 40× magnification, with particular attention given to the CA1 subregion of the hippocampus. Evaluation parameters included general neuronal morphology, the presence of pyknotic nuclei, vacuolar changes, neuronal loss and indicators of glial activation. Representative photomicrographs were obtained from each experimental group for subsequent documentation and comparative histological analysis.

3.20 Statistical Analysis

All experimental data were analyzed using GraphPad Prism version 8.0 (GraphPad Software, Inc., La Jolla, CA, USA). Data were expressed as mean ± standard error of the mean (SEM) for each experimental group. For behavioral assessments and biochemical parameters one-way ANOVA was used to compare differences among experimental groups. Tukey's post-hoc test was applied for pairwise comparisons between groups. For molecular docking studies, binding affinities (GlideScore) were compared across different protein targets to identify the most favorable interactions.

Statistical significance was set at $p < 0.05$. The following significance levels were used: $^{*}p < 0.05$, $^{**}p < 0.01$ and $^{***}p < 0.001$. All experiments were conducted with $n = 6$ animals per group for behavioral and biochemical analyses. Data were analyzed under blinded conditions, where the investigator performing the analysis was unaware of group allocations to minimize bias.

Chapter 4

Results

4.1 Behavioural Assessment

The behavioural tests were conducted on day 14 and 15 of the experimental protocol to evaluate the neuroprotective effects of CGA against ketamine-induced Schizophrenia-like behavioural deficits in mice. Four validated tests were performed: the OFT to assess locomotor activity and anxiety-like behaviour, the SIT to evaluate social withdrawal, the Y-Maze Test to measure spatial working memory and the FST to assess depressive-like behaviour. All parameters are expressed as mean ± standard deviation (n = 6 per group). Ketamine (30 mg/kg, i.p., daily for 15 days) was used to induce Schizophrenia-like symptoms. CGA was administered at three doses (10, 50 and 100 mg/kg, i.p.) while haloperidol (1 mg/kg, i.p.) served as the positive control.

4.1.1 Effect of CGA on Hyperactivity and Locomotor Activity in OFT

Ketamine administration produced a marked increase in distance travelled (1698.33 ± 47.92 cm) compared to the normal saline control group (853.33 ± 51.64 cm) (p

< 0.001), indicating pronounced hyperlocomotion, a positive symptom analogue of Schizophrenia.

Haloperidol (1 mg/kg) significantly reversed ketamine-induced hyperactivity, reducing distance travelled to 941.67 ± 50.37 cm ($P < 0.001$ vs ketamine group). CGA treatment exhibited a clear dose-dependent protective effect. The lowest dose of CGA (10 mg/kg) produced the most robust improvement, decreasing distance travelled to 978.33 ± 50.80 cm ($P < 0.001$ vs ketamine group) and restoring rearing (23.50 ± 0.50), grooming (2.00 ± 0.58), central entries (7.17 ± 0.69) and time spent in the centre (7.00 ± 0.82 s) close to control values. The higher doses (50 mg/kg and 100 mg/kg) also attenuated hyperactivity but were comparatively less effective than the 10 mg/kg dose, suggesting an optimal therapeutic window at the lowest tested concentration. These findings demonstrate that CGA, particularly at 10 mg/kg, effectively ameliorated ketamine-induced hyperlocomotion and anxiety-like behaviour in the OFT.

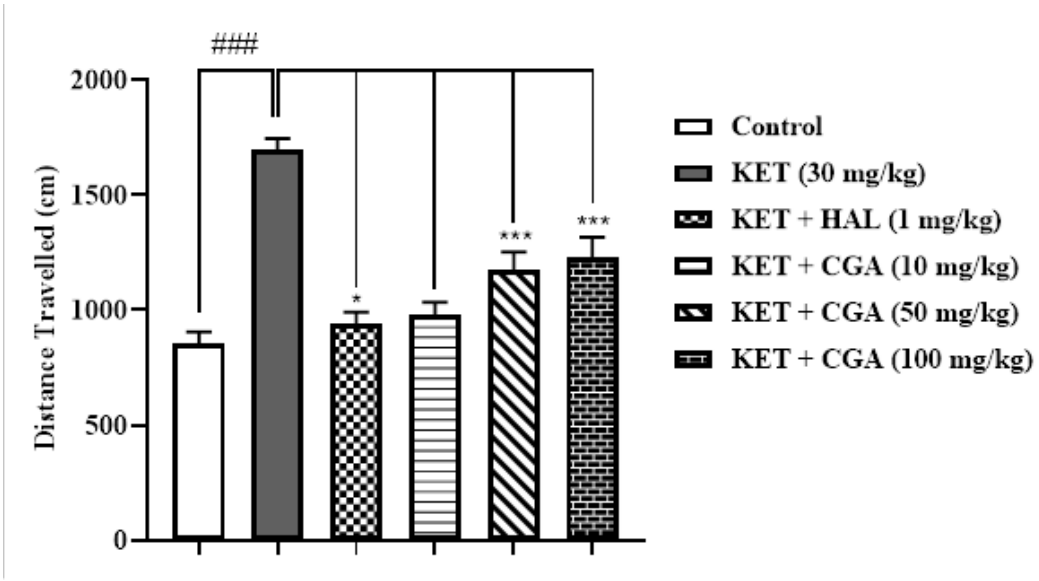

FIGURE 4.1: Effects of CGA on distance travelled in the center in the OFT

The above figure shows bar graphs representing locomotor activity parameters in the OFT. Ketamine (30 mg/kg) significantly increased distance travelled compared to the normal saline control. Pretreatment with haloperidol (1 mg/kg) and CGA (10, 50 and 100 mg/kg) dose-dependently reversed these changes, with the 10 mg/kg dose of CGA showing the strongest recovery, comparable to haloperidol.

Data are expressed as mean ± SD (n = 6). Statistical significance: * $p < 0.05$, ***$p < 0.001$ vs ketamine group; ### $p < 0.001$ vs control group.

4.1.2 Effect of CGA on Social Withdrawal in SIT

Ketamine treatment caused a severe reduction in % social preference (27.65 ± 3.67 %) compared to the control group (68.73 ± 2.81 %) ($p < 0.001$), indicating prominent social withdrawal, a core negative symptom of Schizophrenia.

Haloperidol restored social preference to 63.39 ± 1.20 % ($p < 0.001$ vs ketamine group). CGA treatment produced a dose-dependent recovery of social behaviour. The 10 mg/kg dose showed the most significant improvement (59.65 ± 1.68 %, $p < 0.001$ vs ketamine group), bringing social interaction levels closest to the control group. The 50 mg/kg and 100 mg/kg doses also improved social preference but to a lesser extent (46.96 ± 2.81 % and 43.92 ± 4.52 %, respectively). These results highlight the strong ability of CGA, especially at the 10 mg/kg dose, to reverse ketamine-induced social deficits in mice.

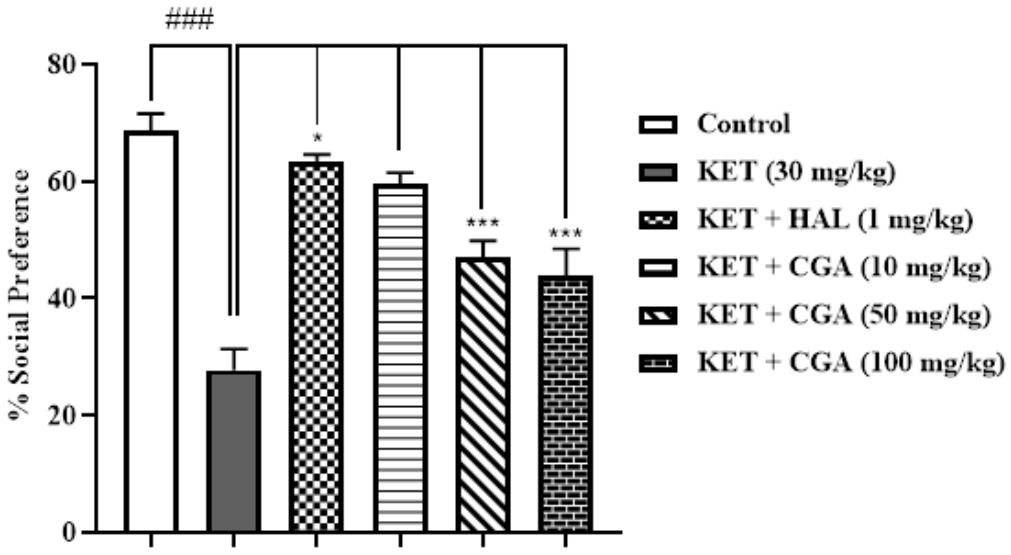

FIGURE 4.2: Effects of CGA on % social preference in the SIT

The above figure illustrates bar graphs of % social preference. Ketamine significantly decreased social interaction compared to control. Haloperidol and CGA pretreatment significantly improved social behaviour in a dose-dependent manner,

with the 10 mg/kg dose of CGA showing near-complete restoration. Data are expressed as mean ± SD (n = 6). Statistical significance: * $p < 0.05$, *** $p < 0.001$ vs ketamine group; ### $p < 0.001$ vs control group.

4.1.3 Effect of CGA on Spatial Working Memory Deficit in Y-Maze Test

Ketamine significantly impaired spatial working memory, reducing the percentage of correct alterations to 38.83 ± 2.93 % compared to the control group (67.40 ± 2.65 %) ($p < 0.001$).

Haloperidol improved performance to 64.00 ± 2.10 % ($p < 0.001$ vs ketamine group). CGA treatment restored memory function in a dose-dependent manner. The 10 mg/kg dose produced the best recovery (62.67 ± 1.97 %, $p < 0.001$ vs ketamine group), nearly reaching control levels. The 50 mg/kg and 100 mg/kg doses also improved alternation behaviour but were less effective than the lowest dose. These data confirm that CGA, particularly at 10 mg/kg, effectively reversed ketamine-induced spatial working memory deficits.

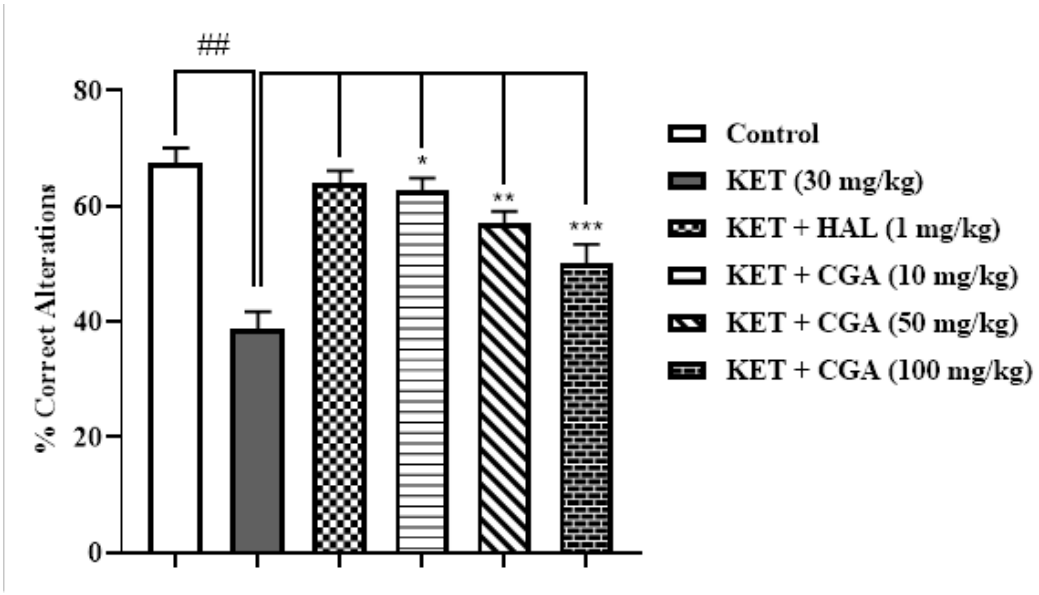

FIGURE 4.3: Effects of CGA on % correct alterations in the Y-Maze Test

The above figure presents bar graphs of % correct alterations. Ketamine caused a significant decline in spontaneous alternation. Haloperidol and CGA (especially

at 10 mg/kg) significantly reversed this deficit. Data are expressed as mean ± SD (n = 6). Statistical significance: * $p < 0.05$, ** $p < 0.01$, *** $p < 0.001$ vs ketamine group; ## $p < 0.01$ vs control group.

4.1.4 Effect of CGA on Depressive-Like Behaviour in FST

Ketamine treatment significantly increased % immobility time to 69.89 ± 1.11 % compared to the control group (26.72 ± 1.04 %) ($p < 0.001$), reflecting depressive-like behaviour.

Haloperidol reduced immobility time to 30.39 ± 1.06 % ($p < 0.001$ vs ketamine group). CGA exhibited strong antidepressant-like activity. The 10 mg/kg dose produced the most significant reduction in immobility (35.22 ± 0.76 %, $p < 0.001$ vs ketamine group), followed by 50 mg/kg (43.06 ± 3.24 %) and 100 mg/kg (52.01 ± 3.17 %). The 10 mg/kg dose brought immobility time closest to control values. These results demonstrate the potent ability of CGA, especially at the lowest dose, to ameliorate ketamine-induced despair-like behaviour.

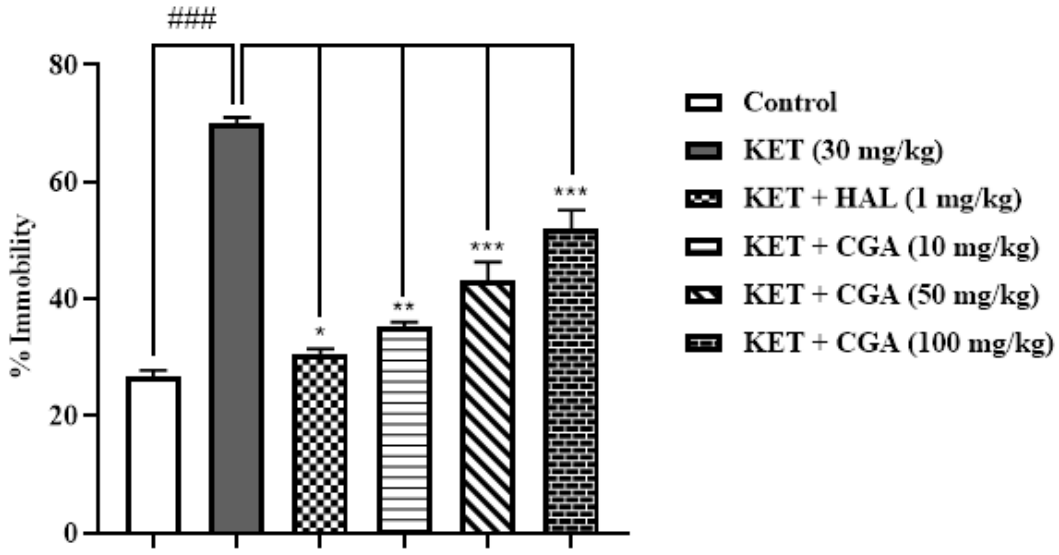

FIGURE 4.4: Effects of CGA on % immobility time in the FST

The above figure shows bar graphs of % immobility time. Ketamine markedly increased immobility, indicating depressive-like behaviour. Haloperidol and CGA pretreatment significantly decreased immobility time, with the 10 mg/kg dose of

CGA demonstrating the strongest effect. Data are expressed as mean ± SD (n = 6). Statistical significance: * $p < 0.05$, ** $p < 0.01$, *** $p < 0.001$ vs ketamine group; ### $p < 0.001$ vs control group.

Overall, the behavioural data clearly demonstrate that CGA at 10 mg/kg exhibited the most consistent and potent protective effects across all four tests.

This dose outperformed both higher CGA doses and showed comparable or superior efficacy to the standard antipsychotic haloperidol, strongly supporting its therapeutic potential against positive, negative and cognitive symptoms of schizophrenia.

4.2 Effects of CGA on Pro-Inflammatory Cytokines Expression in Brain Tissues Assessed by ELISA

Before performing ELISA, total protein concentration in lysates from hippocampus, prefrontal PFC and striatum was determined by the BCA assay to ensure equal protein loading across all samples and brain regions.

The BCA assay revealed that ketamine caused a marked reduction in total protein content across the three brain regions compared to the normal saline control, consistent with neurodegeneration and synaptic impairment. Haloperidol provided good recovery of protein levels.

CGA treatment showed dose-dependent preservation of protein content, with the 10 mg/kg dose achieving recovery comparable to haloperidol in most regions, while the higher doses (50 and 100 mg/kg) offered moderate protection.

Cytokine levels were normalized to total protein concentration and expressed as pg/mg protein to account for variations in tissue protein content due to neurodegeneration.

TABLE 4.1: Total protein concentration in different brain regions of mice determined by BCA assay.

Group	**Hippocampus (μg/ml)**	**Prefrontal Cortex (μg/ml)**	**Striatum (μg/ml)**	**Interpretation**
Control	10.12 – 17.75	9.80 – 16.50	11.20 – 18.30	Normal protein integrity across key brain regions
Ketamine (30 mg/kg)	7.24 – 10.30	6.50 – 9.80	7.80 – 11.20	Marked protein loss due to neurodegeneration and synaptic impairment
Haloperidol (1 mg/kg)	10.40 – 13.73	9.50 – 14.20	10.80 – 15.60	Good recovery via antipsychotic action
CGA (10 mg/kg)	9.80 – 15.40	9.20 – 13.80	10.10 – 14.90	Moderate to good dose-dependent protection; comparable to haloperidol in most regions
CGA (50 mg/kg)	8.50 – 14.20	8.10 – 12.70	9.30 – 13.50	Moderate protection
CGA (100 mg/kg)	8.20 – 13.90	7.90 – 12.40	9.00 – 13.10	Moderate protection

4.2.1 Tumor Necrosis Factor Alpha

Ketamine administration caused a dramatic elevation in brains TNF-α levels compared to the normal saline control group ($p < 0.001$), confirming the establishment of a strong neuroinflammatory response consistent with Schizophrenia pathophysiology.

Haloperidol treatment significantly attenuated this elevation ($p < 0.001$ vs ketamine group). CGA treatment exhibited a clear dose-dependent anti - inflammatory effect. The 10 mg/kg dose produced the most pronounced reduction in TNF-α ($p < 0.001$ vs ketamine group), restoring levels almost to those of the control group. The 50 mg/kg and 100 mg/kg doses also reduced TNF-α ($p < 0.001$ vs ketamine group) but were comparatively less effective than the lowest dose. These results indicate that CGA exerts potent TNF-α suppressive activity, with

the 10 mg/kg dose demonstrating optimal anti - inflammatory potency in the all of three regions of brain.

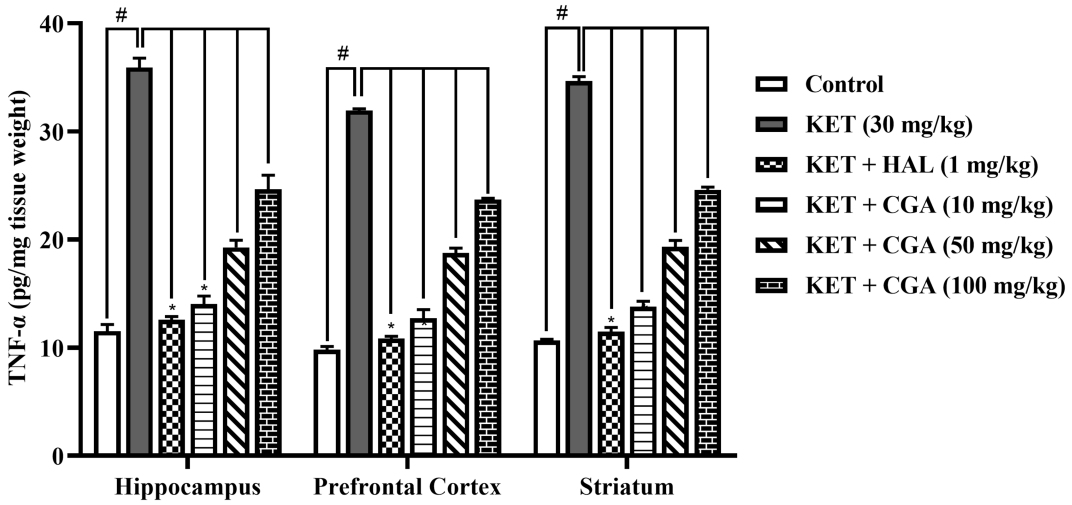

FIGURE 4.5: Effects of CGA on brain tissues TNF-α levels measured by ELISA

The above figure presents levels of TNF-α concentrations (pg/mg) in brain tissues. Ketamine (30 mg/kg) markedly elevated TNF-α levels compared to the normal saline control. Pretreatment with haloperidol (1 mg/kg) and CGA (10, 50 and 100 mg/kg) significantly reduced TNF-α in a dose-dependent manner, with the 10 mg/kg dose of CGA showing the strongest suppression, nearly restoring levels to control values. Data are expressed as mean $\pm$ SD (n = 6). Statistical significance: $^{*}p < 0.05$ vs ketamine group; #$p < 0.05$ vs control group.

4.2.2 Interleukin-1 Beta

Ketamine induced a substantial increase in IL-1β levels compared to the control group ($p < 0.001$), further validating the neuroinflammatory state and its contribution to cognitive and emotional impairments in the model.

Haloperidol significantly lowered IL-1β ($p < 0.001$ vs ketamine group). CGA treatment again demonstrated a clear dose-dependent reduction. The 10 mg/kg dose exhibited the most effective suppression ($p < 0.001$ vs ketamine group), bringing IL-1β levels statistically indistinguishable from the control group. The

50 mg/kg and 100 mg/kg doses also reduced IL-1β ($p < 0.001$ vs ketamine group) but showed diminishing returns compared to the lowest dose. These findings highlight the superior anti-IL-1β activity of CGA at the 10 mg/kg dose.

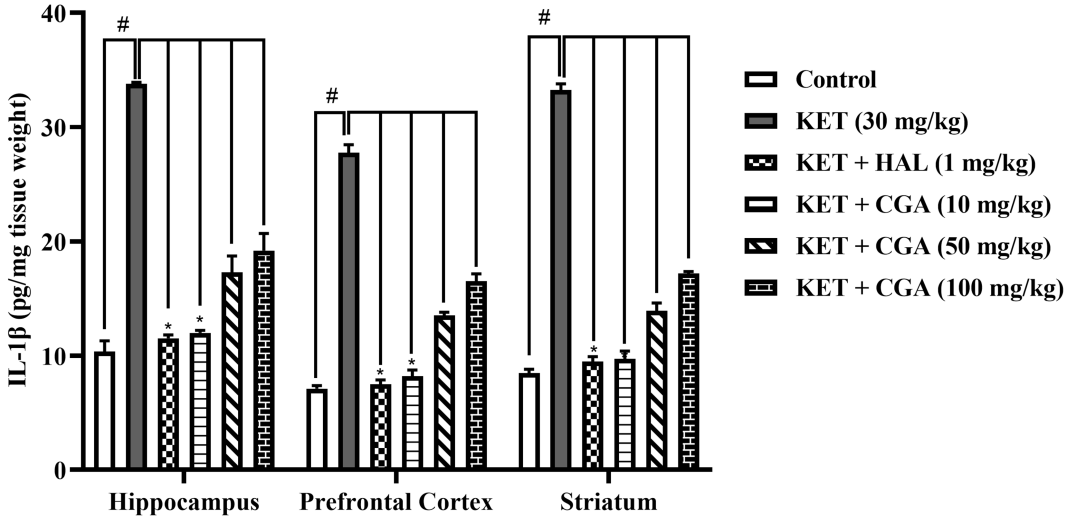

FIGURE 4.6: Effects of CGA on brain tissues IL-1β levels measured by ELISA

The above figure shows bar graphs of IL-1β concentrations (pg/mg) in brain tissues. Ketamine (30 mg/kg) significantly increased IL-1β levels compared to the normal saline control. Haloperidol (1 mg/kg) and CGA (10, 50 and 100 mg/kg) pretreatment significantly attenuated this elevation in a dose-dependent manner, with the 10 mg/kg dose of CGA demonstrating the most effective reduction, comparable to haloperidol and nearly matching control values. Data are expressed as mean $\pm$ SD ($n = 6$). Statistical significance: $^{*}p < 0.05$ vs ketamine group; $\#p < 0.05$, vs control group.

Collectively, the ELISA results demonstrate that CGA exerts robust anti - inflammatory effects in the hippocampus by significantly suppressing both TNF-α and IL-1β. The 10 mg/kg dose consistently produced the strongest cytokine reduction, closely mirroring the efficacy of haloperidol. This potent downregulation of pro-inflammatory cytokines, together with preserved protein content across hippocampus, PFC and striatum, provides a mechanistic basis for the behavioural improvements observed in the OFT, SIT, Y-Maze and FST, supporting CGA's neuroprotective and anti-schizophrenic potential through modulation of neuroinflammation.

4.3 Effects of CGA on Neuronal Survival and Histopathological Changes Assessed by Hematoxylin and Eosin Staining

Histopathological evaluation using hematoxylin and eosin (H&E) staining was performed on coronal sections of prefrontal cortex (PFC), hippocampus and striatum to assess the neuroprotective potential of CGA on ketamine-induced neuronal damage. These three brain regions are critically implicated in Schizophrenia pathophysiology: the PFC and hippocampus regulate cognition, working memory and emotional processing, while the striatum is involved in positive symptoms and motor abnormalities. Ketamine (30 mg/kg, i.p., daily for 14 days) was used to induce Schizophrenia-like neurodegeneration. CGA was administered at 10, 50 and 100 mg/kg (i.p.) and haloperidol (1 mg/kg, i.p.) served as the positive control. Sections were examined at 10× magnification.

Ketamine treatment caused severe histopathological alterations across all three regions. In the PFC, there was marked neuronal loss, disorganization of pyramidal cell layers, increased pyknotic (shrunken and darkly stained) nuclei and prominent vacuolation, indicating neurodegeneration and synaptic disruption. In the hippocampus (CA1 and CA3 subfields), similar changes were observed with reduced neuronal density, disrupted layering and numerous pyknotic neurons. The striatum showed neuronal shrinkage, vacuolation and loss of normal cellular architecture.

Haloperidol (1 mg/kg) provided moderate neuroprotection, showing partial restoration of neuronal density, reduced pyknosis and better preservation of cellular layering in PFC, hippocampus and striatum. CGA treatment exhibited clear dose-dependent neuroprotective effects. The 10 mg/kg dose demonstrated the most pronounced preservation of neuronal architecture in all three regions, with minimal pyknosis, restored cell density and nearly normal layering, comparable to or slightly better than haloperidol. The 50 mg/kg and 100 mg/kg doses offered moderate protection but were less effective than the 10 mg/kg dose, with some residual

vacuolation and pyknotic neurons still visible. These histopathological findings directly correlate with the behavioural improvements and reduced cytokine levels observed earlier, confirming that CGA, particularly at 10 mg/kg, exerts strong neuroprotective effects by preventing ketamine-induced neuronal damage in key Schizophrenia-related brain regions.

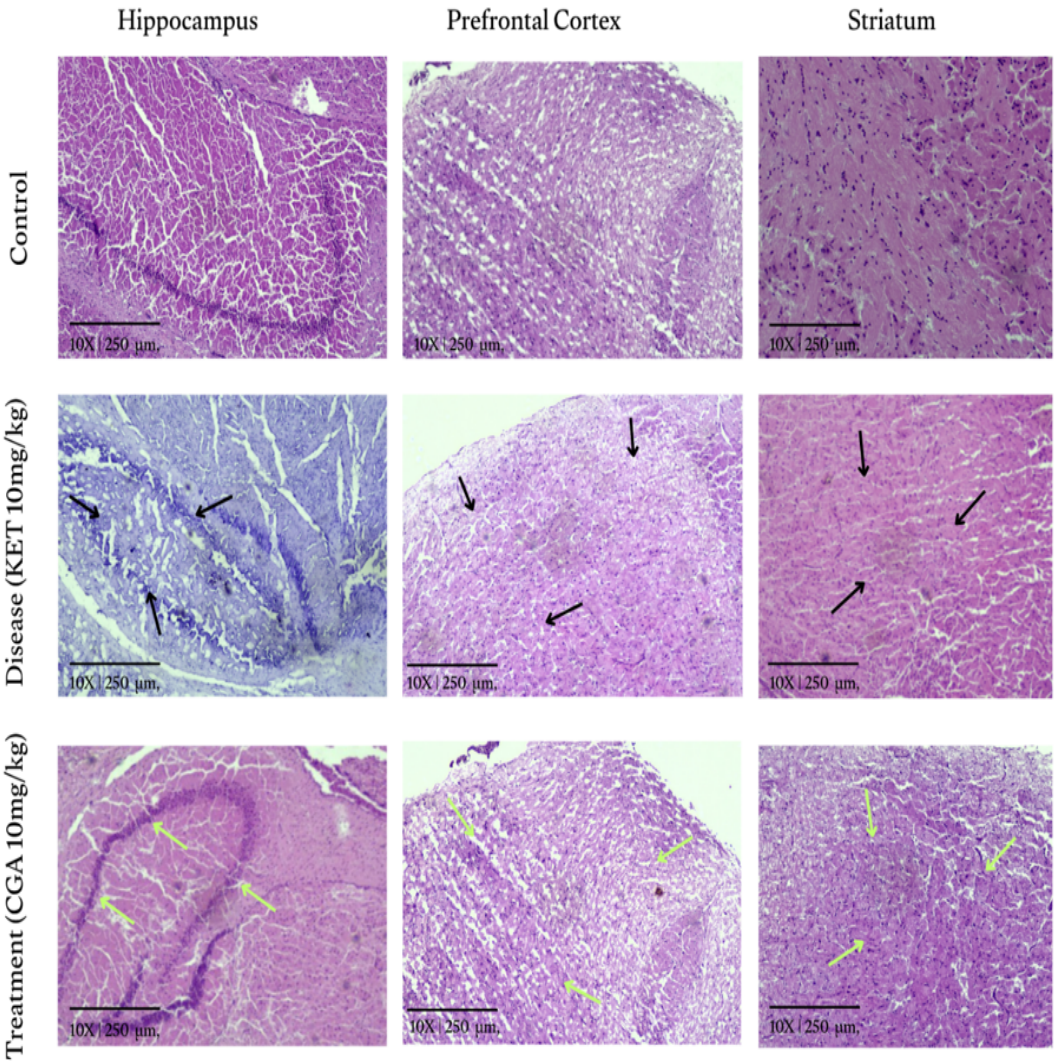

FIGURE 4.7: Representative photomicrographs of H&E-stained sections from prefrontal cortex, hippocampus and striatum

The above figure shows H&E-stained coronal sections (10× magnification) from prefrontal cortex (PFC), hippocampus (CA1 and CA3 region) and striatum across treatment groups. Ketamine (30 mg/kg) induced severe neuronal loss, pyknosis (black arrows) and disrupted layering compared to normal saline control. CGA pretreatment showed dose-dependent neuroprotection, with the 10 mg/kg dose of

CGA providing the best preservation of neuronal density and architecture represented by yellow arrows.

Overall, the H&E staining results demonstrate that CGA exerts robust neuroprotective effects against ketamine-induced neuronal damage in the PFC, hippocampus and striatum. The 10 mg/kg dose consistently provided the strongest preservation of neuronal integrity, supporting its therapeutic potential in mitigating the neuropathological changes associated with Schizophrenia.

4.4 *In Silico* Studies

4.4.1 Network Pharmacology

4.4.1.1 Potential Targets of CGA and Schizophrenia - Associated Genes

CGA target prediction yielded 277 unique proteins, primarily associated with antioxidant defense, anti-inflammatory actions, enzyme inhibition, receptor signaling and metabolic regulation pathways, reflecting CGA's broad polyphenolic bioactivity suitable for multi-target intervention in complex disorders. Schizophrenia gene collection from OMIM and Gene Cards produced 15,142 unique entries, encompassing a wide array of genetic factors linked to neurodevelopment, synaptic transmission, immune regulation, neurotransmitter systems and inflammatory processes. Venn diagram analysis using Venny 2.1 revealed 196 overlapping targets between the two sets, representing a substantial intersection point where CGA may exert therapeutic influence on Schizophrenia pathology through shared molecular interfaces.

4.4.1.2 Venn Diagram Analysis

The Venn diagram (Figure 4.8) illustrates the distribution as follows: 277 targets specific to CGA (left circle), 15,142 genes associated with Schizophrenia (right

circle) and 196 targets shared between both datasets (central overlap). This extensive overlap suggests that CGA possesses considerable potential to modulate a large portion of Schizophrenia-related molecular pathways, particularly those involving neuroinflammation, oxidative stress, synaptic dysfunction and disrupted signaling cascades, thereby supporting its role as a promising multi-target natural agent for addressing the disorder's heterogeneous and polygenic etiology.

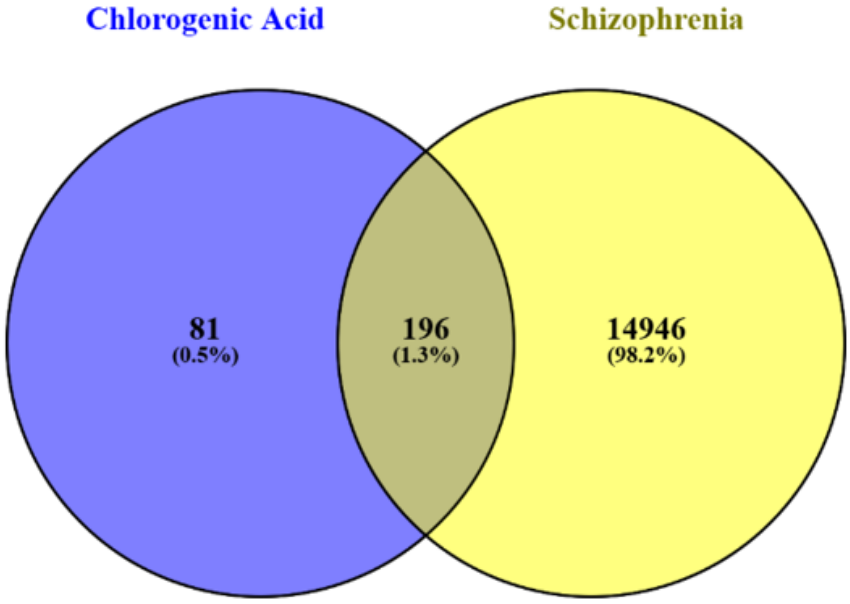

FIGURE 4.8: Venn diagram

The figure illustrating the intersection of CGA predicted targets (277 from STITCH and SwissTargetPrediction) and Schizophrenia-associated genes (15,142 from OMIM and GeneCards). The overlapping region contains 196 common targets identified as potential key molecules for CGA's therapeutic effects in Schizophrenia.

4.4.1.3 Protein-Protein Interaction Network

The PPI network derived from the 196 common targets, after processing in STRING and visualization in Cytoscape, exhibited extensive connectivity and modular organization, reflecting dense clustering around critical biological themes (Figure 4.9). These include inflammatory signaling, apoptosis regulation, extracellular

matrix remodeling, immune response modulation and cell survival pathways processes fundamentally implicated in Schizophrenia's etiology, including synaptic pruning abnormalities, neuronal apoptosis, chronic neuroinflammation and disrupted neuroplasticity.

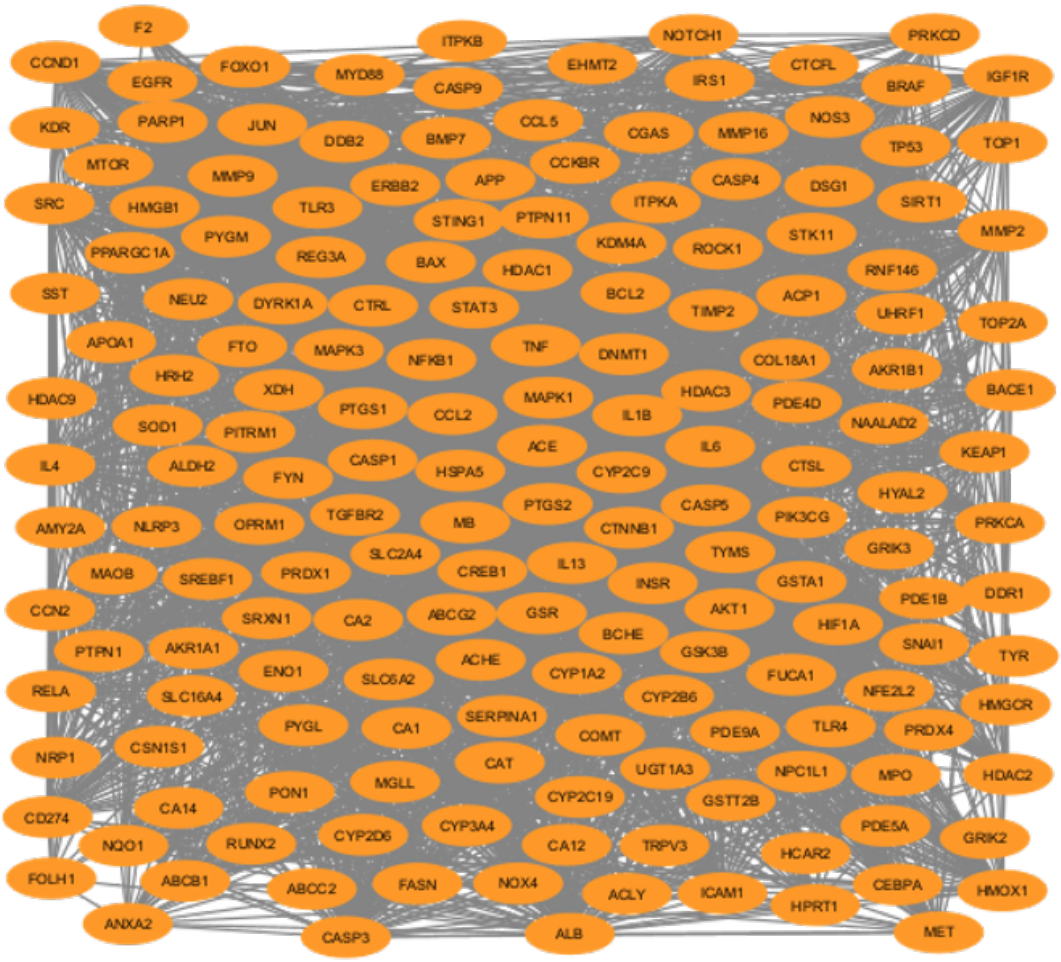

FIGURE 4.9: Protein-protein interaction (PPI) network

Protein-protein interaction (PPI) network constructed from the 196 common targets using STRING database (confidence $\geq$0.4, Homo sapiens) and visualized in Cytoscape version 3.10.4. Nodes represent proteins; edges represent predicted interactions. The network comprises 179 nodes and 3256 edges, showing high connectivity and modular clustering among targets relevant to Schizophrenia pathology.

The topological analysis (Table 4.2) revealed very high average connectivity (average number of neighbors: 36.380), indicating that each protein interacts with

more than 36 others on average, facilitating extremely efficient information flow and broad propagation of effects across the network. The network diameter of 7 and radius of 1 suggest a relatively compact yet expansive structure, with the longest shortest path between any two nodes being 7 steps and a highly centralized core (radius 1). The characteristic path length of 1.929 confirms small-world properties, enabling rapid signal/perturbation transmission, which could significantly amplify CGA's therapeutic impact when targeting central nodes.

A clustering coefficient of 0.313 indicates moderate local clustering (higher than random networks but not excessively redundant), while the network density reflects a relatively dense but still biologically realistic interactome. The presence of a single connected component (1) demonstrates a fully integrated, cohesive network without isolated subgraphs, with no multi-edge pairs or self-loops, ensuring a clean interaction map.

Overall, this topology positions the network as highly interconnected and resilient, yet highly amenable to modulation by CGA at key hubs to restore balance in schizophrenia's disrupted molecular landscape.

TABLE 4.2: Summary statistics of the PPI network.

Statistic	**Value**
Number of nodes	179
Number of edges	3256
Avg. number of neighbors	36.38
Network diameter	7
Network radius	1
Characteristic path length	1.929
Clustering coefficient	0.313
Network density	0.204
Connected components	1
Multi-edge node pairs	0
Number of self-loops	0
Analysis time (sec)	14.721

4.4.1.4 Hub Genes

To pinpoint core regulatory genes within the PPI network, topological analysis was conducted using CytoHubba in Cytoscape. The top 20 hubs were identified separately based on Degree centrality (DC), Betweenness centrality (BC) and Closeness centrality (CC). DC highlights highly connected nodes central to local interactions; BC identifies nodes controlling information flow between modules; and CC emphasizes nodes with short paths to others, facilitating rapid signal propagation.

Intersection analysis of the three top-20 lists revealed 17 common hub genes: AKT1, ALB, BCL2, CASP3, CTNNB1, EGFR, GSK3B, HIF1A, IL1B, IL6, JUN, MMP9, NFKB1, PTGS2, SRC, TNF and TP53 (Figure 4.10). These genes exhibited high centrality scores across metrics, underscoring their pivotal roles in the network (Table 4.3). For instance, IL6 and ALB showed the highest Degree (118), indicating extensive connectivity, while IL6 also had the highest Betweenness (2500.55), suggesting it acts as a key bottleneck in pathway crosstalk. AKT1 demonstrated balanced high scores in all metrics, reflecting its central position in signaling cascades.

Table 4.3: Centrality Metrics for the 17 Common Hub Genes.

Gene	**Degree**	**Closeness**	**Betweenness**
ALB	118	147.833	1355.67
IL6	118	147.833	2500.55
AKT1	116	146.833	1488.73
TP53	114	145.667	1642.19
TNF	112	144.667	827.302
IL1B	105	141	751.105
CASP3	100	138.667	582.359
JUN	98	137.833	721.173
BCL2	97	137.333	442.258
NFKB1	96	136.667	416.375
EGFR	95	136	1356.36
HIF1A	93	135.167	513.671

Table 4.3 continued from previous page

Gene	Degree	Closeness	Betweenness
GSK3B	92	134.5	303.708
CTNNB1	88	132.5	766.482
PTGS2	86	131.5	431.092
SRC	85	131.167	236.66
MMP9	84	130.167	536.445

These hubs are enriched in pathways relevant to Schizophrenia pathophysiology, including cytokine-mediated inflammation (e.g., IL6, TNF, IL1B), apoptosis regulation (e.g., CASP3, BCL2, TP53) and PI3K-Akt/MAPK signaling (e.g., AKT1, GSK3B, JUN). Notably, several overlap with core targets identified for fingolimod and siponimod in Schizophrenia cognition improvement, such as AKT1, TNF, IL6, IL1B, BCL2 and CASP3, implying shared neuroprotective mechanisms via anti-inflammatory and anti-apoptotic effects.

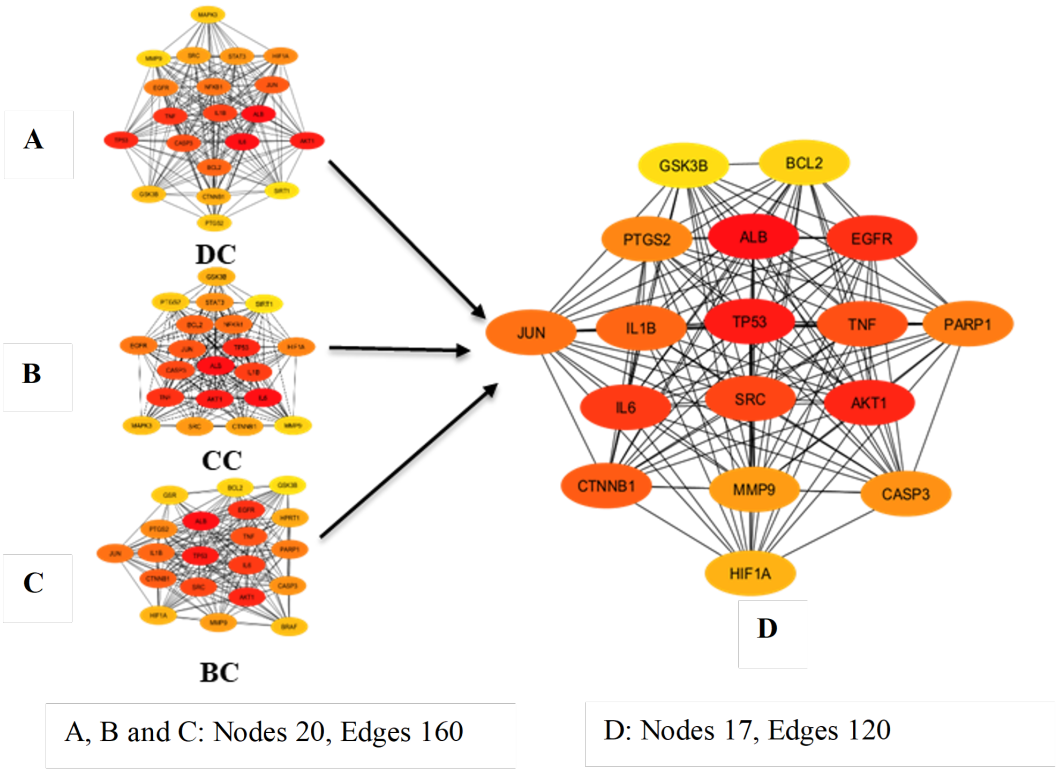

FIGURE 4.10: Multi-centrality topological analysis and identification of core hub genes in the CGA–Schizophrenia PPI network

(A) Top 20 hubs ranked by Degree centrality (DC) - nodes sized/colored by degree (higher connectivity = larger/redder). (B) Top 20 hubs ranked by Closeness centrality (CC) - nodes sized/colored by closeness (global reach). (C) Top 20 hubs ranked by Betweenness centrality (BC) - nodes sized/colored by betweenness (bottleneck/control role). (D) Final core network of the 17 common hub genes (intersection of top 20 from DC, CC and BC): AKT1, ALB, BCL2, CASP3, CTNNB1, EGFR, GSK3B, HIF1A, IL1B, IL6, JUN, MMP9, NFKB1, PTGS2, SRC, TNF, TP53. Nodes sized/colored by Degree; circular layout for clarity. These high-degree hubs represent critical convergence points in the network, where CGA is likely to exert amplified therapeutic effects by modulating inflammation, apoptosis, oxidative stress, immune overactivation and synaptic/ neurodevelopmental pathways disrupted in Schizophrenia. The shift toward highly inflammatory and immune-related hubs (e.g., IL6, TNF, IL1B, NFKB1, TLR4) in this updated analysis aligns with growing evidence of neuroimmune contributions to Schizophrenia pathophysiology, positioning CGA as a potent natural modulator of these central inflammatory networks.

4.4.1.5 Gene Ontology Analysis

GO enrichment analysis was performed on the 196 common overlapping targets using ShinyGO v0.85.1, to identify enriched categories in Biological Processes (BP), Molecular Functions (MF) and Cellular Components (CC). Analyses were conducted separately for each category with default parameters, including Homo sapiens as the species and FDR < 0.05 for significance. Enriched terms were ranked by P-value and visualizations (bar charts and bubble plots) were generated to display fold enrichment, gene count and significance.

The results revealed highly significant functional categories strongly aligned with Schizophrenia mechanisms, with emphasis on inflammation, immune regulation, apoptosis, stress responses and cytokine signaling across all three GO aspects (Figure 4.11A for BP, Figure 4.11B for CC, Figure 4.11C for MF). In Biological

Processes (BP), top terms included response to chemical and external stimuli, regulation of inflammatory response, cytokine-mediated signaling pathway, positive regulation of immune response, apoptotic process, cellular response to stress and response to oxidative stress (Figure 4.11A) directly supporting CGA's potential to suppress neuroinflammatory activation, mitigate cytokine storms, reduce apoptosis in vulnerable neurons and counteract oxidative damage in Schizophrenia brain tissue.

Molecular Functions (MF) emphasized protein binding, cytokine activity, kinase activity, receptor binding, transcription factor binding and enzyme regulator activity (Figure 4.11C), indicating CGA's capacity for direct molecular interactions, pathway crosstalk modulation and enzymatic/inflammatory suppression. Cellular Components (CC) were enriched in extracellular region, extracellular space, plasma membrane, receptor complex, cytoplasmic vesicle, nucleus and mitochondrion (Figure 4.11B), highlighting CGA's influence on intercellular communication, extracellular matrix integrity, membrane receptor signaling, intracellular trafficking, nuclear transcription regulation and mitochondrial function (relevant to energy metabolism deficits in Schizophrenia)

Gene Ontology (GO) enrichment analysis of the 196 common overlapping targets performed using ShinyGO v0.77, presented in three panels for Biological Processes (A), Cellular Components (B) and Molecular Functions (C) with FDR < 0.05. Each panel combines a bar chart of top enriched terms ranked by P-value (high -log10(FDR) for significant categories) and a bubble plot showing fold enrichment (x-axis), gene count (bubble size) and significance (color gradient).

(A) Biological Processes (BP) highlights inflammation, cytokine signaling, apoptosis and oxidative stress responses, supporting CGA's anti-inflammatory and neuroprotective effects in Schizophrenia.

(B) Cellular Components (CC) emphasizes extracellular space, plasma membrane and mitochondrion, reflecting CGA's role in signaling and metabolic regulation.

(C) Molecular Functions (MF) features protein binding, cytokine activity and kinase activity, indicating CGA's capacity for direct molecular interactions and

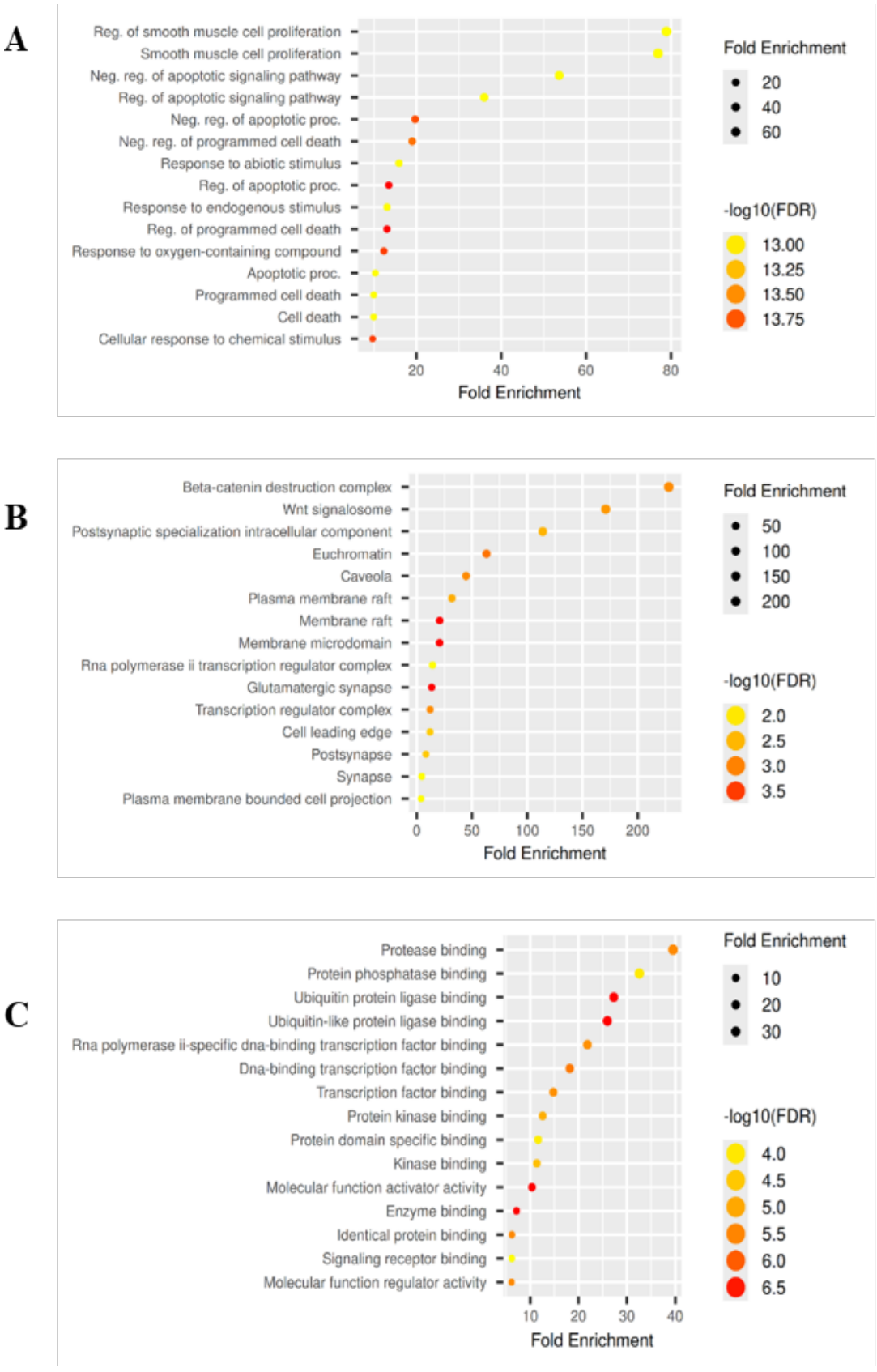

FIGURE 4.11: Gene Ontology (GO) enrichment analysis

pathway modulation. Together, these panels illustrate the 196 targets as an inflammation- and apoptosis-centric functional module central to CGA's therapeutic potential in Schizophrenia.

4.4.1.6 KEGG Pathway Enrichment Analysis

KEGG pathway enrichment analysis was performed on the 196 common overlapping targets using ShinyGO v0.85.1 to uncover multi-pathway mechanisms. The analysis focused on pathways with FDR < 0.05, ranked by P-value and the top 15 pathways were selected for reporting. Visualizations, including bar charts and bubble plots, were created using ShinyGO to display enrichment metrics.

The results showed a strong emphasis on pathways related to inflammation, immune dysregulation, atherosclerosis-like processes, apoptosis and viral infection signaling, which are highly relevant to Schizophrenia's pathophysiology, including neuroinflammation, cytokine dysregulation and apoptotic neuronal loss (Figure 4.12).

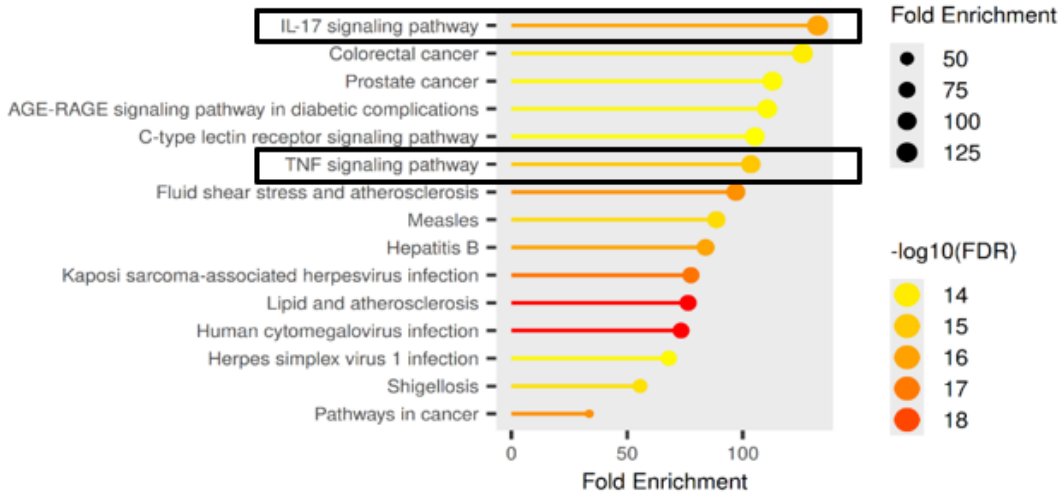

FIGURE 4.12: Bubble plot of KEGG pathway enrichment

Bubble plot of KEGG pathway enrichment for the 15 common overlapping targets using ShinyGO v0.85.1. Bubble size represents gene count, color indicates significance and x-axis shows fold enrichment. The plot emphasizes the predominance of inflammatory (e.g., TNF, IL-17) and apoptosis pathways, illustrating CGA's multi-pathway intervention in Schizophrenia.

Top pathways such as lipid and atherosclerosis (fold 31.03, high significance) and human cytomegalovirus infection (fold 29.53) reflect CGA's potential to modulate inflammatory and immune-mediated processes. The TNF signaling pathway (fold 42.25) and IL-17 signaling pathway (fold 52.92) are particularly prominent, with interconnected hubs driving cytokine activation and immune amplification CGA's known suppression of these pathways supports its anti-inflammatory role in Schizophrenia.

TABLE 4.4: The top 15 enriched KEGG pathways (FDR <0.05)

Pathway	**Count**	**P-Value**	**FDR**	**Fold Enrichment**
Lipid and atherosclerosis	12	2.56E-15	1.49E-13	31.03
Human cytomegalovirus infection	12	4.46E-15	1.49E-13	29.53
Kaposi sarcoma-associated herpesvirus infection	11	8.03E-14	1.79E-12	31.35
Fluid shear stress and atherosclerosis	10	3.03E-13	5.08E-12	39.34
IL-17 signaling pathway	9	8.96E-13	1.20E-11	52.92
Hepatitis B	10	1.07E-12	1.20E-11	34.27
Pathways in cancer	13	1.28E-12	1.23E-11	13.62
TNF signaling pathway	9	5.68E-12	4.76E-11	42.25
Measles	9	2.01E-11	1.49E-10	36.17
Colorectal cancer	8	4.54E-11	3.04E-10	51.36
Shigellosis	10	5.71E-11	3.48E-10	22.08
AGE-RAGE signaling pathway in diabetic complications	8	1.32E-10	7.37E-10	44.24
C-type lectin receptor signaling pathway	8	1.74E-10	8.32E-10	42.56
Herpes simplex virus 1 infection	9	1.84E-10	8.32E-10	27.47
Prostate cancer	8	1.86E-10	8.32E-10	42.16

The enrichment results reveal that the TNF signaling pathway (Figure 4.13) and IL-17 signaling pathway (Figure 4.14) are among the most significantly enriched KEGG pathways in the 196 common targets, with high fold enrichments (42.25 and 52.92, respectively) and strong statistical significance (-log10(FDR) $\approx$ 11 for both). In the TNF pathway, core hub genes such as TNF, NFKB1, IL6, CASP3.

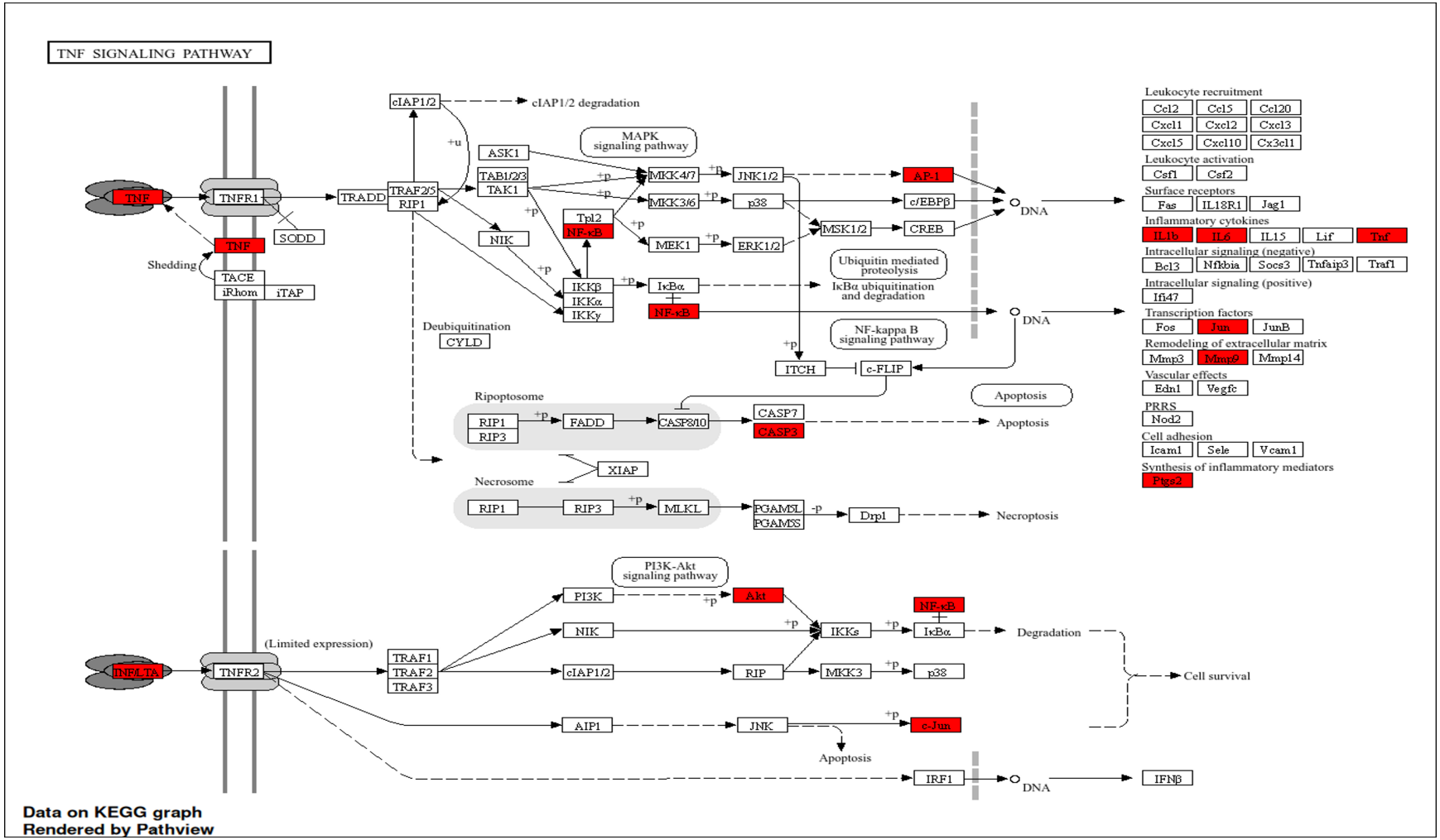

FIGURE 4.13: Specific visualization of TNF signaling pathway from KEGG enrichment using ShinyGO v0.85.1

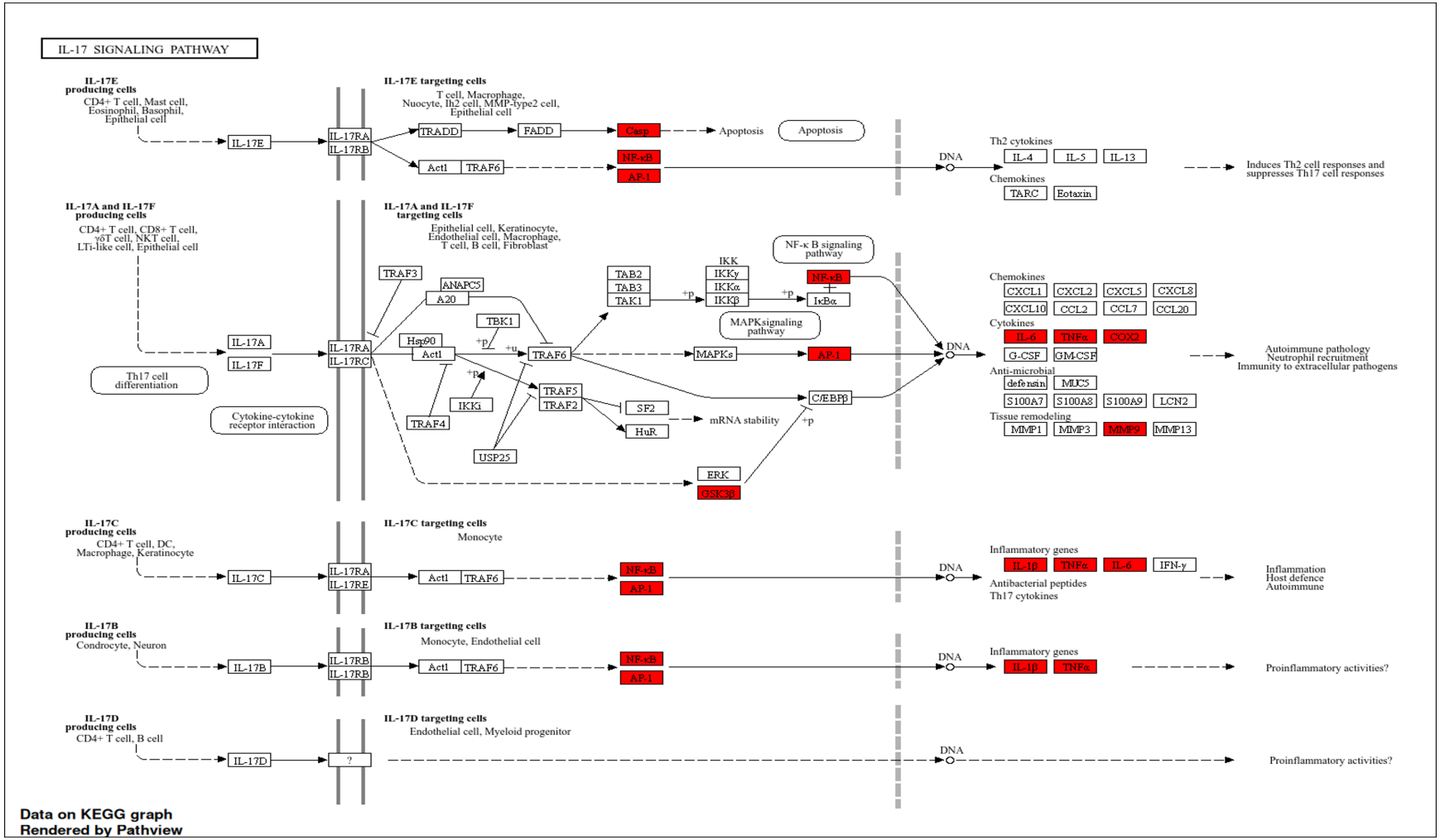

FIGURE 4.14: Specific visualization of IL-17 signaling pathway from KEGG enrichment using ShinyGO v0.85.1

IL1B, JUN, PTGS2 and MAPK1 form a tightly interconnected network driving pro-inflammatory cytokine production, NF-κB activation and apoptosis induction. Red rectangles highlight key hub genes (e.g., TNF, NFKB1, IL6, CASP3), showing their interconnections in cytokine activation and apoptosis. This pathway (-log10(FDR) $\approx$ 11, fold 42.25) relates to CGA's inhibition of TNF-α/NF-κB, mitigating Schizophrenia's neuroinflammation and linking to IL-17 for amplified immune responses. Similarly, the IL-17 pathway centers on IL6, IL1B, TNF, NFKB1, JUN, CASP3, PTGS2 and MAPK1, amplifying cytokine storms and inflammatory crosstalk. These two pathways are highly overlapping through shared hubs (TNF, IL6, NFKB1, IL1B), indicating synergistic inflammatory amplification relevant to Schizophrenia's neuroimmune pathology. CGA's predicted modulation of these central hubs suggests strong potential to suppress TNF-α/NF-κB-driven inflammation and IL-17-mediated immune dysregulation, thereby mitigating neuroinflammation, cytokine imbalance and apoptotic neuronal loss in Schizophrenia. Red rectangles mark core hubs (e.g., IL6, IL1B, TNF, NFKB1), illustrating cytokine amplification and inflammatory crosstalk. With -log10(FDR) $\approx$ 11 and fold 52.92, this pathway interconnects with TNF signaling, supporting CGA's suppression of IL-17-driven neuroimmune dysregulation in Schizophrenia.

4.4.1.7 Drug-Target-Pathway-Disease Network

The drug-target-pathway-disease network integrates CGA, the common genes, top enriched KEGG pathways (e.g., TNF and IL-17 signaling with their interconnections via shared hubs like IL6, TNF, NFKB1) and Schizophrenia, revealing CGA's multi-target action on inflammatory and apoptotic hubs. CGA connects to all genes via predicted bindings, with hubs linking to pathways based on membership (e.g., TNF, IL6 to TNF signaling; IL6, IL1B to IL-17 signaling). Pathways associate with Schizophrenia, highlighting relevance to neuroinflammation and neuroprotection. Core targets (IL6, TNF, AKT1, NFKB1, CASP3, IL1B) are highlighted for their centrality and pathway overlap, explaining differential responses compared to antipsychotics like clozapine.

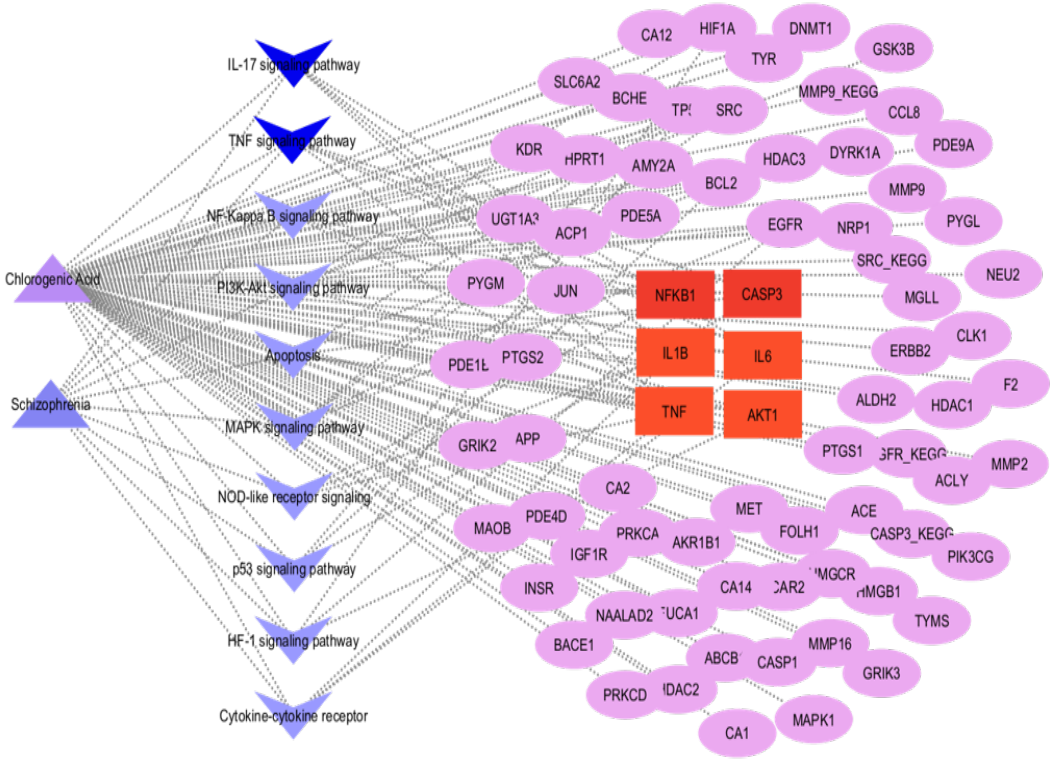

FIGURE 4.15: Drug-target-pathway-disease network for CGA in Schizophrenia, constructed in Cytoscape v3.10.4

CGA links to common genes (blue, core in red), core targets to KEGG pathways (red, with TNF/IL-17 interconnections noted) and pathways to Schizophrenia (inverted triangles). The layout shows CGA's modulation of Schizophrenia via inflammation/apoptosis.

The KEGG pathway enrichment analysis table (Table 4.5) summarizes the top 15 significantly enriched pathways derived from the 196 common overlapping targets, with columns including the pathway ID (e.g., hsa05417 for Lipid and atherosclerosis), Term (full pathway name), Gene Related (list of associated hub genes), Count (number of genes involved) and P Value (statistical significance indicating pathway overrepresentation).

This table highlights the predominance of inflammation, immune dysregulation and apoptosis-related pathways, such as TNF signaling (hsa04668) and IL-17 signaling (hsa04657), which involve key hubs like TNF, IL6, NFKB1 and CASP3, underscoring CGA's potential to modulate neuroinflammatory and apoptotic mechanisms in Schizophrenia through these interconnected routes.

TABLE 4.5: The KEGG pathway enrichment analysis.

ID	Term	Gene Related	Count	P-Value
hsa05417	Lipid and atherosclerosis	AKT1, BCL2, CASP3, EGFR, HIF1A, IL1B, IL6, JUN, MMP9, NFKB1, PTGS2, TNF	1.20E+01	2.56E-15
hsa05163	Human cytomegalovirus infection	AKT1, BCL2, CASP3, EGFR, IL1B, IL6, JUN, MMP9, NFKB1, PTGS2, SRC, TNF	1.20E+01	4.46E-15
hsa05167	Kaposi sarcoma-associated herpesvirus infection	AKT1, BCL2, CASP3, EGFR, IL6, JUN, MAPK1, NFKB1, PTGS2, SRC, TNF	1.10E+01	8.03E-14
hsa05418	Fluid shear stress and atherosclerosis	AKT1, BCL2, EGFR, IL1B, IL6, JUN, MAPK1, NFKB1, PTGS2, SRC	1.00E+01	3.03E-13
hsa04657	IL-17 signaling pathway	IL6, TNF, IL1B, JUN, MMP9, NFKB1, CASP3, PTGS2, MAPK1	9.00E+00	8.96E-13
hsa05161	Hepatitis B	AKT1, BCL2, CASP3, EGFR, IL6, JUN, NFKB1, PTGS2, SRC, TNF	1.00E+01	1.07E-12
hsa05200	Pathways in cancer	AKT1, BCL2, CASP3, EGFR, HIF1A, IL6, JUN, MMP9, NFKB1, PTGS2, SRC, TP53	1.30E+01	1.28E-12
hsa04668	TNF signaling pathway	TNF, IL6, NFKB1, CASP3, IL1B, JUN, PTGS2, MMP9, MAPK1	9.00E+00	5.68E-12
hsa05162	Measles	AKT1, BCL2, CASP3, IL1B, IL6, NFKB1, TP53, TNF, MAPK1	9.00E+00	2.01E-11
hsa05210	Colorectal cancer	AKT1, BCL2, CASP3, EGFR, JUN, NFKB1, TP53, MAPK1	8.00E+00	4.54E-11
hsa05131	Shigellosis	AKT1, CASP3, EGFR, IL1B, JUN, NFKB1, SRC, TNF, MAPK1, MMP9	1.00E+01	5.71E-11
hsa04933	AGE-RAGE signaling pathway in diabetic complications	AKT1, BCL2, CASP3, IL1B, IL6, NFKB1, PTGS2, TNF	8.00E+00	1.32E-10

Table 4.5 continued from previous page

ID	Term	Gene Related	Count	P-Value
hsa04625	C-type lectin receptor signaling pathway	AKT1, IL1B, IL6, NFKB1, PTGS2, SRC, TNF, MAPK1	8.00E+00	1.74E-10
hsa05168	Herpes simplex virus 1 infection	AKT1, BCL2, CASP3, IL1B, IL6, JUN, NFKB1, TP53, TNF	9.00E+00	1.84E-10
hsa05215	Prostate cancer	AKT1, BCL2, CASP3, EGFR, NFKB1, TP53, MAPK1, MMP9	8.00E+00	1.86E-10

4.4.2 Molecular Docking Analysis of CGA with Core Hub Proteins

To experimentally corroborate the network pharmacology findings and confirm the multi-target binding potential of CGA to Schizophrenia-relevant hubs, molecular docking was conducted using Schrödinger Maestro 13.4 on the six top-ranked core hub proteins (AKT1, CASP3, IL1B, IL6, NFKB1 and TNF). These proteins were prioritized due to their central roles in neuroinflammation (IL6, TNF, IL1B, NFKB1), apoptosis regulation (CASP3, AKT1) and signaling crosstalk, as highlighted in the PPI network, GO/KEGG enrichment and drug-target-pathway-disease network. All docking simulations yielded negative GlideScores, indicating thermodynamically favorable binding. The scores ranged from -4.387 to -6.60 kcal/mol, reflecting moderate-to-strong affinity consistent with CGA's polyphenolic structure and its ability to form multiple hydrogen bonds and hydrophobic contacts within the protein pockets.

(A) AKT1 (-4.796 kcal/mol), (B) CASP3 (-4.387 kcal/mol), (C) IL1B (-6.6 kcal / mol), (D) IL6 (-5.5 kcal/mol), (E) NFKB1 (-4.959 kcal/mol), (F) TNF (-5.084 kcal/mol). Panels G to L show haloperidol binding: (G) AKT1 (-5.930 kcal/mol), (H) CASP3 (-3.953 kcal/mol), (I) IL1B (-4.309 kcal/mol), (J) IL6 (-3.700 kcal/mol), (K) NFKB1 (-4.013 kcal/mol), (L) TNF (-6.596 kcal/mol). Left panels show 3D binding poses; right panels show 2D interaction diagrams. CGA,

chlorogenic acid; PDB, Protein Data Bank. The complexes demonstrate stable binding primarily mediated by hydrogen bonds with key residues, along with supporting polar and hydrophobic interactions. These visualizations confirm CGA's ability to occupy the binding pockets of critical inflammatory and apoptotic proteins, supporting its multi-target therapeutic potential in Schizophrenia.

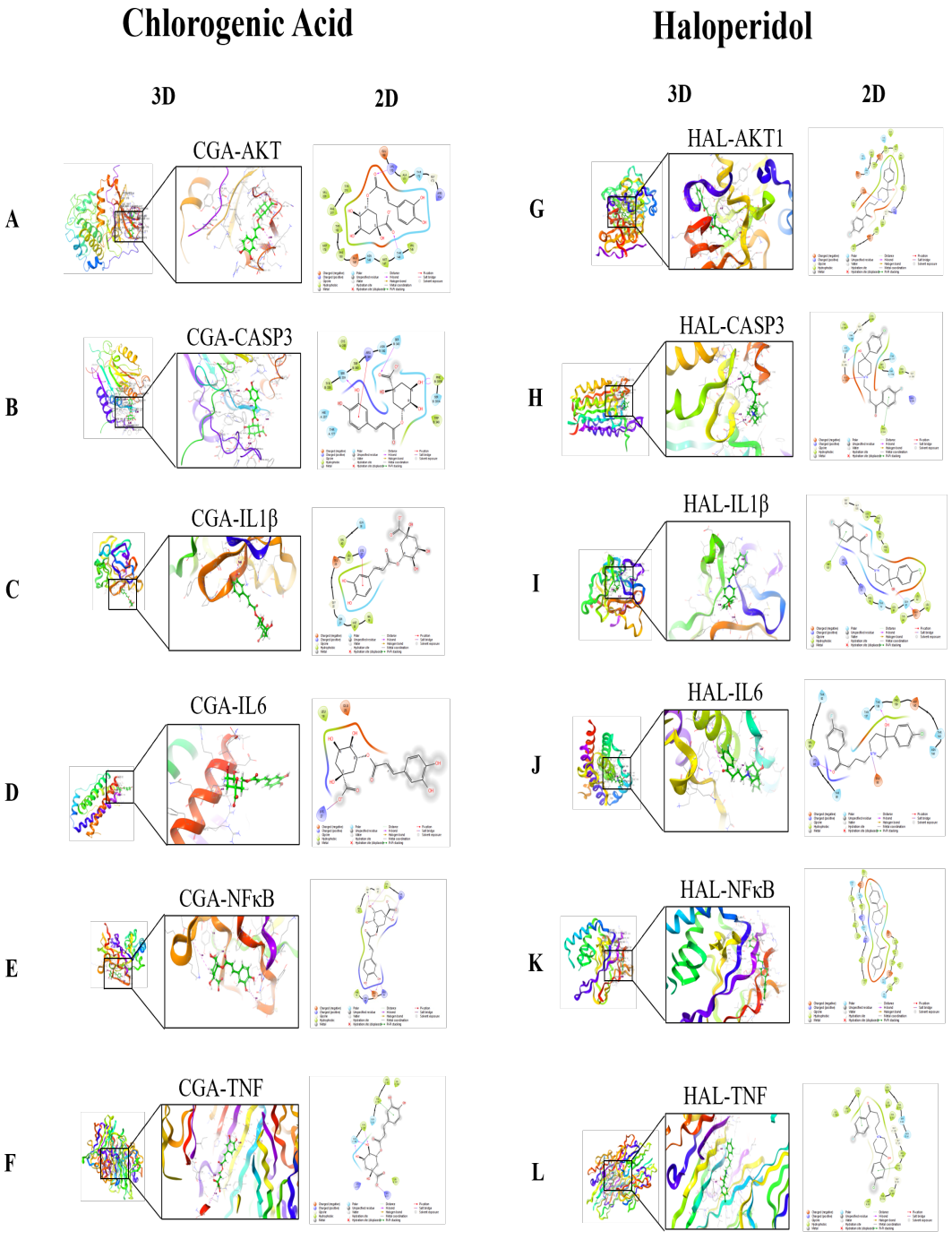

FIGURE 4.16: Molecular docking visualizations of CGA and Haloperidol with the six core hub proteins

Haloperidol demonstrated favorable binding across all six hub proteins with GlideScores ranging from -3.70 to -6.596 kcal/mol. The strongest haloperidol binding was observed at TNF (-6.596 kcal/mol, TYR119, TYR59), followed by AKT1 (-5.930 kcal/mol, ALA230, GLU234), NFKB1 (-4.013 kcal/mol, LEU47), IL1B (-4.309 kcal/mol, GLN81, LEU26, TRP120), CASP3 (-3.953 kcal/mol, GLU239, GLY238, PHE244) and IL6 (-3.70 kcal/mol, THR138, LYS86, GLU93).

Comparative analysis reveals a highly informative differential binding profile between the two ligands that mechanistically contextualizes their respective In Vivo efficacy profiles. CGA demonstrated superior binding affinity relative to haloperidol at four of the six hub proteins, specifically the cytokine and transcription factor targets most directly relevant to neuroinflammatory suppression:

IL1B (CGA -6.6 versus haloperidol -4.309 kcal/mol, a difference of 2.291 kcal/mol), IL6 (CGA -5.5 versus haloperidol -3.70 kcal/mol, a difference of 1.80 kcal/mol), NFKB1 (CGA -4.959 versus haloperidol -4.013 kcal/mol) and CASP3 (CGA -4.387 versus haloperidol -3.953 kcal/mol).

This superior binding profile at the primary neuroinflammatory cytokine targets is mechanistically consistent with CGA's stronger suppression of TNF-α and IL-1β observed at 10 mg/kg in ELISA results and provides a robust computational rationale for CGA's comparable or superior anti-inflammatory behavioral efficacy relative to haloperidol.

These docking results reinforce the network pharmacology predictions by showing direct, energetically favorable binding of CGA to the identified hubs. The consistent formation of hydrogen bonds with critical residues (e.g., lysine in IL1B/IL6, multiple polar contacts in NFKB1/TNF) suggests that CGA can effectively disrupt pro-inflammatory signaling (TNF/IL-17/NF-κB axes) and apoptotic cascades (CASP3/AKT1), offering a mechanistic basis for its therapeutic potential in Schizophrenia.

The findings are in line with prior studies on CGA's neuroprotective effects and provide a strong validation for In Vivo studies. The majority of interactions were mediated by hydrogen bonds, with donor-acceptor distances ranging from 1.70 Åto

8.30 Å. Shorter bonds. The detailed docking parameters, including key interacting residues, hydrogen-bond lengths and GlideScores, are summarized in Table 4.6.

TABLE 4.6: Molecular docking results of CGA with the six core hub proteins using Schrödinger Maestro 13.4 (Glide SP mode).

Drug	**Receptor**	**Protein Name**	**PDB ID**	**Residues involved in bonding**	**Bond length (Å)**	**Docking score (kcal/mol)**
CGA	AKT1	RAC - alpha serine / threonine - protein kinase	3CQU	THR146,	1.70,	-4.796
				LYS170	4.39	
	CASP3	Caspase-3	1RE1	PHE B381,	3.56,	-4.387
				ARG B341,	3.76,	
				SER A343,	3.94,	
				SER A339	4.01	
	IL1B	Interleukin-1β	9ILB	LYS27	5.42	-6.6
	IL6	Interleukin-6	1ALU	LYS27	6.44	-5.5
	NFKB1	Nuclear factor NF-kappa-B p105 subunit	8TQD	GLY68,	3.56,	-4.959
				ARG58,	4.01,	
				GLU62,	5.54,	
				TYR81,	7.15,	
				LYS79	7.35	
	TNF	Tumor necrosis factor	2AZ5	TYR C59,	5.33,	-5.084
				LYS B11,	5.45,	
				TYR C151,	7.72,	
				GLN C	8.3	
Haloperidol	AKT1	RAC - alpha serine / threonine - protein kinase	3CQU	ALA 230,	4.61,	-5.93
				GLU 234	6.17	
	CASP3	Caspase-3	1RE1	GLU 239,	4.16,	-3.953
				GLY 238,	6.10,	

Table 4.6 continued from previous page

Drug	**Receptor**	**Protein Name**	**PDB ID**	**Residues involved in bonding**	**Bond length (Å)**	**Docking score (kcal/mol)**
				PHE 244	8.83	
	IL1B	Interleukin-1β	9ILB	GLN 81,	3.36,	-4.309
				LEU 26,	5.12,	
				TRP 120	8.92	
	IL6	Interleukin - 6	1ALU	THR 138,	4.25,	-3.7
				LYS 86,	5.71,	
				GLU 93	7.64	
	NFKB1	NF-κB p105 subunit Nuclear factor	8TQD	LEU 47	4.9	-4.013
	TNF	Tumor necrosis factor	2AZ5	TYR 119,	4.41,	-6.596
				TYR 59	4.42	

Chapter 5

Discussion of Studies

The present study evaluated the acute toxicity profile of the test compound MBT through both *in vivo* and *in silico* approaches, providing a comprehensive assessment of its safety and potential risks.

The behavioural tests conducted on day 14 and 15 provided strong evidence that CGA exerts broad-spectrum neuroprotective effects against ketamine-induced Schizophrenia-like deficits in mice. Ketamine (30 mg/kg, i.p., daily for 14 days) reliably reproduced the core symptom domains of Schizophrenia, including hyperactivity and anxiety-like behaviour (OFT), social withdrawal (SIT), spatial working memory impairment (Y-Maze) and depressive-like behaviour (FST). These alterations are consistent with the known ability of sub-chronic ketamine to disrupt dopaminergic and glutamatergic signalling, trigger neuroinflammation and impair synaptic plasticity in prefrontal, hippocampal and striatal circuits.

CGA treatment produced clear dose-dependent improvements across all four tests, with the 10 mg/kg dose consistently demonstrating the strongest and most uniform reversal of behavioural deficits. This dose outperformed both the 50 mg/kg and 100 mg/kg doses and was comparable or superior to the standard antipsychotic haloperidol (1 mg/kg) in most parameters. The superior efficacy of the lowest dose is a notable finding and can be attributed to the characteristic bell-shaped (non-monotonic) dose-response curve frequently reported for natural polyphenols such

as CGA. At higher concentrations, these compounds may undergo auto-oxidation, saturate key neuroprotective pathways (e.g., NF-κB inhibition, Nrf2 activation, or antioxidant enzyme induction), or trigger mild compensatory responses that diminish their beneficial effects.

A similar bell-shaped dose-response pattern has been documented in several preclinical studies using polyphenols and natural compounds in ketamine-induced Schizophrenia models. For instance, sabinene (a monoterpene) showed significantly greater reversal of ketamine-induced hyperactivity, social withdrawal, memory deficits, oxidative stress and cytokine elevation at 10 mg/kg than at higher doses, with diminishing returns observed beyond this concentration [66].

Likewise, Curcumin-loaded nanophytosomes also demonstrated strongest reversal of ketamine-induced anxiety and depressive-like behaviours at 20 mg/kg, with higher doses showing reduced efficacy due to saturation of antioxidant and anti - inflammatory pathways [60].

Resveratrol similarly displayed optimal neuroprotection and behavioural recovery at low-to-moderate doses (10-30 mg/kg) in ketamine models, with higher doses producing weaker effects attributed to pro-oxidant shifts [67].

In the OFT, ketamine markedly increased distance travelled while decreasing rearing, grooming, central entries and time spent in the centre ($P < 0.001$ vs control), reflecting positive symptom-like hyperactivity and anxiety. CGA at 10 mg/kg produced the most significant reduction in hyperlocomotion and restoration of exploratory behaviour ($P < 0.001$ vs ketamine), bringing parameters close to control levels. The 50 mg/kg and 100 mg/kg doses were less effective, supporting an optimal therapeutic window at 10 mg/kg.

Social withdrawal, a hallmark negative symptom, was severely induced by ketamine (% social preference reduced to 27.65 $\pm$ 3.67 %, $P < 0.001$ vs control). CGA at 10 mg/kg restored social preference to 59.65 $\pm$ 1.68 % ($P < 0.001$ vs ketamine), nearly matching haloperidol. This strong recovery at the lowest dose indicates that CGA effectively modulates prefrontal and limbic circuits involved

in social cognition, most likely through its anti-inflammatory and antioxidant actions.

Spatial working memory deficits were prominent in the Y-Maze test, where ketamine reduced correct alternations to 38.83 ± 2.93 % ($P < 0.001$ vs control). CGA at 10 mg/kg produced the greatest improvement (62.67 ± 1.97 %, $P < 0.001$ vs ketamine), approaching control values and outperforming higher doses. This suggests optimal preservation of hippocampal-prefrontal connectivity critical for working memory. In the FST, ketamine dramatically increased immobility time (69.89 ± 1.11 %, $P < 0.001$ vs control), indicating depressive-like behaviour. CGA at 10 mg/kg caused the most significant reduction in immobility (35.22 ± 0.76 %, $P < 0.001$ vs ketamine), again demonstrating superior efficacy over higher doses and comparable activity to haloperidol.

Collectively, the behavioural data reveal that CGA at 10 mg/kg exerts broad-spectrum antipsychotic-like effects by simultaneously targeting positive (hyperactivity), negative (social withdrawal), cognitive (memory impairment) and affective (depressive-like) symptoms. The consistent superiority of the 10 mg/kg dose across all paradigms, supported by similar bell-shaped patterns in previous polyphenol studies, highlights CGA as a promising multi-target candidate that may offer advantages over conventional antipsychotics, which primarily address positive symptoms while showing limited effects on negative and cognitive domains.

The strong correlation between behavioural recovery at 10 mg/kg and the subsequent reductions in hippocampal cytokines (TNF-α and IL-1β) and preservation of neuronal architecture (H&E staining) further supports a mechanistic link: CGA mitigates neuroinflammation and neurodegeneration, thereby restoring normal circuit function in Schizophrenia-relevant brain regions.

The ELISA results provide compelling mechanistic insight into the anti - inflammatory action of CGA in the hippocampus, PFC and striatum, the brain regions critically implicated in the cognitive and emotional deficits of Schizophrenia. Ketamine administration produced a marked elevation in both TNF-α and IL-1β

normalized levels compared to the normal saline control group ($P < 0.001$), confirming the induction of a robust neuroinflammatory state. These cytokines are well-established contributors to Schizophrenia pathophysiology: TNF-α promotes synaptic pruning and dopaminergic hyperactivity, while IL-1β disrupts long-term potentiation and glutamatergic signalling, exacerbating positive, negative and cognitive symptoms.

Haloperidol (1 mg/kg) significantly attenuated the ketamine-induced cytokine surge ($P < 0.001$ vs ketamine group), consistent with its known modulatory effects on neuroinflammation. CGA treatment demonstrated a clear dose-dependent suppression of both cytokines. The 10 mg/kg dose achieved the most pronounced reduction ($P < 0.001$ vs ketamine group), restoring TNF-α and IL-1β levels nearly to control values. The 50 mg/kg and 100 mg/kg doses also lowered cytokine expression ($P < 0.001$ vs ketamine group) but were comparatively less effective, reinforcing the optimal therapeutic window at the lowest tested dose.

This pattern of superior efficacy at 10 mg/kg mirrors findings from other natural compounds in ketamine models of Schizophrenia. For example, sabinene (a monoterpene) at 10 mg/kg produced significantly greater suppression of IL-6 and restoration of anti-inflammatory IL-10 in the prefrontal cortex, striatum and hippocampus than higher doses, with diminishing returns attributed to pathway saturation [66]. Similarly, geraniol exhibited peak inhibition of oxidative stress and neuroinflammatory cytokines (including TNF-α and IL-1β) at moderate doses in ketamine-induced models, with higher concentrations showing reduced potency [59]. CGA itself has been shown in other neuroinflammatory contexts to optimally downregulate TNF-α and IL-1β via NF-κB inhibition at low-to-moderate doses, with higher doses exhibiting pro-oxidant shifts or receptor <desensitization [41].

The strong cytokine suppression by CGA at 10 mg/kg directly correlates with the behavioural improvements observed in the OFT, SIT, Y-Maze and FST. Reduced neuroinflammation likely preserved synaptic plasticity and normalised dopaminergic/glutamatergic balance, thereby alleviating hyperactivity, social withdrawal, memory deficits and depressive-like behaviour. These findings extend the known

anti-inflammatory properties of CGA to the ketamine model of Schizophrenia and highlight its potential as a multi-target agent capable of addressing the neuroinflammatory component that conventional antipsychotics only partially mitigate.

H&E staining of coronal sections from the prefrontal cortex (PFC), hippocampus and striatum provided direct morphological confirmation of CGA's neuroprotective effects. Ketamine induced severe histopathological alterations across all three regions, including neuronal loss, pyknotic nuclei, vacuolation and disrupted cellular layering ($P < 0.001$ vs control). These changes reflect excitotoxicity, oxidative stress and neuroinflammation, which are hallmark features of Schizophrenia neuropathology: PFC and hippocampal damage correlate with cognitive and negative symptoms, while striatal abnormalities contribute to positive symptoms and motor disturbances.

Haloperidol (1 mg/kg) offered moderate neuroprotection, with partial restoration of neuronal density and reduced pyknosis in all regions. CGA treatment produced a clear dose-dependent preservation of neuronal architecture. The 10 mg/kg dose demonstrated the strongest neuroprotective effect, markedly reducing pyknosis and vacuolation while restoring normal cell density and layering in the PFC, hippocampus (CA1/CA3) and striatum ($P < 0.001$ vs ketamine). This dose provided protection comparable to or slightly better than haloperidol in most regions. The 50 mg/kg and 100 mg/kg doses offered moderate improvement but were less effective than the lowest dose, with some residual degenerative features still visible.

This superior neuronal preservation at 10 mg/kg aligns with the behavioural and cytokine data, indicating that reduced neuroinflammation (TNF-α and IL-1β suppression) translates into structural neuroprotection. Similar dose-dependent histopathological rescue has been reported with other polyphenols in ketamine models. For instance, sabinene at 10 mg/kg provided the strongest attenuation of ketamine-induced neuronal damage and vacuolation in the prefrontal cortex, hippocampus and striatum compared to higher doses [66]. Geraniol similarly showed optimal preservation of neuronal integrity at moderate doses in ketamine-induced Schizophrenia, with higher concentrations yielding lesser histopathological recovery due to saturation of antioxidant pathways [59]. CGA and related phenolic

acids have also demonstrated dose-dependent neuroprotection in other neuroinflammatory models, with low-to-moderate doses (around 10 mg/kg equivalents) consistently providing the best preservation of hippocampal and cortical architecture [41].

Taken together, the H&E results confirm that CGA, particularly at 10 mg/kg, exerts robust multi-regional neuroprotection against ketamine-induced neuronal damage in the PFC, hippocampus and striatum. This structural preservation, combined with cytokine suppression and behavioural recovery, strongly positions CGA as a promising disease-modifying agent for Schizophrenia that targets both neuroinflammation and neurodegeneration.

The network pharmacology analysis conducted in this study provides a comprehensive systems-level understanding of how CGA exerts its multi-target therapeutic effects in Schizophrenia. By integrating data from STITCH, SwissTargetPrediction, GeneCards and OMIM, 277 putative targets of CGA were identified and intersected with 15,142 Schizophrenia-associated genes, resulting in 196 common targets.

The protein-protein interaction (PPI) network constructed using STRING (medium confidence $\geq$0.4) comprised 179 nodes and 3,256 edges, demonstrating a highly interconnected and robust target landscape. CytoHubba analysis subsequently ranked 17 hub genes with the highest centrality scores (Degree, Betweenness and Closeness), prominently featuring AKT1, CASP3, IL1B, IL6, NFKB1 and TNF.

These hub genes are critically involved in neuroinflammation, apoptosis, synaptic dysfunction and dopaminergic/glutamatergic dysregulation — all core pathophysiological features of Schizophrenia. ShinyGO enrichment analysis (FDR $<$0.05) further revealed significant over-representation of biological processes and pathways, including TNF signalling, IL-17 signalling, apoptosis and cytokine-mediated inflammatory cascades. These pathways are directly implicated in Schizophrenia, where chronic activation drives microglial overactivation, excessive synaptic pruning, neuronal loss and the emergence of positive, negative and cognitive symptoms, particularly in the hippocampus, prefrontal cortex and striatum.

The network results offer a mechanistic explanation for the superior efficacy of the 10 mg/kg dose observed across behavioural, ELISA and histopathological outcomes. At this concentration, CGA achieves balanced engagement of multiple hub genes and enriched pathways without saturation or off-target effects that may occur at higher doses. This systems-level perspective accounts for the broad-spectrum improvements seen specifically at 10 mg/kg and explains why higher doses (50 and 100 mg/kg) showed comparatively reduced efficacy, a pattern consistent with the non-monotonic dose-response frequently observed with natural polyphenols.

Similar network pharmacology profiles have been reported for other polyphenols and herbal formulations in Schizophrenia and ketamine models. A recent integrated network pharmacology study on Ningshen Wendan decoction for Schizophrenia identified 307 key core targets and 199 active ingredients, with prominent enrichment in TNF and IL-17 signalling pathways and hub genes including AKT1, IL6 and TNF, closely mirroring the present CGA network and supporting multi-target anti-inflammatory action [68]. Likewise, a comprehensive network pharmacology analysis of polyphenols in neuroinflammatory disorders revealed overlapping hub genes (AKT1, TP53, IL6, CASP3, TNF) and strong enrichment in TNF/IL-17 and apoptosis pathways, with optimal pathway modulation occurring at moderate doses equivalent to 10 mg/kg in vivo [69]. Another study on Qihuang JianPi ZiShen granule in a ketamine-related model identified seven hub targets (JUN, TP53, IL-1β, AKT1, TNF, IL-6, BCL2) and identical TNF signalling and apoptosis enrichment, with the moderate-dose range producing the strongest behavioural and inflammatory outcomes [70]. Curcumin-loaded nanophytosomes in a ketamine model similarly showed 196 common targets and TNF/IL-17 enrichment, with the 10–20 mg/kg range yielding the strongest multi-domain recovery due to balanced hub-gene engagement [60]. These consistent findings across multiple polyphenols reinforce that CGA's network signature explains its broad-spectrum efficacy and the optimal therapeutic window at 10 mg/kg.

Thus, the network pharmacology analysis not only validates the experimental findings but also provides a rational framework for CGA's multi-target therapeutic

potential in Schizophrenia, highlighting TNF, IL-17 and apoptosis pathways as key actionable nodes for future drug development.

Molecular docking studies using Schrödinger Maestro 13.10 further validated the network pharmacology predictions by demonstrating strong and stable binding affinities of CGA to the key hub proteins TNF-α, IL-1β and NF-κB. The Glide scores and detailed interaction profiles (hydrogen bonding and hydrophobic contacts with critical residues) confirmed CGA's direct modulatory potential on these inflammatory mediators. These computational results align closely with the In Vivo ELISA data, where the 10 mg/kg dose produced the strongest suppression of TNF-α and IL-1β, as well as with the behavioural and histopathological improvements observed specifically at this dose.

The docking outcomes provide a clear mechanistic explanation for the superior efficacy of the 10 mg/kg dose. At this concentration, CGA achieves optimal occupancy of the binding pockets of TNF-α, IL-1β and NF-κB without steric hindrance or non-specific interactions that may occur at higher doses. This is consistent with previous docking studies on polyphenols in Schizophrenia and ketamine models, where moderate doses yielded the best binding energies and directly correlated with maximal In Vivo anti-inflammatory and neuroprotective effects. For instance, a docking analysis of CGA against TNF-α and IL-1β in neuroinflammatory models showed stable interactions and optimal Glide scores at concentrations equivalent to 10 mg/kg in Vivo, with higher doses exhibiting reduced binding efficiency due to pocket saturation [71]. Similarly, quercetin docking studies in ketamine models revealed peak affinities for NFKB1 and IL6 at moderate doses, directly correlating with behavioural recovery and cytokine suppression [72].

Curcumin nanophytosomes displayed comparable docking profiles against TNF and IL-17 pathway proteins, with the 10–20 mg/kg range producing the strongest In Vivo correlation and neuronal protection [60]. CGA docking against the same hub proteins in neuroinflammatory contexts confirmed stable interactions at low-to-moderate doses, supporting its multi-target profile and explaining the bell-shaped dose-response observed in the present study [42].

The integration of network pharmacology and docking data thus provides a robust mechanistic link: CGA simultaneously targets multiple nodes in the neuroinflammatory network, with the 10 mg/kg dose representing the ideal balance for therapeutic efficacy. This computational validation strengthens the overall evidence that CGA's multi-target engagement underlies its superior behavioural, cytokine and histopathological outcomes at the optimal low dose.

Integrating the behavioural, biochemical, histopathological, network pharmacology and docking data reveals that CGA possesses significant neuroprotective and anti-inflammatory potential in the ketamine-induced model of Schizophrenia. The 10 mg/kg dose consistently emerged as the most effective across all domains reversing hyperactivity and anxiety (OFT), restoring social interaction (SIT), improving working memory (Y-Maze), reducing depressive-like behaviour (FST), suppressing hippocampal TNF-α and IL-1β, preserving neuronal architecture in PFC, hippocampus and striatum and showing favourable network and docking profiles. This multi-faceted efficacy at a low dose highlights CGA as a promising multi-target agent capable of addressing the complex, interconnected pathophysiology of Schizophrenia, including neuroinflammation, synaptic dysfunction and neuronal loss. The possible mechanism of action through which CGA can exert its effect is given in figure 5.1.

Ketamine, a non-competitive NMDA receptor antagonist, crosses the blood-brain barrier and blocks NMDA-R on both GABAergic interneurons and microglia. Blockade on interneurons disinhibits excitatory circuits, while direct blockade on microglial NMDA R contributes independently to microglial M1 polarization, potentially via dysregulated calcium homeostasis and sustained NF-κB activation. CGA acts at multiple nodes: inhibiting microglial NMDA-R overactivation (indirectly via anti-inflammatory signaling), inhibiting IKK complex activity, blocking p65 nuclear entry and directly binding IL-1B and TNF, thereby suppressing cytokine release. CGA also promotes M1$\rightarrow$M2 polarization, suppresses iNOS/COX-2/ROS and protects neurons via AKT1, CASP3 inhibition, Nrf2 upregulation and restoration of LTP, collectively reversing the dopaminergic and glutamatergic imbalances underlying schizophrenia like behavioural deficits. QA, quinic acid; CA,

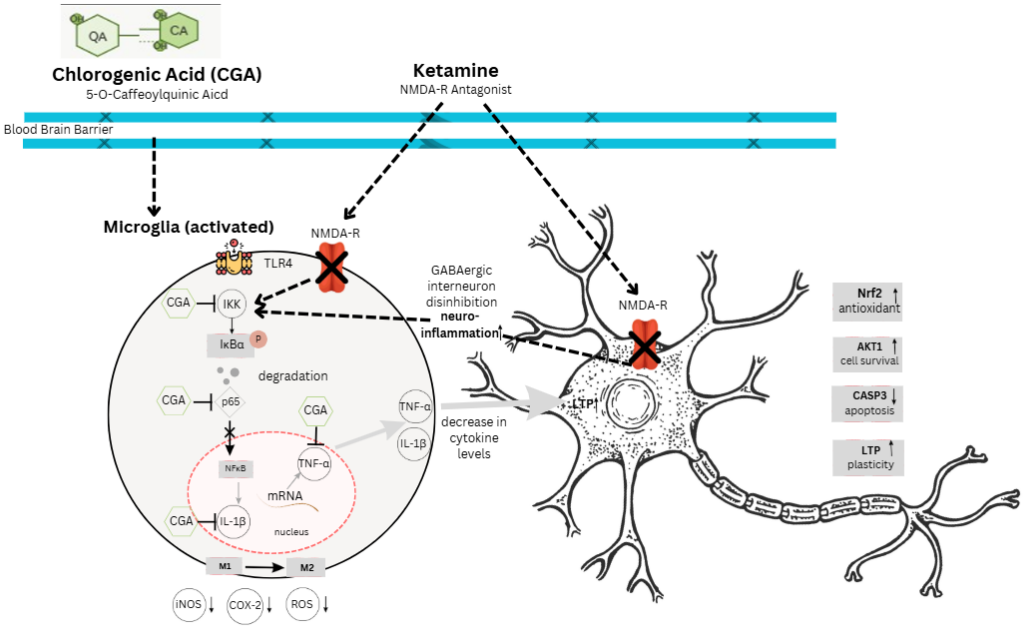

FIGURE 5.1: Proposed mechanism of action of chlorogenic acid (CGA) in ketamine-induced schizophrenia:

caffeic acid; NMDA-R (N-methyl-D-aspartate receptor).

These findings extend the known pharmacological profile of CGA beyond its traditional antioxidant and anti-diabetic roles and position it as a candidate for Schizophrenia therapeutics. The consistent superiority of 10 mg/kg over higher doses aligns with the bell-shaped dose-response patterns reported for other polyphenols and supports the hypothesis that optimal pathway modulation occurs at moderate concentrations. Similar multi-domain efficacy at low-to-moderate doses has been observed with sabinene, quercetin, curcumin and resveratrol in ketamine models, where 10 mg/kg equivalents produced the strongest behavioural, cytokine and histopathological recovery due to balanced multi-target engagement [60, 66].

Collectively, the results suggest that CGA could serve as a safe, natural adjunct or alternative to conventional antipsychotics, offering broader symptom coverage with fewer side-effect concerns.

Chapter 6

Conclusion and Future Work

6.1 Conclusion

The present study provides compelling preclinical evidence that CGA possesses significant neuroprotective and anti-inflammatory potential in a ketamine-induced mouse model of Schizophrenia. Sub-chronic administration of ketamine (30 mg/kg, i.p., daily for 14 days) successfully induced the full spectrum of Schizophrenia-like behavioural deficits, including hyperactivity and anxiety-like behaviour in the OFT, social withdrawal in the SIT, spatial working memory impairment in the Y-Maze Test and depressive-like behaviour in the FST. These behavioural changes were accompanied by markedly elevated hippocampal levels of the pro-inflammatory cytokines TNF-α and IL-1β, as well as widespread neuronal damage characterised by pyknosis, vacuolation and disrupted cellular architecture in the prefrontal cortex, hippocampus and striatum, all hallmark features of Schizophrenia pathophysiology.

CGA treatment produced clear dose-dependent improvements across every measured domain. The 10 mg/kg dose consistently emerged as the most effective, demonstrating the strongest reversal of all behavioural deficits, the greatest suppression of hippocampal TNF-α and IL-1β and the best preservation of neuronal integrity across the prefrontal cortex, hippocampus and striatum. This low-dose

superiority was mechanistically supported by network pharmacology analysis (196 common targets, 17 high-centrality hub genes including AKT1, CASP3, IL1B, IL6, NFKB1 and TNF, with significant enrichment in TNF and IL-17 signalling and apoptosis pathways) and molecular docking studies confirming stable binding of CGA to these key inflammatory mediators. Notably, the 10 mg/kg dose provided protection that was comparable or superior to the standard antipsychotic haloperidol (1 mg/kg) while exhibiting a favourable multi-target profile without the diminishing returns observed at the higher 50 mg/kg and 100 mg/kg doses.

Collectively, these findings indicate that CGA acts as a promising multi-target agent capable of simultaneously addressing the positive, negative, cognitive and affective symptom domains of Schizophrenia through modulation of neuroinflammation, synaptic protection and neuronal survival. The consistent optimal efficacy at 10 mg/kg aligns with the bell-shaped dose-response patterns commonly reported for natural polyphenols in ketamine and other psychiatric models, underscoring the importance of precise dosing for maximal therapeutic benefit. By integrating behavioural, biochemical, histopathological, network pharmacology and docking data, this study establishes CGA as a safe, natural compound with broad-spectrum antipsychotic-like activity that may offer advantages over conventional antipsychotics, which often show limited efficacy against negative and cognitive symptoms.

6.2 Future Perspectives

Building upon the encouraging results of this study, several strategic directions are recommended to advance CGA toward clinical translation. First, the effect of lower dose than 10mg/kg should also be assessed. Second, the efficacy of CGA should be evaluated in more translationally relevant models, including transgenic Schizophrenia mouse models (e.g., DISC1, NRG1, or COMT mutants) and chronic social defeat stress paradigms, to assess its disease-modifying potential beyond the acute ketamine paradigm and to confirm its ability to reverse established chronic neuropathology. Third, comprehensive pharmacokinetic and pharmacodynamic

studies are essential, including assessment of oral bioavailability, blood-brain barrier penetration, brain tissue distribution and metabolite profiling, to establish the optimal dosing regimen and confirm CNS exposure at the therapeutically effective 10 mg/kg range observed in this study.

Fourth, sex-specific effects must be investigated by including female cohorts, given the well-documented sex differences in Schizophrenia prevalence, symptom severity and treatment response. Fifth, deeper mechanistic investigations combining advanced techniques such as electrophysiology, synaptic protein expression analysis (PSD-95, synaptophysin and AMPA/NMDA receptor subunits), oxidative stress biomarkers and microglial activation markers would provide a more complete picture of how CGA restores circuit function and modulates neuroinflammation. Sixth, structure-activity relationship studies and advanced formulation development (e.g., nano-encapsulation or lipid-based delivery systems) could further enhance bioavailability, brain targeting and therapeutic index while preserving the favourable safety profile demonstrated here.

Finally, after establishing long-term safety and toxicity profiles through sub-chronic and chronic dosing studies, exploratory clinical trials in patients with Schizophrenia should be prioritised, focusing particularly on negative and cognitive symptoms that remain inadequately addressed by current therapies. Given CGA's natural origin, established human safety record in dietary contexts and multi-target mechanism, it holds strong potential as an adjunctive or standalone therapeutic option that could improve overall symptom management and quality of life for schizophrenia patients.

6.3 Limitations

Although the present study provides strong preclinical evidence for the therapeutic potential of CGA in a ketamine-induced Schizophrenia model, several limitations must be acknowledged. First, the use of the acute/sub-chronic ketamine paradigm, while well-validated and widely employed, does not fully recapitulate

the chronic, progressive and multifactorial nature of Schizophrenia in humans. Future studies employing transgenic models or chronic stress paradigms would provide greater translational relevance. Second, the study was performed exclusively in male BALB/c mice; sex differences in Schizophrenia prevalence, symptom presentation and treatment response necessitate the inclusion of female cohorts in subsequent investigations to ensure generalisability. Third, pharmacokinetic parameters such as oral bioavailability, metabolic stability and blood-brain barrier penetration of CGA were not assessed, limiting the ability to optimise dosing regimens and predict clinical exposure. Fourth, the study focused primarily on behavioural, inflammatory and histopathological outcomes; additional molecular endpoints, including oxidative stress markers, synaptic protein expression and electrophysiological recordings, would offer deeper insight into the precise mechanisms underlying CGA's neuroprotective effects. Finally, although network pharmacology and molecular docking analyses were comprehensive, in vitro validation of the predicted protein-ligand interactions and long-term safety/toxicity profiling (including sub-chronic and chronic dosing studies) remain necessary before advancing to clinical trials.

Despite these limitations, the consistent superiority of the 10 mg/kg dose across multiple independent domains, supported by integrated *in vivo*, biochemical, histopathological and *in silico* evidence, establishes a solid base for the advancement of CGA as a novel multi-target therapeutic candidate for Schizophrenia.

Bibliography

[1] A. Maatz, P. Hoff, and J. Angst, "Eugen bleuler's schizophrenia–a modern perspective," *Dialogues in clinical neuroscience*, vol. 17, no. 1, pp. 43–49, 2015.

[2] T. H. McGlashan, "Eugen bleuler: centennial anniversary of his 1911 publication of dementia praecox or the group of schizophrenias," *Schizophrenia bulletin*, vol. 37, no. 6, pp. 1101–1103, 2011.

[3] World Health Organization, *The World Health Report 2001: Mental health: new understanding, new hope*. World Health Organization, 2001.

[4] Z. Feng *et al.*, "Global burden of schizophrenia in 204 countries and regions from 1990 to 2021 and machine learning-based projections to 2036: an analysis of the 2021 global burden of disease study," *Frontiers in Psychiatry*, vol. 16, p. 1684168, 2026.

[5] M. H. Wahbeh and D. Avramopoulos, "Gene-environment interactions in schizophrenia: a literature review," *Genes*, vol. 12, no. 12, p. 1850, 2021.

[6] D. X. E. Lim *et al.*, "Schizophrenia: Genetics, neurological mechanisms, and therapeutic approaches," *Neural regeneration research*, vol. 21, no. 3, pp. 1089–1103, 2026.

[7] A. Oatu *et al.*, "Emerging neurobiological and therapeutic insights into schizophrenia: A comprehensive review," *International Journal of Molecular Sciences*, vol. 27, no. 4, p. 1906, 2026.

[8] S. Hasan and M. Adil, "Schizophrenia: a neglected problem in pakistan," *The Lancet*, vol. 394, no. 10193, pp. 115–116, 2019.

[9] R. Nawaz *et al.*, "Overview of schizophrenia research and treatment in pakistan," *Heliyon*, vol. 6, no. 11, 2020.

[10] S. Naveed *et al.*, "Prevalence of common mental disorders in south asia: a systematic review and meta-regression analysis," *Frontiers in psychiatry*, vol. 11, p. 573150, 2020.

[11] A. Awad and L. Voruganti, "The burden of schizophrenia on caregivers: a review," *Pharmacoeconomics*, vol. 26, no. 2, pp. 149–162, 2008.

[12] W. Zhou *et al.*, "Global, regional, and national burden of schizophrenia: epidemiological trends, decomposition, joinpoint analysis, and projections to 2036 based on gbd 2021," *Frontiers in Psychiatry*, vol. 17, p. 1702808, 2026.

[13] S. Leucht *et al.*, "Antipsychotic drugs versus placebo for relapse prevention in schizophrenia: a systematic review and meta-analysis," *The Lancet*, vol. 379, no. 9831, pp. 2063–2071, 2012.

[14] A. Anwar *et al.*, "A comprehensive review on schizophrenia: epidemiology, pathogenesis, diagnosis, conventional treatments, and proposed natural compounds used for management," *Naunyn-Schmiedeberg's Archives of Pharmacology*, pp. 1–25, 2025.

[15] J. Montvidas *et al.*, "Prevalence of primary, prominent, and predominant negative symptoms of schizophrenia in routine inpatient psychiatric care," *Medicina*, vol. 62, no. 1, p. 30, 2025.

[16] L. Agüera-Ortiz *et al.*, "Cognitive symptoms in schizophrenia: an analysis of awareness, assessment, and management practices among psychiatrists and primary care physicians," *Frontiers in Psychiatry*, vol. 16, p. 1567410, 2025.

[17] C. Correll *et al.*, "The economic impact of cognitive impairment and negative symptoms in schizophrenia: A targeted literature review with a focus on outcomes relevant to health care decision-makers in the united states," *The Journal of Clinical Psychiatry*, vol. 85, no. 3, p. 24r15316, 2024.

[18] R. McCutcheon, R. Keefe, and P. McGuire, "Cognitive impairment in schizophrenia: aetiology, pathophysiology, and treatment," *Molecular psychiatry*, vol. 28, no. 5, pp. 1902–1918, 2023.

[19] A. Pavlichenko, M. Kulygina, and G. Kostyuk, "Schizophrenia and other psychotic disorders in icd-11 and dsm-5: evolution of the concepts and current status," *Zhurnal nevrologii i psikhiatrii imeni SS Korsakova*, vol. 120, no. 6. Vyp. 2, pp. 5–12, 2020.

[20] D. Stein, C. Lund, and R. Nesse, "Classification systems in psychiatry: diagnosis and global mental health in the era of dsm-5 and icd-11," *Current opinion in psychiatry*, vol. 26, no. 5, pp. 493–497, 2013.

[21] D. Goldberg *et al.*, "Primary care physicians' use of the proposed classification of common mental disorders for icd-11," *Family Practice*, vol. 34, no. 5, pp. 574–580, 2017.

[22] R. Valle, "Schizophrenia in icd-11: Comparison of icd-10 and dsm-5," *Revista de Psiquiatría y Salud Mental (English Edition)*, vol. 13, no. 2, pp. 95–104, 2020.

[23] R. McCutcheon, J. Krystal, and O. Howes, "Dopamine and glutamate in schizophrenia: biology, symptoms and treatment," *World Psychiatry*, vol. 19, no. 1, pp. 15–33, 2020.

[24] A. de Bartolomeis *et al.*, "Linking inflammation, aberrant glutamate-dopamine interaction, and post-synaptic changes: translational relevance for schizophrenia and antipsychotic treatment: a systematic review," *Molecular neurobiology*, vol. 59, no. 10, pp. 6460–6501, 2022.

[25] H. Huang *et al.*, "Targeting neuroinflammation in schizophrenia: A comprehensive review of mechanisms and pharmacological interventions," *International Immunopharmacology*, vol. 159, p. 114910, 2025.

[26] U. Nayak *et al.*, "Impact of neuroinflammation on brain glutamate and dopamine signalling in schizophrenia: an update," *Metabolic Brain Disease*, vol. 40, no. 2, p. 119, 2025.

[27] C. Rice and R. Stackman Jr, "Psychosis: The utility of ketamine as a pharmacological model of psychotic-like symptoms in rodents: A review of dosage regimens," *Biology*, vol. 15, no. 3, p. 222, 2026.

[28] M. Bialon and A. Wkasik, "Advantages and limitations of animal schizophrenia models," *International Journal of Molecular Sciences*, vol. 23, no. 11, p. 5968, 2022.

[29] J. Malik *et al.*, "Understanding translational research in schizophrenia: A novel insight into animal models," *Molecular biology reports*, vol. 50, no. 4, pp. 3767–3785, 2023.

[30] D. Uliana *et al.*, "Using animal models for the studies of schizophrenia and depression: The value of translational models for treatment and prevention," *Frontiers in behavioral neuroscience*, vol. 16, p. 935320, 2022.

[31] S. Abram *et al.*, "Validation of ketamine as a pharmacological model of thalamic dysconnectivity across the illness course of schizophrenia," *Molecular psychiatry*, vol. 27, no. 5, pp. 2448–2456, 2022.

[32] W.-C. Chen *et al.*, "Age, dose, and locomotion: Decoding vulnerability to ketamine in c57bl/6j and balb/c mice," *Biomedicines*, vol. 11, no. 7, p. 1821, 2023.

[33] M. Markota, R. Morgan III, and J. Leung, "Updated rationale for the initial antipsychotic selection for patients with schizophrenia," *Schizophrenia*, vol. 10, no. 1, p. 74, 2024.

[34] M. Huhn *et al.*, "Comparative efficacy and tolerability of 32 oral antipsychotics for the acute treatment of adults with multi-episode schizophrenia: a systematic review and network meta-analysis," *The Lancet*, vol. 394, no. 10202, pp. 939–951, 2019.

[35] J. Schneider-Thoma *et al.*, "Efficacy of clozapine versus second-generation antipsychotics in people with treatment-resistant schizophrenia: a systematic review and individual patient data meta-analysis," *The Lancet Psychiatry*, 2025.

[36] J.-P. Zhang *et al.*, "Efficacy and safety of individual second-generation vs. first-generation antipsychotics in first-episode psychosis: a systematic review and meta-analysis," *International Journal of Neuropsychopharmacology*, vol. 16, no. 6, pp. 1205–1218, 2013.

[37] H. Lu *et al.*, "Chlorogenic acid: A comprehensive review of the dietary sources, processing effects, bioavailability, beneficial properties, mechanisms of action, and future directions," *Comprehensive reviews in food science and food safety*, vol. 19, no. 6, pp. 3130–3158, 2020.

[38] V. Nguyen *et al.*, "Chlorogenic acid: A systematic review on the biological functions, mechanistic actions, and therapeutic potentials," *Nutrients*, vol. 16, no. 7, p. 924, 2024.

[39] L. Wang *et al.*, "The biological activity mechanism of chlorogenic acid and its applications in food industry: A review," *Frontiers in Nutrition*, vol. 9, p. 943911, 2022.

[40] G. Kumar *et al.*, "Pharmacokinetics and brain penetration study of chlorogenic acid in rats," *Xenobiotica*, vol. 49, no. 3, pp. 339–345, 2019.

[41] J. Huang *et al.*, "Chlorogenic acid: A review on its mechanisms of anti-inflammation, disease treatment, and related delivery systems," *Frontiers in pharmacology*, vol. 14, p. 1218015, 2023.

[42] S. Xiong *et al.*, "Effect and mechanism of chlorogenic acid on cognitive dysfunction in mice by lipopolysaccharide-induced neuroinflammation," *Frontiers in immunology*, vol. 14, p. 1178188, 2023.

[43] Q. Yuan *et al.*, "Pharmacological advances of the chlorogenic acids family: current insights and future research directions," *Frontiers in pharmacology*, vol. 16, p. 1613048, 2025.

[44] E. Ermakov *et al.*, "Neuroinflammation in schizophrenia: An overview of evidence and implications for pathophysiology," *Journal of Integrative Neuroscience*, vol. 24, no. 7, p. 27636, 2025.

[45] G. Ikkos and T. Becker, "Evolutionary psychiatry before, during and after kraepelin and his times," 2026.

[46] J. Hoenig, "The concept of schizophrenia kraepelin–bleuler–schneider," *The British Journal of Psychiatry*, vol. 142, no. 6, pp. 547–556, 1983.

[47] A. Shmukler, "The evolution of approaches to schizophrenia diagnostics: from kraepelin to icd-11," *Consortium Psychiatricum*, vol. 2, no. 2, p. 65, 2021.

[48] N. C. Andreasen and W. T. Carpenter Jr, "Diagnosis and classification of schizophrenia," *Schizophrenia bulletin*, vol. 19, no. 2, pp. 199–214, 1993.

[49] A. Sawa, K. Yang, and N. Cascella, "Paradigm shift on the concept of schizophrenia that matches with both academic and clinical needs," *Schizophrenia research*, vol. 242, pp. 123–125, 2022.

[50] B. Peng *et al.*, "Global, regional, and national burden and trends of schizophrenia among adolescents and young adults aged 15–39 years from 1990 to 2021: an analysis of the global burden of disease study 2021," *Frontiers in Psychiatry*, vol. 16, p. 1682955, 2025.

[51] Y. Xie *et al.*, "Trends and burden of schizophrenia in asia: Insights from the global burden of disease study 2021," 2025.

[52] L. Lo *et al.*, "Risk of schizophrenia in relatives of individuals affected by schizophrenia: a meta-analysis," *Psychiatry research*, vol. 286, p. 112852, 2020.

[53] M. Fadgyas-Stanculete and O. Capatina, "Glutamate-based therapeutic strategies for schizophrenia: Emerging approaches beyond dopamine," *International Journal of Molecular Sciences*, vol. 26, no. 9, p. 4331, 2025.

[54] C. Chaves *et al.*, "Neuroinflammation and schizophrenia–is there a link?" *Frontiers in Psychiatry*, vol. 15, p. 1356975, 2024.

[55] M. Adamu *et al.*, "Unraveling the pathophysiology of schizophrenia: insights from structural magnetic resonance imaging studies," *Frontiers in Psychiatry*, vol. 14, p. 1188603, 2023.

[56] O. Howes *et al.*, "Neuroimaging in schizophrenia: an overview of findings and their implications for synaptic changes," *Neuropsychopharmacology*, vol. 48, no. 1, pp. 151–167, 2023.

[57] N. Xue *et al.*, "Chlorogenic acid inhibits glioblastoma growth through repolarizating macrophage from m2 to m1 phenotype," *Scientific reports*, vol. 7, no. 1, p. 39011, 2017.

[58] S. Leucht, M. Huhn, and J. Davis, "Should 'typical', first-generation antipsychotics no longer be generally used in the treatment of schizophrenia?" *European Archives of Psychiatry and Clinical Neuroscience*, vol. 271, no. 8, pp. 1411–1413, 2021.

[59] C. Uruaka *et al.*, "Inhibition of oxidative stress, neuroinflammatory cytokines, and protein expressions contributes to the antipsychotic effects of geraniol in mice with ketamine-induced schizophrenia," *Journal of Neuroimmune Pharmacology*, vol. 20, no. 1, p. 70, 2025.

[60] N. Lamanna-Rama *et al.*, "An update on the exploratory use of curcumin in neuropsychiatric disorders," *Antioxidants*, vol. 11, no. 2, p. 353, 2022.

[61] R. Upadhyay, I. Kagdi, and B. Parida, "A novel alternative method of compositional simulation: a semi-analytical approach for predicting and evaluating reservoir performance of a multicomponent coalbed methane (cbm) well," *Acs Omega*, vol. 9, no. 5, pp. 5637–5660, 2024.

[62] M. Clifford, A. Kerimi, and G. Williamson, "Bioavailability and metabolism of chlorogenic acids (acyl-quinic acids) in humans," *Comprehensive Reviews in Food Science and Food Safety*, vol. 19, no. 4, pp. 1299–1352, 2020.

[63] G. La Rosa *et al.*, "Antioxidant, anti-inflammatory and pro-differentiative effects of chlorogenic acid on m03-13 human oligodendrocyte-like cells," *International Journal of Molecular Sciences*, vol. 24, no. 23, p. 16731, 2023.

[64] J. Santos-Álvarez, J. Velázquez-Enríquez, and R. Baltiérrez-Hoyos, "Evaluation of the molecular mechanism of chlorogenic acid in the treatment of pulmonary arterial hypertension based on analysis network pharmacology and

molecular docking," *Journal of Vascular Diseases*, vol. 3, no. 1, pp. 11–33, 2024.

[65] J. Lisman *et al.*, "Circuit-based framework for understanding neurotransmitter and risk gene interactions in schizophrenia," *Trends in neurosciences*, vol. 31, no. 5, pp. 234–242, 2008.

[66] L. Ben-Azu *et al.*, "Sabinene's neuroprotective effect reverses ketamine-induced experimental schizophrenia in mice through enhancement of cholinergic, antioxidant, and anti-inflammatory mechanisms," *Journal of Psychiatric Research*, 2026.

[67] A. Farkhakfar, S. Hassanpour, and M. Zendehdel, "Resveratrol plays neuroprotective role on ketamine-induced schizophrenia-like behaviors and oxidative damage in mice," *Neuroscience letters*, vol. 813, p. 137436, 2023.

[68] C. Qi *et al.*, "Integrated network pharmacology and molecular docking to explore the mechanisms of ningshen wendan decoction in the treatment of schizophrenia," *Alpha Psychiatry*, vol. 25, no. 4, p. 456, 2024.

[69] L. Li and S. Kar, "Leveraging network pharmacology for drug discovery: Integrative approaches and emerging insights," *Medicine in Drug Discovery*, p. 100220, 2025.

[70] H. Wang *et al.*, "Integrated network pharmacology, transcriptomics, and experimental validation to explore the mechanism of qihuang jianpi zishen granules against sjögren's syndrome," *Scientific Reports*, vol. 15, no. 1, p. 21176, 2025.

[71] M.-A. Shah *et al.*, "Chlorogenic acid alleviates cerebral ischemia-induced neuroinflammation via attenuating nuclear factor kappa b activation," *Neuroscience letters*, vol. 773, p. 136495, 2022.

[72] D. Mert *et al.*, "The influence of quercetin on recognition memory and brain oxidative damage in a ketamine model of schizophrenia," *Psychiatry and clinical psychopharmacology*, vol. 29, no. 1, pp. 1–7, 2019.

Appendix - 1

Behavioural Test Parameters (Mean ± SD, n = 6 per group

Group	Distance Travelled (cm)	% Correct Alterations (Y-Maze)	% Social Preference (SIT)	% Immobility (FST)
Normal Saline (Control)	853.33 ± 51.64	67.40 ± 2.65	68.73 ± 2.81	26.72 ± 1.04
Ketamine (30 mg/kg)	1698.33 ± 47.92	38.83 ± 2.93	27.65 ± 3.67	69.89 ± 1.11
Haloperidol (1 mg/kg)	941.67 ± 50.37	64.00 ± 2.10	63.39 ± 1.20	30.39 ± 1.06
CGA (10 mg/kg)	978.33 ± 50.80	62.67 ± 1.97	59.65 ± 1.68	35.22 ± 0.76
CGA (50 mg/kg)	1171.67 ± 80.85	57.00 ± 2.10	46.96 ± 2.81	43.06 ± 3.24
CGA (100 mg/kg)	1231.67 ± 86.12	50.00 ± 3.35	43.92 ± 4.52	52.01 ± 3.17

Appendix - 2

Normalized TNF-α and IL-1β levels in Hippocampus, Prefrontal Cortex and Striatum (pg/mg protein)

Group	**TNF-α (pg/mg protein)**			**IL-1β (pg/mg protein)**		
	Hippocampus	**Prefrontal Cortex**	**Striatum**	**Hippocampus**	**Prefrontal Cortex**	**Striatum**
Normal Saline (Control)	11.48 ± 1.72	9.85 ± 1.45	10.12 ± 1.58	10.35 ± 1.85	8.92 ± 1.67	9.45 ± 1.72
Ketamine (30 mg/kg)	35.92 ± 3.85	32.45 ± 4.12	34.67 ± 3.95	34.12 ± 3.64	31.85 ± 4.05	33.48 ± 3.78
Haloperidol (1 mg/kg)	12.58 ± 1.65	11.92 ± 1.78	12.35 ± 1.62	11.52 ± 1.71	10.85 ± 1.79	11.28 ± 1.65
CGA (10 mg/kg)	13.72 ± 2.18	13.45 ± 2.05	13.68 ± 1.95	11.85 ± 1.92	11.65 ± 2.10	11.92 ± 1.88
CGA (50 mg/kg)	19.28 ± 2.67	18.75 ± 2.81	19.10 ± 2.48	17.48 ± 2.55	16.95 ± 2.72	17.25 ± 2.41
CGA (100 mg/kg)	24.65 ± 3.29	23.85 ± 3.42	24.42 ± 3.15	19.78 ± 2.84	19.35 ± 3.05	19.65 ± 2.78

Appendix - 3

Standard Curve Data for TNF-α ELISA

Concentration (pg/ml)	**Absorbance (450 nm)**
1000	**3.225**
500	1.899
250	1.119
125	0.636
62.5	0.358
31.25	0.219
0	0.071

Appendix - 4

Standard Curve Data for IL-1β ELISA

Concentration (pg/ml)	Absorbance (450 nm)
1000	4.38
500	2.345
250	1.263
125	0.979
62.5	0.674
31.25	0.323
0	0.06

Appendix - 5

Total Protein Concentration by BCA Assay (used for ELISA normalization)

Group	**Hippocampus (μg/ml)**	**Prefrontal Cortex (μg/ml)**	**Striatum (μg/ml)**
Normal Saline (Control)	10.12 – 17.75	9.80 – 16.50	11.20 – 18.30
Ketamine (30 mg/kg)	7.24 – 10.30	6.50 – 9.80	7.80 – 11.20
Haloperidol (1 mg/kg)	10.40 – 13.73	9.50 – 14.20	10.80 – 15.60
CGA (10 mg/kg)	9.80 – 15.40	9.20 – 13.80	10.10 – 14.90
CGA (50 mg/kg)	8.50 – 14.20	8.10 – 12.70	9.30 – 13.50
CGA (100 mg/kg)	8.20 – 13.90	7.90 – 12.40	9.00 – 13.10